

**A FORCE SENSING RESISTOR  
FOR MONITORING PLANTAR FORCE  
UNDER FOOT**

**A FORCE SENSING RESISTOR  
FOR MONITORING PLANTAR FORCE  
UNDER FOOT**

By

David Martin Hiemstra, B.Eng.Mgt.

A Project

Submitted to the School of Graduate Studies  
in Partial Fulfilment of the Requirements  
for the Degree  
Master of Engineering  
McMaster University

MASTER OF ENGINEERING (1992)

(Electrical Engineering)

McMASTER UNIVERSITY

Hamilton, Ontario

TITLE: A Force Sensing Resistor for Monitoring Plantar Force

AUTHOR: David Martin Hiemstra, B.Eng.Mgt. McMaster University

SUPERVISOR: Dr. H. de Bruin

NUMBER OF PAGES: vii,93

## ABSTRACT

The needs for obtaining quantitative plantar force information range from basic research into foot function to assisting patients in the use of prosthetic devices. This project reviews present force monitoring techniques, describes the evaluation of a Force Sensing Resistor for monitoring plantar force and proposes a low power portable plantar force monitoring system utilizing an array of force sensing resistors.

## TABLE OF CONTENTS

	page
Chapter 1 INTRODUCTION	1
1.0 Project Summary	1
1.1 Need for Monitoring Plantar Force	2
1.2 Review of Force Sensing Techniques	2
a)Resistive Techniques	3
i)Resistive Strain Gage	3
ii)Semiconductor Strain Gage	3
iii)Force Sensing Resistor	4
b)Piezoelectric Techniques	5
i)Polycrystalline Ceramics	5
ii)Polymers	5
c)Capacitive Techniques	6
1.3 Transducer Types	6
Chapter 2 BACKGROUND	9
2.0 Review of Plantar Force Monitoring Techniques	9
a)Qualitative Techniques	9
b)Stationary Sensors	9
c)Insole Sensors	10
d)Outside Sole Sensors	10
2.1 Time Domain Characteristics of Plantar Force	11
2.2 Ideal Characteristics of a Plantar Force Sensor	13
Chapter 3 IMPLEMENTATION OF THE SENSOR	15
3.0 The Force Sensing Resistor	15
a)FSR Construction	15

b)FSR Principle of Operation	16
c)FSR Characteristics	17
3.1 PSPICE Macromodel of FSR	21
3.2 Readout Circuitry for Evaluation of Force Sensing Resistor	25
a)Schematic of Readout Circuitry for FSR	25
b)Technical Description of Readout Circuitry	28
c)Simulation of Readout Circuitry	29
i) DC Analysis	29
ii) AC Analysis	33
iii)Transient Analysis	36
iv) Noise Analysis	39
d)Evaluation of Force Sensing Resistor/Readout Circuitry	42
Chapter IV A PROPOSED LOW POWER PORTABLE PLANTAR FORCE READOUT SYSTEM	47
4.0 Force Sensing Resistor Configuration	47
4.1 Readout Electronics Configuration	49
Chapter V CONCLUSIONS	51
Appendix	
1)PSPICE Circuit File Listing for FSR Readout Circuitry	52
2)Technical Overview Force and Position Sensing Resistor	61

3)Test Data Sheet FSR/Readout Electronics DC Transfer Characteristic	67
4)Test Data Analysis DC Transfer Characteristic	69
5)Active Component Data Sheets for FSR Evaluation Readout Circuitry	75
6)Active Component Data Sheets for Proposed Readout Circuitry	79
References	92

# CHAPTER 1

## INTRODUCTION

### 1.0 Project Summary

This project entitled "A FORCE SENSING RESISTOR FOR MONITORING PLANTAR FORCE UNDER FOOT" first covers the need for monitoring plantar force. This is followed by a review of force sensor characteristics, which leads into an evaluation of present techniques for plantar force monitoring. A quantitative discussion of plantar force time domain characteristics is then provided. This leads into a brief description of the ideal characteristics of a sensor to monitor plantar force. Once the background has been established a detailed description of the "FORCE SENSING RESISTOR (FSR)" is provided including construction, principle of operation, terminal characteristics and a macromodel. A suitable readout circuit for FSR evaluation is presented in schematic form, along with a technical description and FSR/readout circuit simulation results. Experimental evaluation of prototype FSR/readout circuitry is presented. Finally a proposal for further work is presented describing a completely portable plantar force monitoring system based upon the "FORCE SENSING RESISTOR". This system shows considerable promise since it is accurate and reliable with relatively low cost.

## **1.1 Need for Monitoring Plantar Force**

The need for obtaining quantitative plantar force information is driven by a diverse range of interests, which range from basic research into foot function to assisting patients in the use of prosthetic devices. The list below provides a detailed summary:

- 1) Provide a description of normal foot function.[12]
- 2) To assess pathological foot function.[15]
- 3) To assess lower limb disorders.[14]
- 4) Research into biomechanics.
- 5) Monitor usefulness of drug therapy, surgery, physiotherapy and orthopaedic foot wear.
- 6) Dynamic change between walking and running.[12]
- 7) Feedback for sensory impaired foot or limb.
- 8) Feedback for prosthetic and assistive devices.[15]

## **1.2 Review of Force Sensing Techniques**

To sense force a transducer is used to convert the force to an electrical signal. This electrical signal may be a direct result of the applied force or due to a change in transducer characteristics as a result of applied force which modulates a electrical excitation. Respectively these are called two port passive and three port active force transducers. Examples of each type are found in the following discussion of different force sensor types.

## a) Resistive Techniques

### i) Resistive Strain Gage

In a resistive strain gage the force is measured indirectly by measuring deflection in a calibrated carrier. The resistive element changes in length and is placed under strain hence causing a change in its resistance. These can be formed with an unbonded wire stretched between two points or the more practical bonded configuration in wire or foil. Figure 1 shows typical patterns of a bonded wire and foil strain gage.[18]

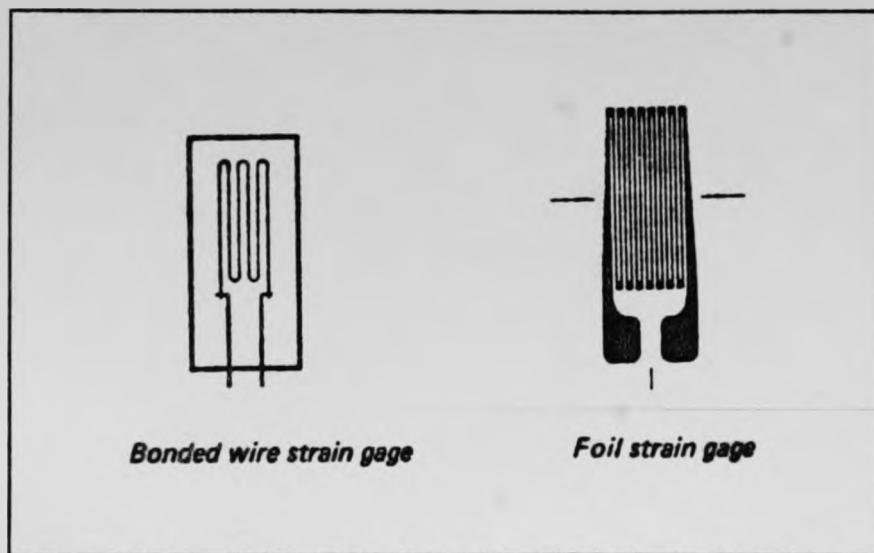


**Figure 1** Bonded Wire and Foil Strain Gage.[18]

### ii) Semiconductor Strain Gage

The semiconductor strain gage principle of operation is similar to the resistive strain gage, improved sensitivity is provided by increased piezoresistive sensitivity at the price of linearity and temperature sensitivity. The ability to micromachine 3-D structures in silicon allows for the fabrication of a diaphragm which flexes under a applied force and results in piezoresistive elements grown on it to change in value. These devices can be

quite user friendly if they include amplifiers and compensation circuitry. Figure 2 shows a picture of a typical device, packaged in a hybrid fashion with readout electronics.[17,18,19,20]

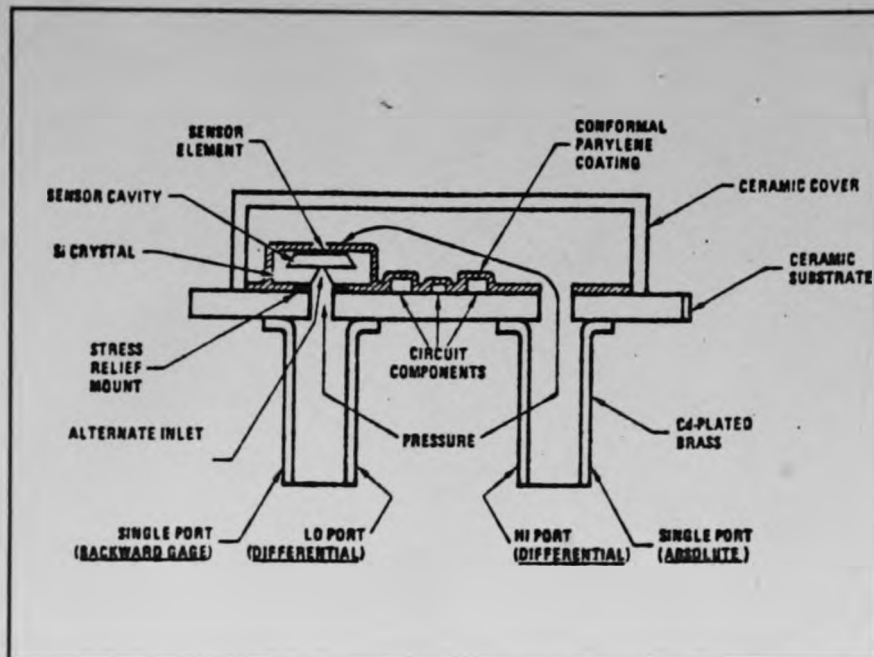


**Figure 2** Typical Semiconductor Strain Gage.[10]

### iii)Force Sensing Resistor

A FSR's terminal resistance responds to force in a piecewise linear power law fashion as shown in Figure 7. This is a result of compression of a conductive polymer against two interdigitated conductors. Figure 3 shows a picture of a typical force sensing resistor.[2]

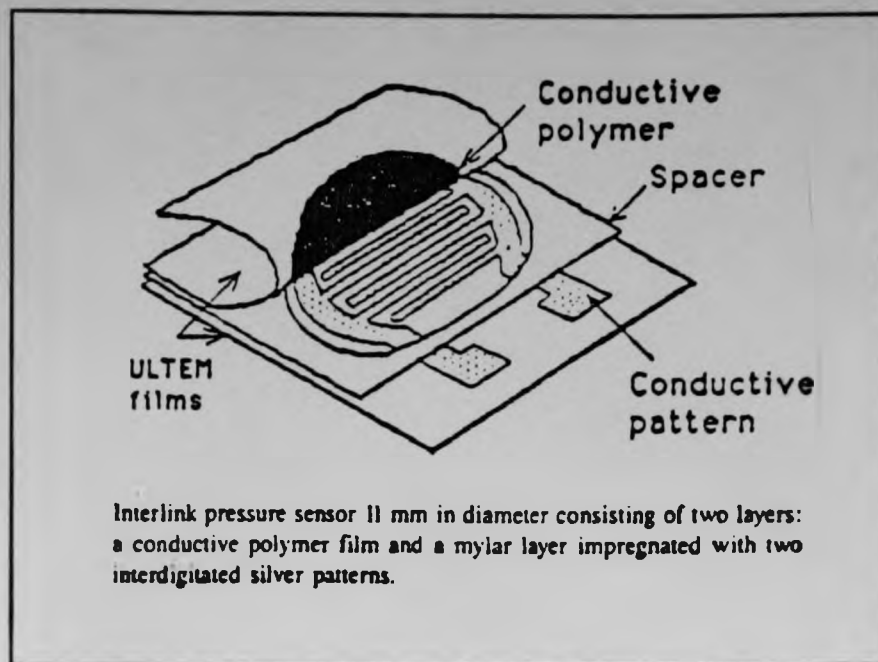


**Figure 3** Circular Force Sensing Resistor. [15]

#### b) Piezoelectric Types

Piezoelectric materials generate an electrical potential when mechanically strained. The electrical potential is a result of lattice distortion due to applied force causing a displacement of charge. The response of piezoelectric devices is inherently AC coupled. These devices are passive in nature and thus require no external excitation.

##### i) Polycrystalline Ceramics

Ceramics such as barium titanate and lead zirconate can be rendered piezoelectric by subjecting them to a strong electric field ( $1\text{E}6 \text{ V/m}$ ) for a given period of time. These passive transducers can produce for example  $140\text{pC/N}$  response. [19]

##### ii) Polymers

Polyvinylidene fluoride film (PVDF) is made piezoelectric by

extruding a sheet, then orienting material by stretching and poling by application of a high electric field. The main advantage of this material is it's flexibility and ability to form complex arrays and shapes.[16]

#### c)Capacitive Types

Capacitive force transducers rely on placing a compliant dielectric material between two plates which are to be subjected to the mechanical force. The response is inherently AC coupled if excitation is DC, but a DC coupled response can be obtained by AC excitation with phase sensitive detector readout circuitry. The material used as the dielectric must be compressible to allow for variation in plate spacing to achieve acceptable sensitivity.[13]

### 1.3 Transducer Types

The chart below provides a quick overview of the different force transducer types.

#### Strain Gage

Terminal Characteristics: Resistance shift with applied strain. Typical resistance is 100-350 Ohms with a total variation of 0.1% for full scale applied force.

Readout Circuitry: Requires high quality low level instrumentation amplifier and stable excitation source.

Accuracy: Better than 0.05% of full scale with suitable compensation.[18]

#### Semiconductor Strain Gage

Terminal Characteristics: Resistance shifts with applied

force. Typical resistance is 1000-4000 Ohms with a total variation of 1% for full scale applied force.

Readout Circuitry: Requires instrumentation amplifier, stable excitation source and temperature compensation is typically included.

Accuracy: Better than 0.5% of full scale possible.[18]

#### Force Sensing Resistor

Terminal Characteristics: Resistance varies in a piecewise linear power law fashion with applied force. Ranges from 1 MOhm to 2 kOhm.

Readout Circuitry: Simple buffer or transimpedance amplifier with low gain. For a linear readout, linearization is best performed digitally in software.

Accuracy: Better than 2% of full scale range possible.[3]

#### Piezoelectric Types

Terminal Characteristics: True charge output device providing AC coupled response up to 50kHz. Is equivalent to a variable capacitor in series with a voltage source.

Readout Circuitry: Charge amplifier with low bias current.[19]

Accuracy: Better than +/-3% of full scale.[14]

#### Capacitive Types

Terminal Characteristics: Capacitance shift with applied force. Capacitance increases inversely with decreasing plate spacing as applied force increases.

Readout Circuitry: Requires a fixed frequency excitation, transimpedance amplifier and phase sensitive detector for DC response. Alternatively a frequency output can be obtained by including sensor in a oscillator circuit.[20]

Accuracy: Better than +/-5% of full scale possible.[13]

## CHAPTER II

### BACKGROUND

#### 2.0 Review of Plantar Force Monitoring Techniques

There are many techniques for establishing plantar force. These techniques can be categorized as qualitative, and quantitative: single step stationary, insole and outside sole.

##### a)Qualitative Techniques

A qualitative measure of plantar force pattern and magnitude can be obtained by clinical observation of patients gait, observations of shoe wear pattern, location of calisites and foot print type studies. Foot print studies can be achieved with contour mats, inked paper and cinematography through glass.[11] These observations though not providing quantitative measures may be useful for determining sensor placement and establishing that the patient's gait is not affected by the quantitative plantar force measuring technique.

##### b)Stationary Sensors

Typically stationary sensors consist of a plate with an integrated array of force transducers. These transducers have been capacitive (NICOL Mat) or resistive (similar to force sensing resistor)[14]. A considerable number of disadvantages with these stationary types arise: 1) Only a limited number of steps can be monitored; 2) Requires exact placement of bare foot; and 3)The

restrictive highly clinical environment may affect patient's gait.[15]

#### c) Insole Sensors

A number of insole sensors have been developed based upon many different transducer types. Insole transducers have the following advantages: 1) They allow the patient to wear normal footwear; 2) The ability to monitor many steps; and 3) The potential for unrestricted portability. The main drawback is that positioning of sensors is critical and previous devices could not provide a high resolution of force distribution.[15]

#### d) Outside Sole Sensors

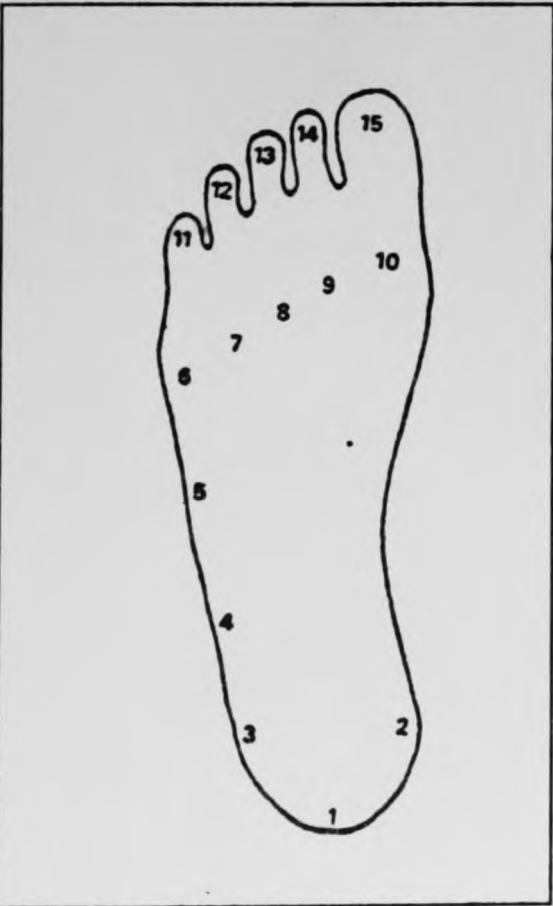
This technique, though allowing multiple steps to be monitored, requires the use of special foot gear over ordinary footwear or socked feet.

Most of the previously discussed sensor types described in Chapter I have been used for monitoring insole plantar forces. Resistive strain gages have been used but they require the development of a custom load cell, which are very expensive and require high quality readout electronics.[11] Piezoelectric ceramics have been imbedded into an insole to form an array of sensors but they are quite brittle, provide only AC response and require high quality charge amplifiers.[14] Capacitive sensors have been demonstrated but they exhibit considerable offset shift with use, are sensitive to stray pickup and require phase sensitive

detection techniques to provide a DC response.[13] The FSR shows significant promise in that these devices can be manufactured in an array of sensors in the shape of an insole which would be very thin, flexible and inexpensive, while not having any of the problems of the other sensor types mentioned previously.

2.1 Time Domain Characteristics of Plantar Force

To properly describe the distribution and timing of plantar force under the foot, Figure 4 below outlines the anatomy of the plantar foot surface.



- 1 Posterior Heel
- 2 Medial Heel
- 3 Lateral Heel
- 4 1/3 lateral heel to
- 5 2/3 5th metatarsal head
- 6 5th metatarsal head
- 7 4th metatarsal head
- 8 3rd metatarsal head
- 9 2nd metatarsal head
- 10 1st metatarsal head
- 11 5th toe
- 12 4th toe
- 13 3rd toe
- 14 2nd toe
- 15 1st toe

Figure 4 Foot Anatomy.[11]

For a typical individual under normal comfortable speed barefoot

walking conditions (1.5 meters/second), at most locations on the foot the force waveform shows a gradual increase to a peak followed by a relatively steep decline, as shown in Figure 5. The total foot plant time is approximately 500 msec. For the first 200 msec. of a foot fall all force is placed upon the heel. From 200 msec to 300 msec the force distribution shifts between heel and metatarsal heads. At 300 msec all force is applied to the metatarsal heads and 460 msec into a foot fall all force is applied to the first toe. The maximum force is in the range of  $8\text{kg}/\text{cm}^2$ . It is interesting to note that use of footwear results in significant redistribution of force, typically peak pressure on heel and metatarsal heads is reduced except for the first metatarsal head, while pressure on the toes is increased.[11,15]

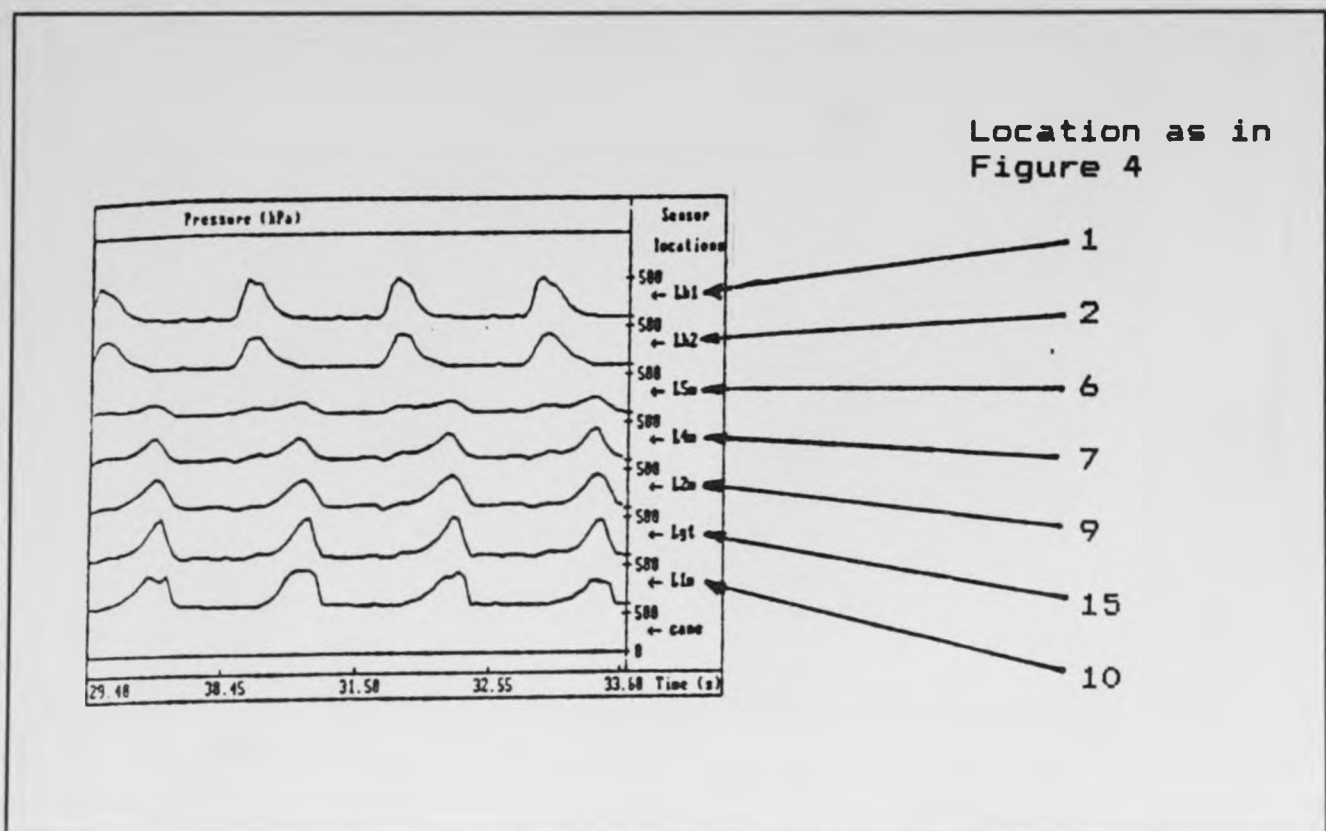


Figure 5 Typical Plantar Force Time Domain Waveforms.[15]

## 2.2 Ideal Characteristics of a Plantar Force Sensor

The ideal plantar force sensor would have the following qualities. A transducer allowing insole monitoring of plantar force would be the ideal configuration considering this would allow for continuous monitoring of plantar force in both clinical and everyday life situations (provided suitable portable readout and data storage electronics is available). To be located insole the transducer must be thin and flexible so that it can not be perceived by the patient and possibly modify the gait. Considering that force distribution under the foot will be different from patient to patient due to normal variations or pathological considerations, an array of sensors for each insole transducer in critical areas would be essential. The configuration of sensors should allow readout electronics to easily multiplex between sensors in critical regions ie. heel, metatarsal heads and toes.

The sensor must be able to withstand high peak forces without degradation, for example as a result of stepping on small objects such as stones on concrete surfaces. The insole transducer must have a undetectable change in dimensions due to applied force, ie. be incompressible. A sensor with this characteristic will likely be more durable and repeatable. The overall accuracy with respect to full scale should be about  $\pm 2\%$  suggesting that factors which can not be calibrated out such as repeatability and hysteresis must be less than this target. The other factors affecting accuracy should be relatively low drift to ensure infrequent calibration and that unsophisticated compensation techniques can be used. The

transducer should be relatively low cost, say less than \$200/insole.

## CHAPTER III

### IMPLEMENTATION OF THE SENSOR

#### 3.0 The Force Sensing Resistor

The force sensing resistor is manufactured by INTERLINK of Santa Barbara, California. This device's response is a piecewise linear power law function, between terminal resistance and applied force. It is available in standard single unit configurations in varying diameters and leadout configurations, costing a few dollars per unit in quantities of 10 or higher. These devices are also available in arrays of sensors in standard dimensions. The possibility exists to develop custom arrays configured as insoles for monitoring plantar force.

##### a)FSR Construction

The construction of a typical "Force Sensing Resistor" is shown in Figure 6 on the next page. It consist of two polymer sheets. On one sheet a set of 2 interdigitated electrodes are deposited with a electrode spacing and width of typically 0.4mm. The second sheet has a semiconductive film deposited on it. The sheets are bonded together.

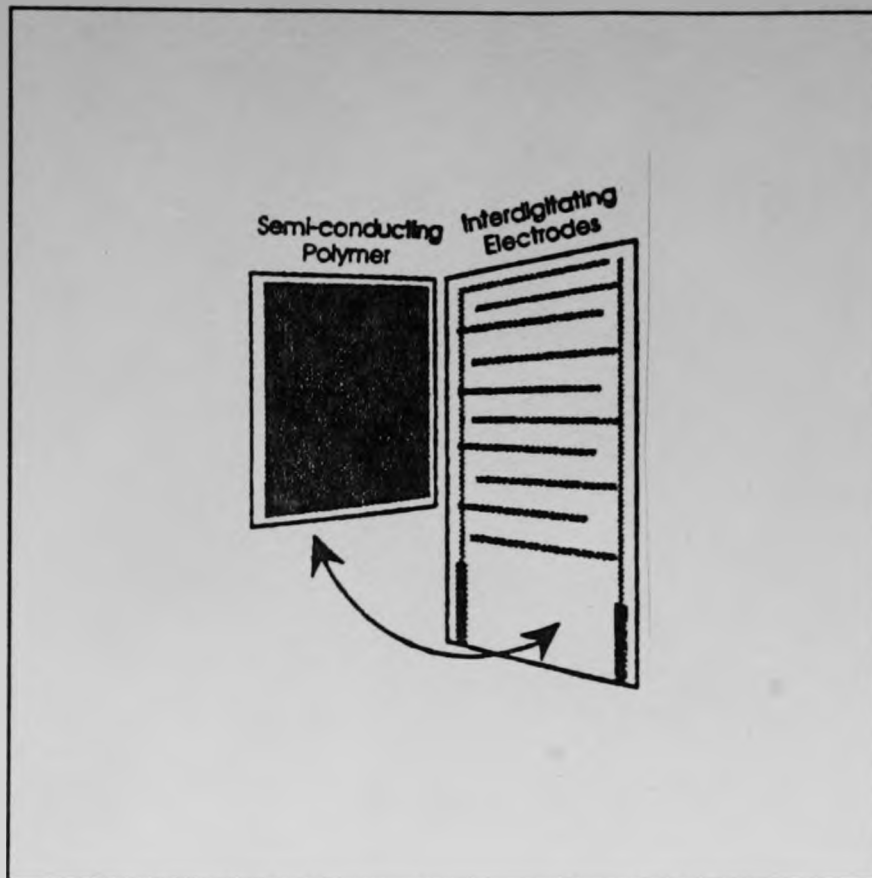


**Figure 6** FSR Construction.[2]

#### b)FSR Principle of Operation

An applied force on the FSR results in interdigitated electrodes being shunted by semiconductive film thus causing a decrease in resistance between electrodes. The FSR responds in a piecewise linear power law manner to force over 3 decades. The conductor design has the most impact on device response, basically the finer the electrode pitch the wider the dynamic range over which the device will respond.

c)FSR Characteristics

The FSR force versus resistance response for a typical device (#302) is shown in Figure 7.

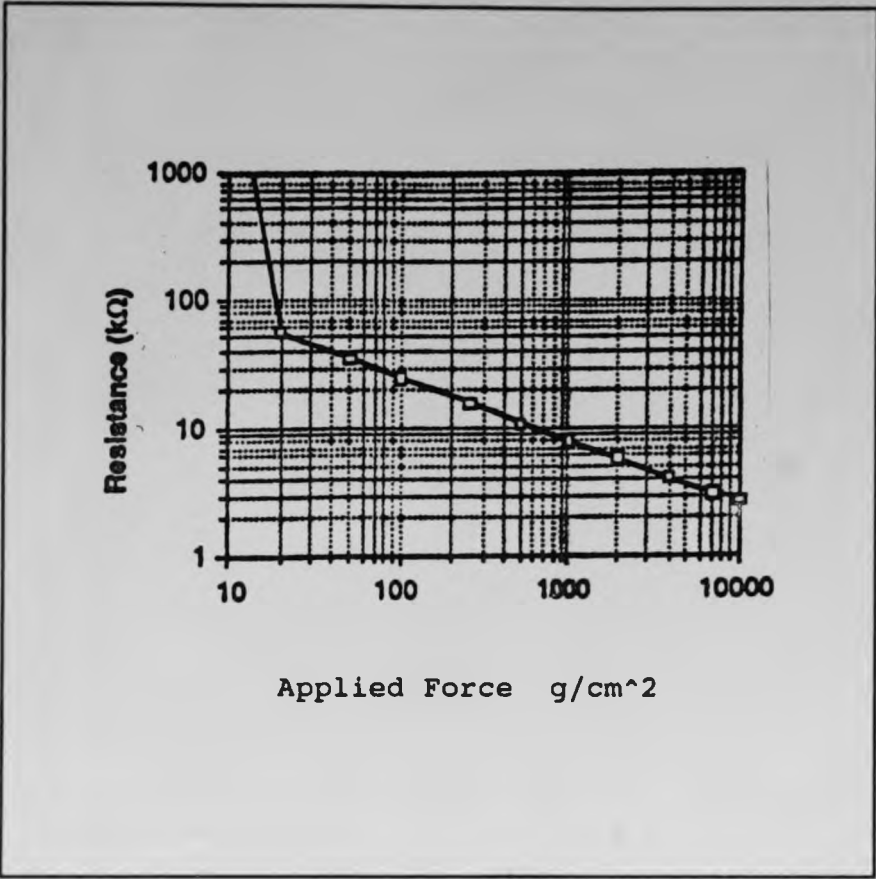


Figure 7 FSR Response.[3]

In general the FSR response follows a piecewise power law characteristic. A clear threshold exists where for low forces, in this case up to 20 g/cm<sup>2</sup>, the FSR resistance ranges from 1 MOhm to approximately 58 kOhm. For forces greater than 20 g/cm<sup>2</sup> and up to 10 kg/cm<sup>2</sup> the resistance ranges from 58 kOhm to 2.7 kOhm approximately. Above 10 kg/cm<sup>2</sup> but not shown the FSR exhibits no further appreciable reduction in resistance for increasing applied force.

The following describes the most important features of the FSR device

- 1) Unlike conventional load cells the FSR's resistance changes by up to 3 decades for a 3 decade range of applied force resulting in extremely high sensitivity , although nonlinear in nature.
- 2) Cycle to cycle repeatability is quite good  $\pm 2\%$  of full scale applied force range. This implies that with proper calibration  $\pm 2\%$  accuracy can be achieved for plantar force measurements.
- 3) The FSR devices are very thin, thickness ranging from 0.1 to 1mm, making them appropriate for incorporating into an insole insert.
- 4) The device is zero travel in nature, leading to exceptionally long term stability ( $\pm 5\%$  for 1,000,000 actuations), and suggesting long intervals between calibrations are possible.
- 5) The FSR's response is directly coupled in nature allowing for static force measurement , unlike piezoelectric devices which can only respond to dynamic forces. Also, unlike piezoelectric devices, they are relatively insensitive to acceleration, acoustic noise and temperature variation.
- 6) The FSR device has a relatively slow response. A typical rise time however corresponds to a minimum bandwidth of 175 Hz, which is more than acceptable for the walking rate of applied plantar forces.
- 7) The FSR's response is proportional to the reciprocal square root area of force applied to the device. This will necessitate arranging force applications to result in a even distribution over the entire device. This is best accommodated by making the sensors smaller than the contact areas for which the force is being measured.

A general FSR technical specification is shown on the following pages.[1,2,3,4]

## FSR™ Technical Specifications

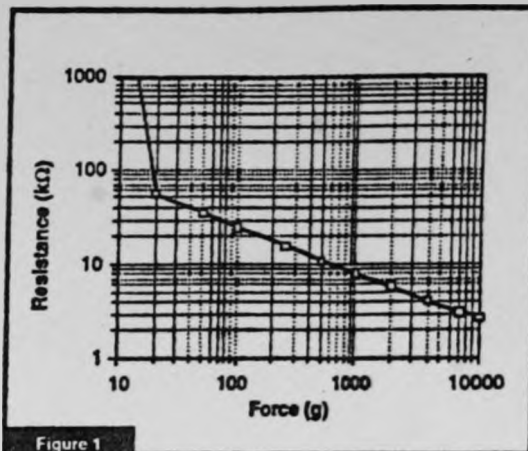
The Force Sensing Resistor™ is a polymer thick film (PTF) device which exhibits a decrease in resistance with any increase in force applied to the active surface. Its force sensitivity is

optimized for use in human touch control of electronic devices. The FSR is not a load cell or strain gauge, though it has similar properties. The FSR is not suited for precision measurement.

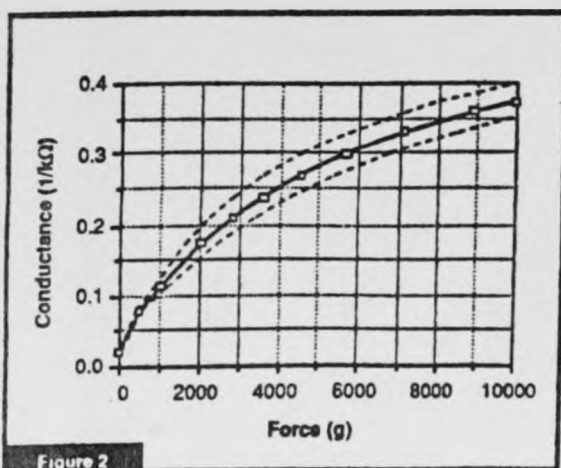
### Force vs. Resistance

The FSR force vs. resistance characteristic shown in Figure 1 provides an overview of the FSR's typical response behavior. For interpretational convenience, the force vs. resistance data are plotted on a log/log format. These data are representative of our typical devices, with this particular force-resistance characteristic being the response of standard part # 302 (1.27 cm diameter circular active area). A 0.56 cm diameter flat stainless steel probe was used to actuate the FSR, and a 0.6 mm thick silicone rubber overlay of 50 durometer was placed on the FSR to even out the force distribution. In general, the FSR's response approximately follows a power-law characteristic.

Referring to Figure 1, at the low force end of the force-resistance characteristic, a switch-like response is evident. This threshold, or "break force", that swings the resistance from greater than 1 MΩ to about 50-100 kΩ (the beginning of the dynamic range that follows a power-law) is determined by the substrate material, overlay thickness and flexibility, and spacer-adhesive thickness (the gap between the conductive elements). Break force increases with increasing substrate and



overlay rigidity, and spacer-adhesive thickness. At the high force end of the dynamic range, the response deviates from the power-law behavior, and eventually saturates to a point where increases in force yield little or no decrease in resistance.



### Force vs. Conductance (or Force vs. Voltage)

In Figure 2, the force is plotted vs. conductance (the inverse of resistance). This format allows interpretation on a linear scale. A simple circuit called a current-to-voltage converter (see TechNotes, Suggested Interfaces, page 1-7) gives a voltage output directly proportional to FSR conductance and can be useful where response linearity is desired. Figure 2 also includes a typical part-to-part repeatability envelope. This error band determines the accuracy of any force measurement. The spread, or width of the band, is strongly dependant on the repeatability of any actuating and measuring system, as well as the manufacturing tolerance held by Interlink during FSR production. Typically, this part-to-part manufacturing tolerance ranges from  $\pm 15\%$  to  $\pm 25\%$  of an established nominal resistance.

## FSR™ Technical Specifications

These are typical parameters. FSRs are custom devices and can be made for use outside these specifications. Consult Applications Engineering with your specific requirements.

Simple FSRs and Arrays		
Parameter	Value	Conditions
Size Range	Max = 20" x 30" (51 x 76 cm) Min = 0.2" x 0.2" (0.5 x 0.5 cm)	Any shape
Device Thickness	0.008" to 0.050" (0.20 to 1.25 mm)	
Force Sensitivity Range	30g to 10kg	
Pressure Sensitivity Range	0.45 to 150 psi (0.03kg/cm <sup>2</sup> to 10kg/cm <sup>2</sup> )	30g to 10kg 1 cm <sup>2</sup> actuator
Part-to-Part Force Repeatability	± 15% full scale	For typical part with consistent actuation
Single Part Force Repeatability	± 2% full scale	
Force Resolution	Better than 0.5% full scale	
Break Force	30 to 100g (1 to 3.5 oz) typical	Dependent on probe size, shape, & sensor construction
Stand-Off Resistance	> 1 MΩ	
Switch Characteristic	Essentially zero travel	
Device Rise Time	1-2 msec (mechanical)	
Lifetime	> 10 million actuations	
Use Temperature	-30°C to +170°C	High temperature adhesives
Maximum Current	1 mA/cm <sup>2</sup> of applied force	
Sensitivity to Noise/Vibration	Not significantly affected	
EMI/ESD	Passive device—not damaged by EMI or ESD	
Lead Attachment	Standard flex circuit techniques	See TechNotes
For Linear Pots and XYZ Pads		
Parameter	Value	Conditions
Positional Resolution	0.003" (0.075 mm) typical	1 cm wide actuator
Positional Accuracy	< ± 1% full scale	

[ 3 ]

### 3.1 PSPICE Macromodel of FSR

An electrical equivalent macromodel of the FSR including analog behavioural models is shown in Figure 8 below.[5] It represents a macromodel for the FSR with characteristics as shown in Figure 7, for a range of force from 20 g/cm<sup>2</sup> to 10 kg/cm<sup>2</sup>.

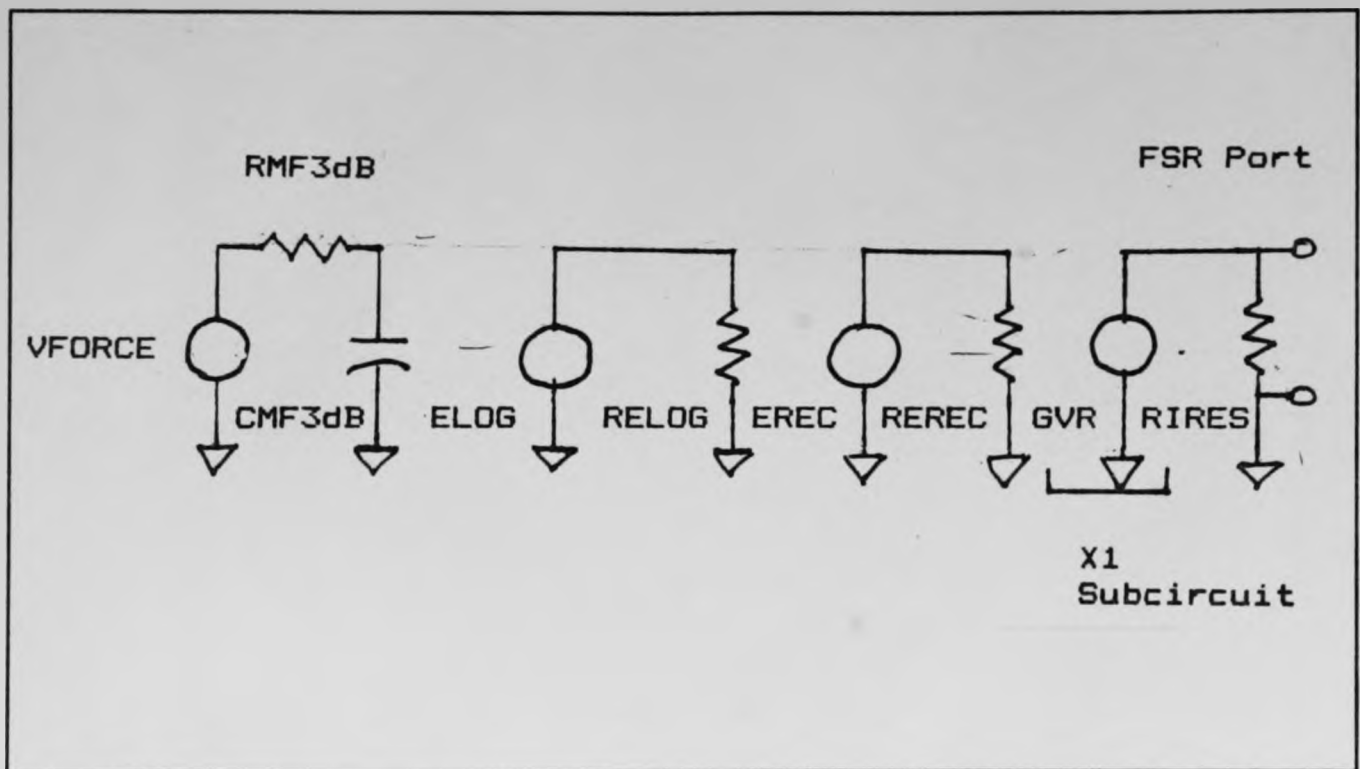


Figure 8 FSR Macromodel

Nomenclature for figure 8.

VFORCE- is a equivalent voltage input representing applied force as a function of time.

RMF3db & CMF3db- is a RC lowpass filter representing the mechanical time constant of the FSR.

ELOG- is a behavioural model providing a logarithmic response between equivalent input force voltage and corresponding output voltage to drive remainder of macromodel's voltage controlled

resistance. Note that the macromodel response is valid for forces above the break point ( $20 \text{ g/cm}^2$ ) and below saturation ( $10 \text{ kg/cm}^2$ ) only.

EREC- is a behavioural model providing an inversion of input voltage from the previous stage. This inversion is needed since the following stage provides a equivalent resistance inversely proportional to the applied voltage.

GVR- is a voltage controlled current source which provides a voltage controlled resistance at its terminals, inversely proportional to the reciprocal of the applied voltage EREC. Upper resistance limit is set by RIRES.[21]

The PSPICE file for this behavioural model is shown below.

#### **PSPICE File for FSR Behaviourial Model.**

```
***VARIABLE RESISTOR MACROMODEL MODEL
VFORCE 5A 0 PWL(***)
RMF3db 5A 5 1K
CMF3db 5 0 455NF
ELOG 4 0 VALUE = {PWR(10,-0.49465*LOG10(V(5))+3.9260)}
RELOG 4 0 1E3
EREC 3 0 VALUE = {(1V/(V(4)))}
REREC 3 0 1E3
RIRES 1 2 1E10
X1 1 2 3 VARISTR
.SUBCKT VARISTR 1 2 3
GVR 1 2 POLY(2) 1 2 3 0 0 0 0 0 1
```

.ENDS

\*\*\*\*\*

The response of the FSR macromodel is shown in Figure 9 on the following page. It compares favourably with the manufactures data Figure 7.

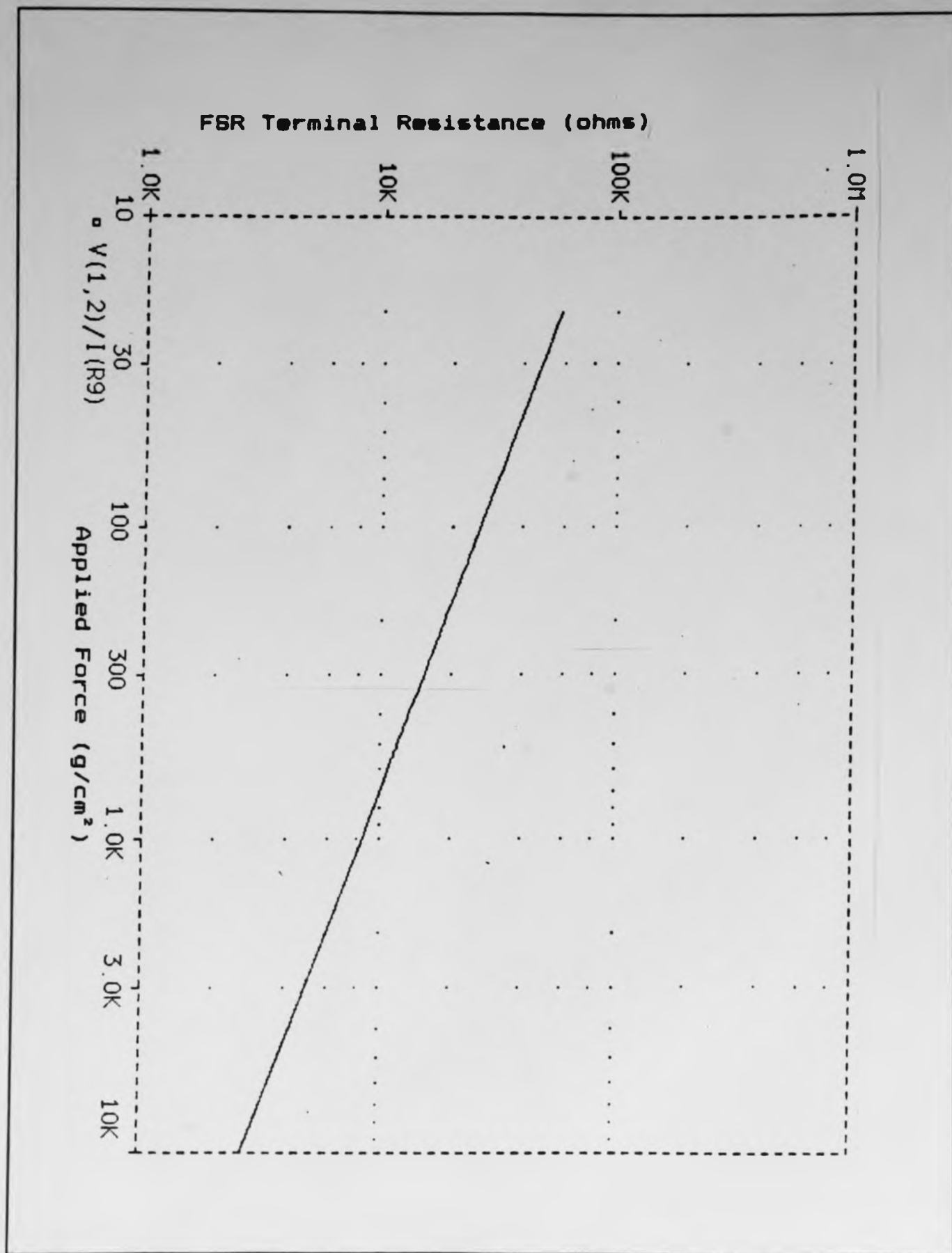


Figure 9 FSR Macromodel Response

### 3.2 Readout Circuitry for Evaluation of Force Sensing Resistor

#### a) Schematic Diagram of Readout Circuitry for FSR

The readout circuitry for FSR is described schematically in Figure 10 below.

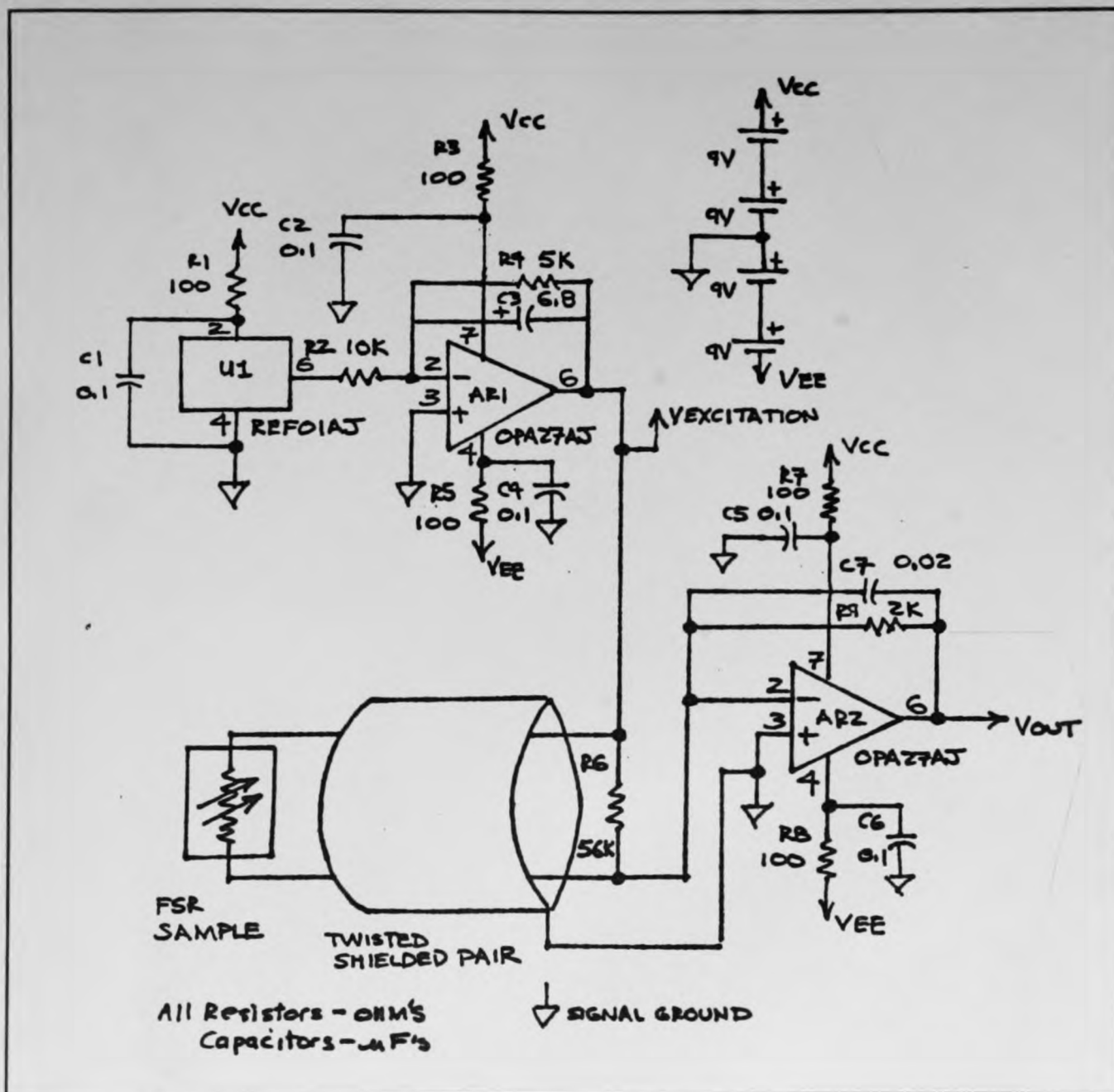


Figure 10 Schematic Diagram Readout Circuitry for FSR

A detailed parts list is shown below.

**Parts List: Readout Circuitry for FSR (Electronic)**

Designation	Part Number	Manufacture	Description	Quantity
U1	REF01AJ	PMI	Precision Reference	1
AR1,AR2	OPA27AJ	Burr-Brown	Opamp Low Noise	2
R1,3,5,7,8	MRS25F100	Phillips	100ohm,1% 1/4W,Metal	5
R2	RN55C1002F	Dale	10Kohm,1% 1/8W,Metal	1
R4	RN55C5001F	Dale	5Kohm,1% 1/8W,Metal	1
R6	RN55C5622F	Dale	56.2Kohm,1% 1/8W,Metal	1
R9	MRS25F2K	Phillips	2Kohm,1% 1/8W,Metal	1
C1,2,4,6	CK05BX1105K	Centerlab	0.1uF,10% 100V,Ceramic	5
C3			6.8uF,10% 35V,Tantalum	1
C7(4X)			4.7nF,2% 100V,Polystyrene	4

**Parts List (cont'd): Readout Circuitry for FSR (Hardware)**

Description	Manufacture	Quantity
3719-5 Prototype Board	Vector	1, trimmed
Twisted Shielded Pair	M27500-22-RC-2506	1 meter
Alligator Clips		4
9V Battery Clips	Radio Shack	4
9V Battery	Signalman	4
22 AWG Wire Insulated		as required

## b) Technical Description of Readout Circuitry

The readout circuitry for the FSR, consists of a transimpedance amplifier formed by AR2 and a precision -5V bias source formed by U1 and AR1. The current flowing through the parallel combination of the FSR device and set resistor R6 is converted to a voltage by the transimpedance amplifier with a gain of 2000 V/A as set by R9. The value of set resistor R6 is chosen near the break point terminal resistance of the FSR device which is approximately 58 kOhm for a applied force of 20 g/cm<sup>2</sup>. This sets the lower limit of measurable force to 20 g/cm<sup>2</sup> which, considering that a tightly laced shoe will apply force greater than this to the foot, leads to no loss of information. This provides a relatively well defined set point for forces < 20 g/cm<sup>2</sup>, of approximately 0.35V. The value of feedback resistor R9 has been chosen to provide a full scale output of approximately 3.9V for a applied force of 10 kg/cm<sup>2</sup>. This signal swing range is compatible with a low voltage/power design based upon +/-5V power rails. The value of feedback capacitance C7 has been chosen to limit electrical bandwidth to 10 times the mechanical bandwidth of the FSR, approximately 4.0 kHz. This bandwidth allows for proper evaluation of the time domain response of the FSR, while limiting noise bandwidth to allow for proper resolution. The low value of R9 in this case minimizes the impact on the closed loop response of the transimpedance amplifier to stray and cable capacitance at it's inverting terminal. The cable shield is connected to the readout circuit ground reference which minimizes coupling of

interfering signals. The precision stable excitation source for the FSR device is provided by voltage reference U1 and the inverting amplifier/ first order lowpass filter formed by AR1. The filter limits noise equivalent bandwidth to 7.4Hz to reduce the excess noise associated with the voltage reference.

#### c) Simulation of Readout Circuitry For FSR

A complete simulation of readout circuitry interfaced to the previously developed macromodel for the FSR has been performed. The PSPICE circuit file listing is contained in Appendix 1.

The results of a complete DC, AC , transient and noise analysis are discussed in the following pages.

##### i)DC Analysis

Figure 11 shows the overall highly nonlinear response of the FSR/readout circuitry combined for forces ranging from 20 g/cm<sup>2</sup> to 10 kg/cm<sup>2</sup>. The response sensitivity ranges from 4 V/(kg/cm<sup>2</sup>) to 0.2 V/(kg/cm<sup>2</sup>) as shown in Figure 12, which is high. The log-log plot's linear characteristic shown in Figure 13 highlights the power law response of FSR/Readout circuitry.

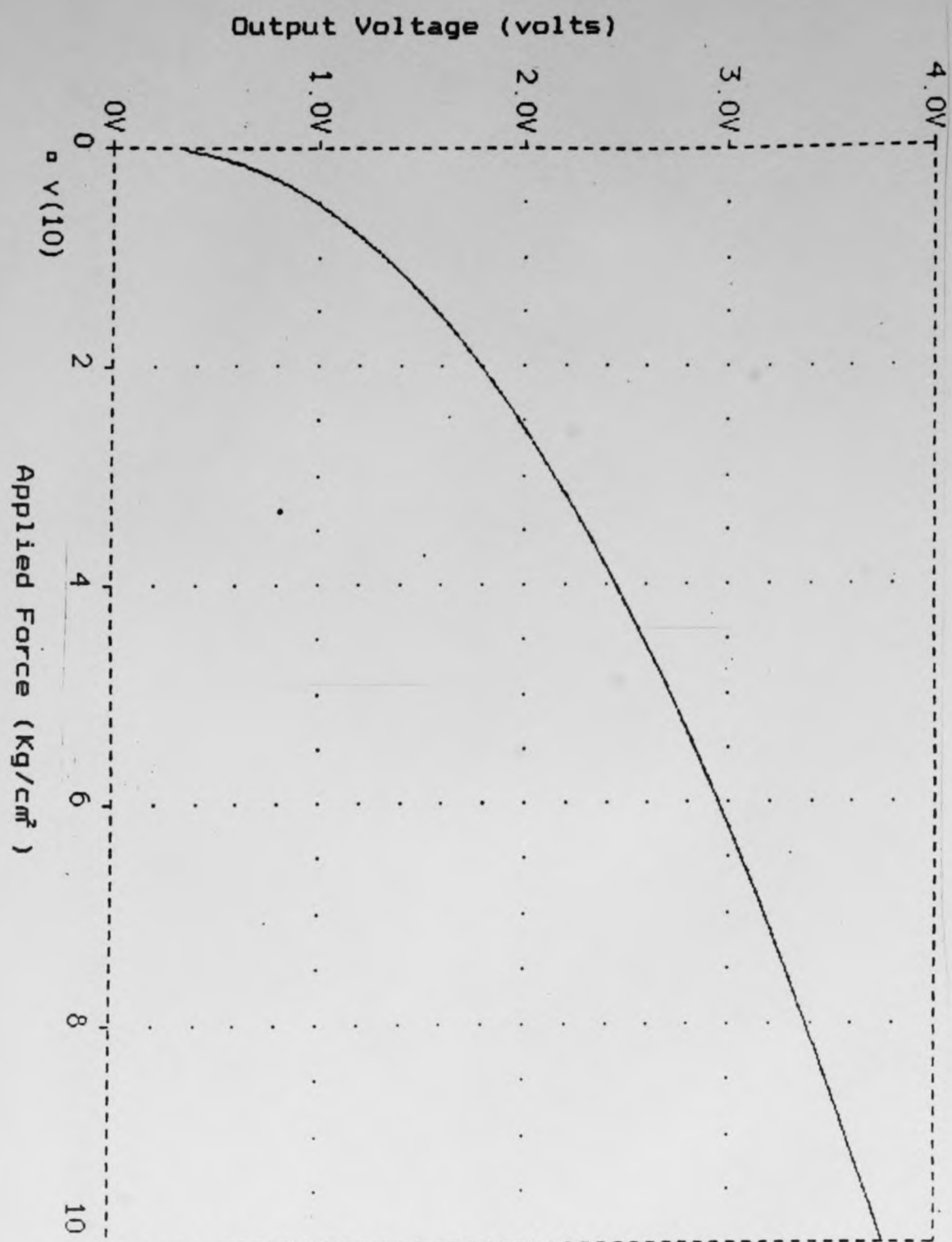


Figure 11 DC Transfer Characteristic of FSR/Readout Circuitry.

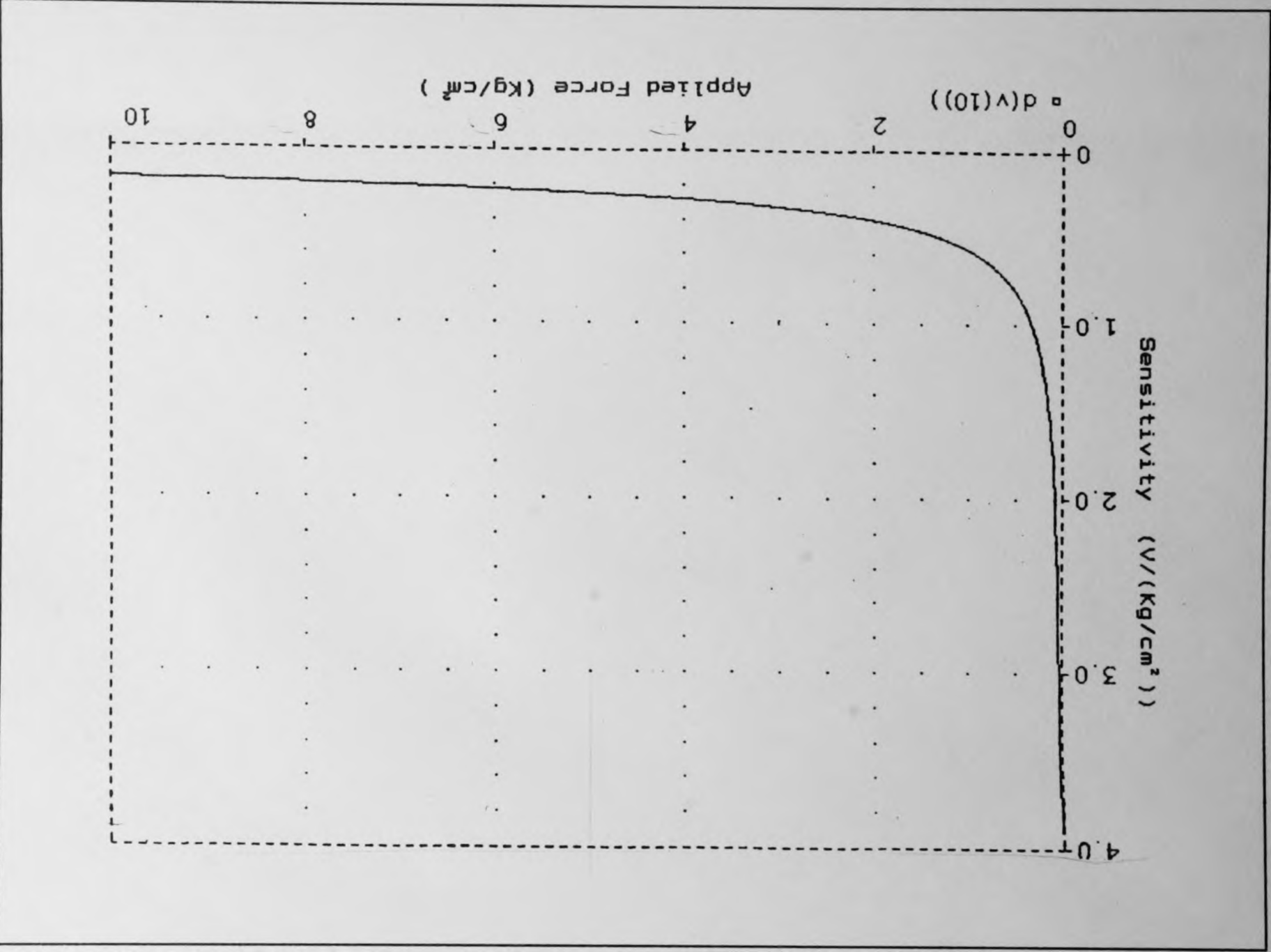


Figure 12 Sensitivity Analysis of FSR Response.

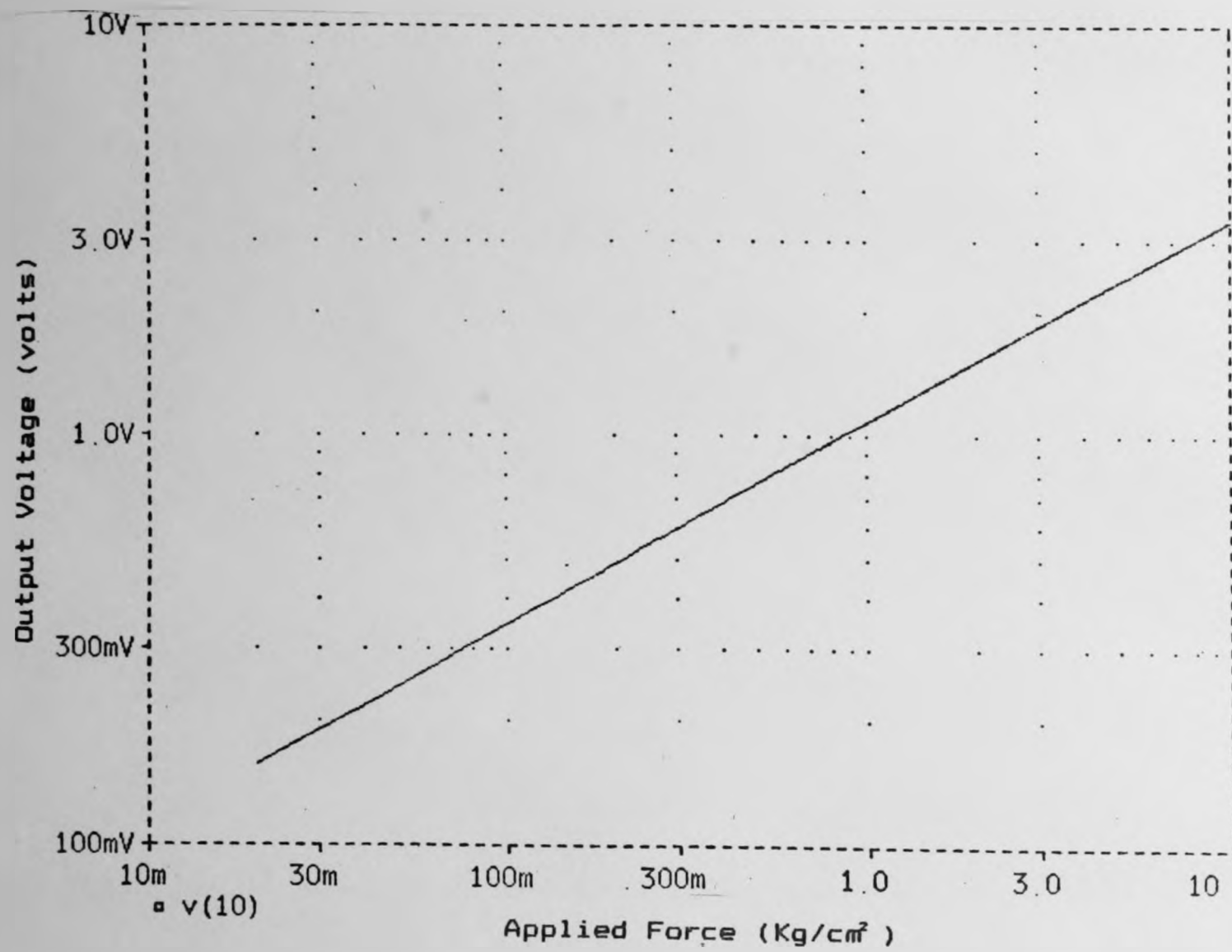


Figure 13 LOG-LOG Plot of FSR/Readout Circuitry Response.

## ii) AC Analysis

An AC analysis was performed at minimum ( $20 \text{ g/cm}^2$ ) and maximum ( $10 \text{ kg/cm}^2$ ) applied force and is shown in Figures 14 and 15, respectively. The overall frequency response is second order in nature and exhibits no peaking, suggesting that gain and phase margin are adequate. The 3dB bandwidth exceeds 316Hz.

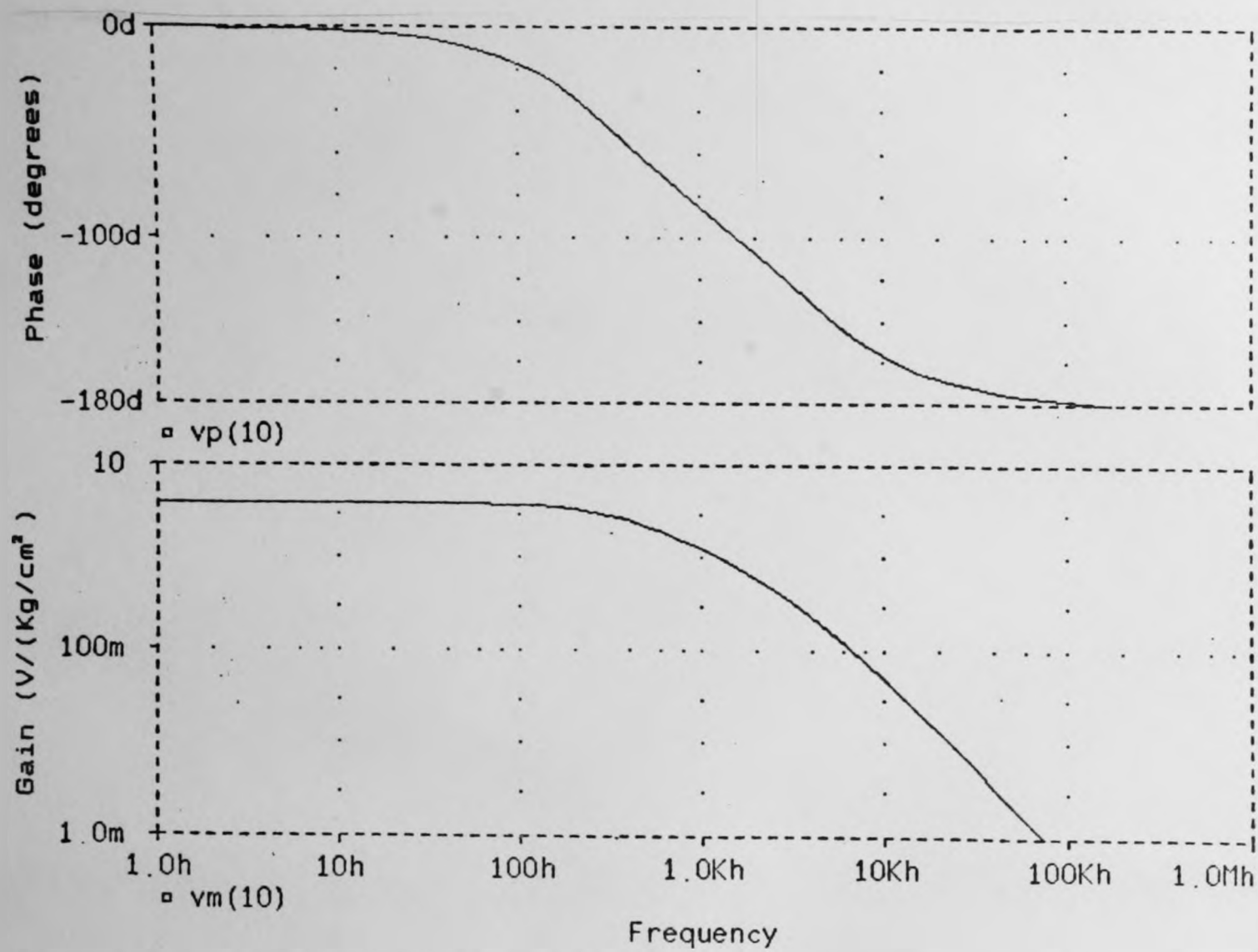


Figure 14 AC Response for a 20g/cm<sup>2</sup> Applied Force

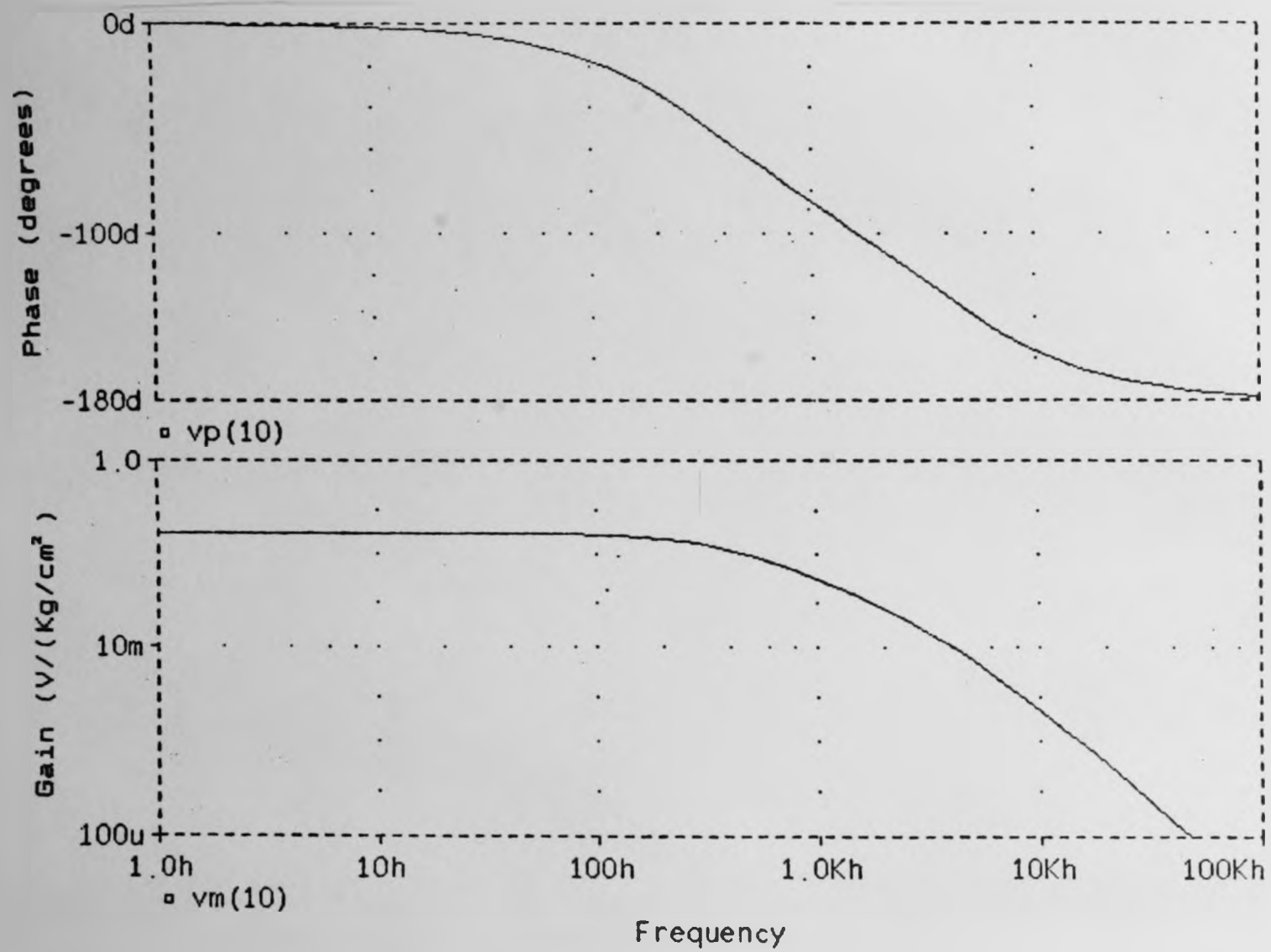


Figure 15 AC Response for 10kg/cm<sup>2</sup> Applied Force

### iii) Transient Analysis

A full scale pulse force ( $10 \text{ kg/cm}^2$ ) with duration of 500 msec was applied to the FSR macromodel. Figure 16 shows a clean damped response with no overshoot. The rise time as shown in Figure 17 is less than 762 usec.

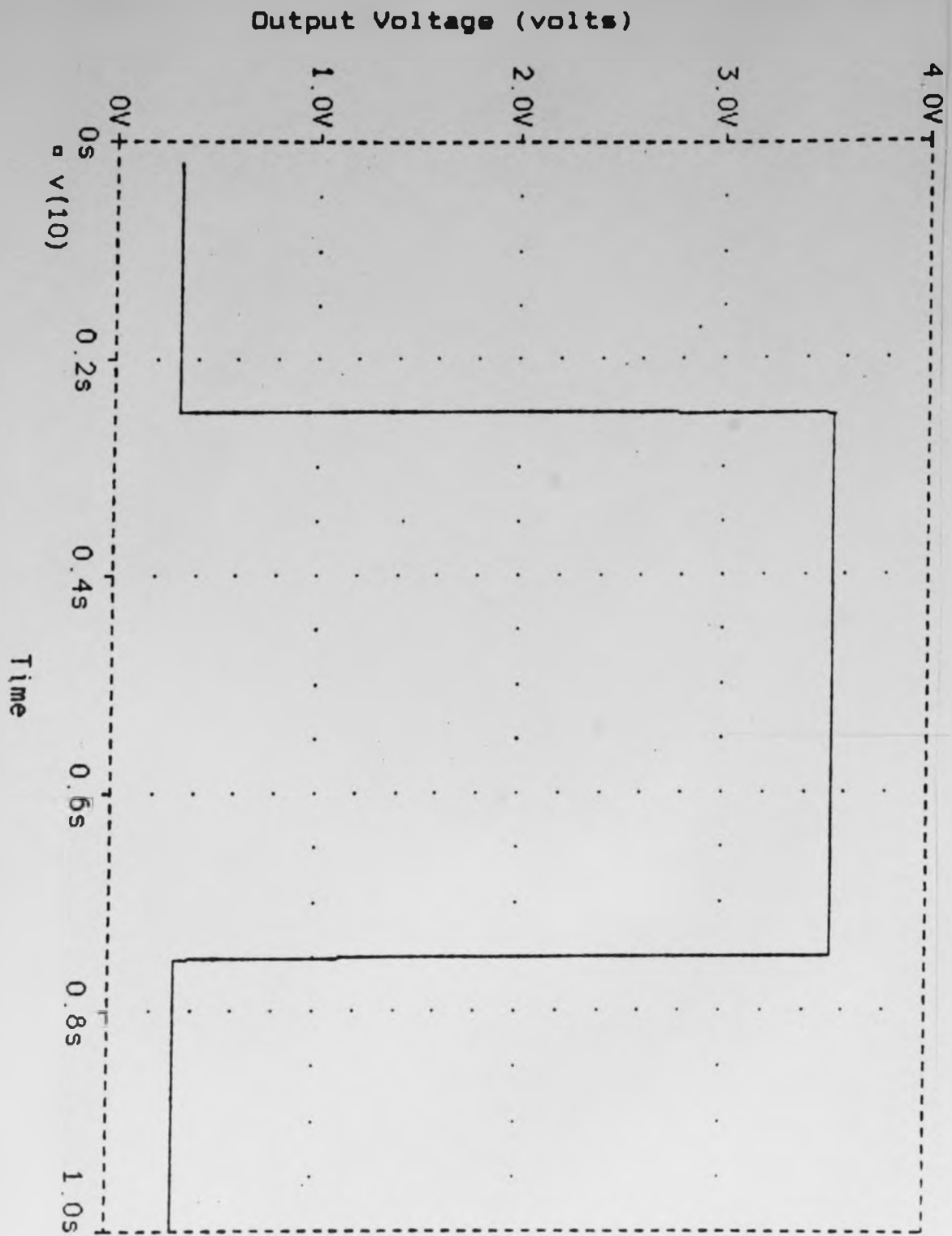


Figure 16 Pulse Response FSR/Readout Circuitry

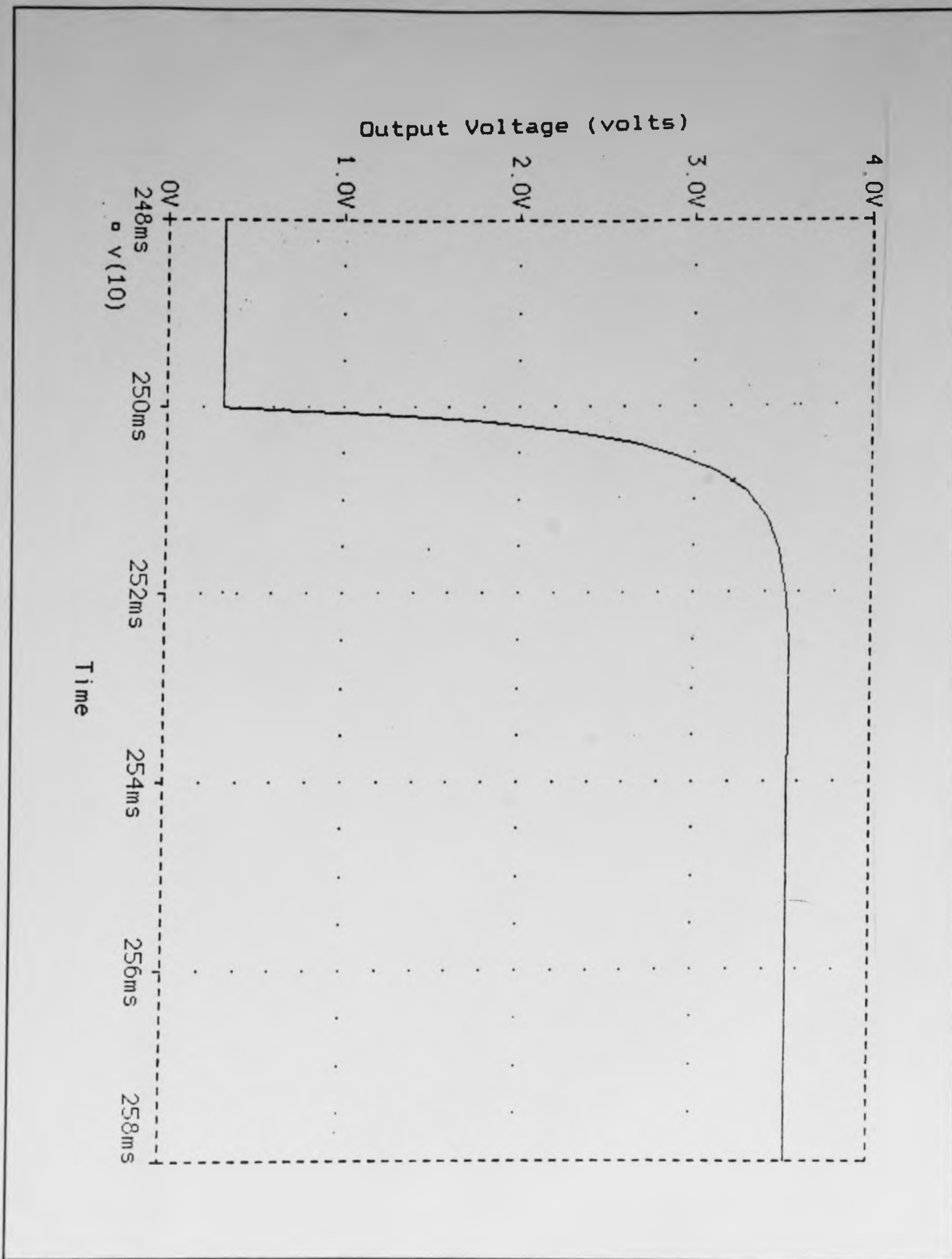


Figure 17 Rise Time FSR/Readout Circuitry

#### iv) Noise Analysis

The noise analysis was performed for both maximum and minimum applied force conditions as shown in Figures 18 and 19, respectively. The total output noise was less than 1.8  $\mu\text{V}_{\text{rms}}$  in both cases which is much less than 1 bit in 12 of a 3.5V range and is more than acceptable.

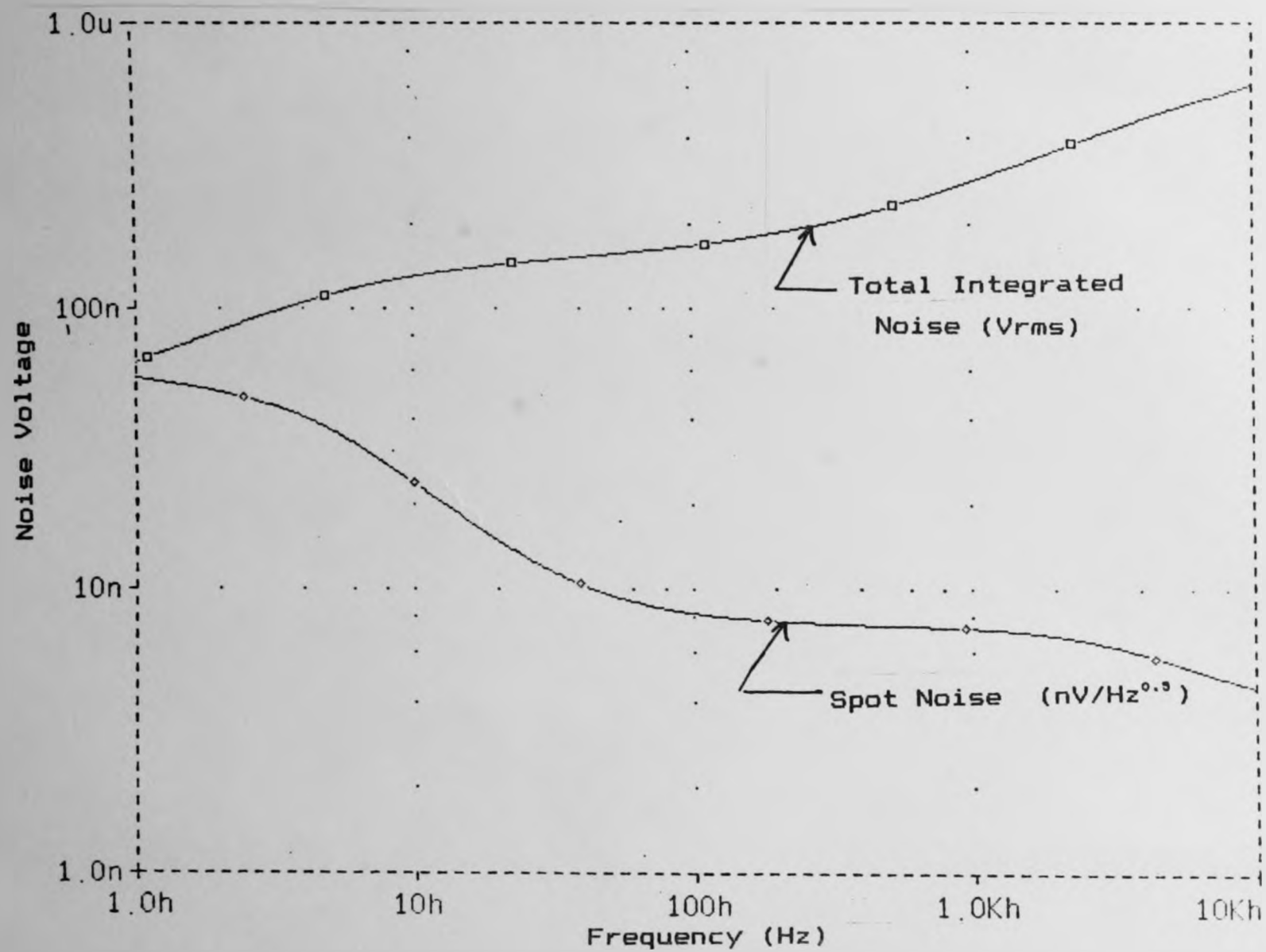


Figure 18 Total Output Noise for 20g/cm<sup>2</sup> Applied Force

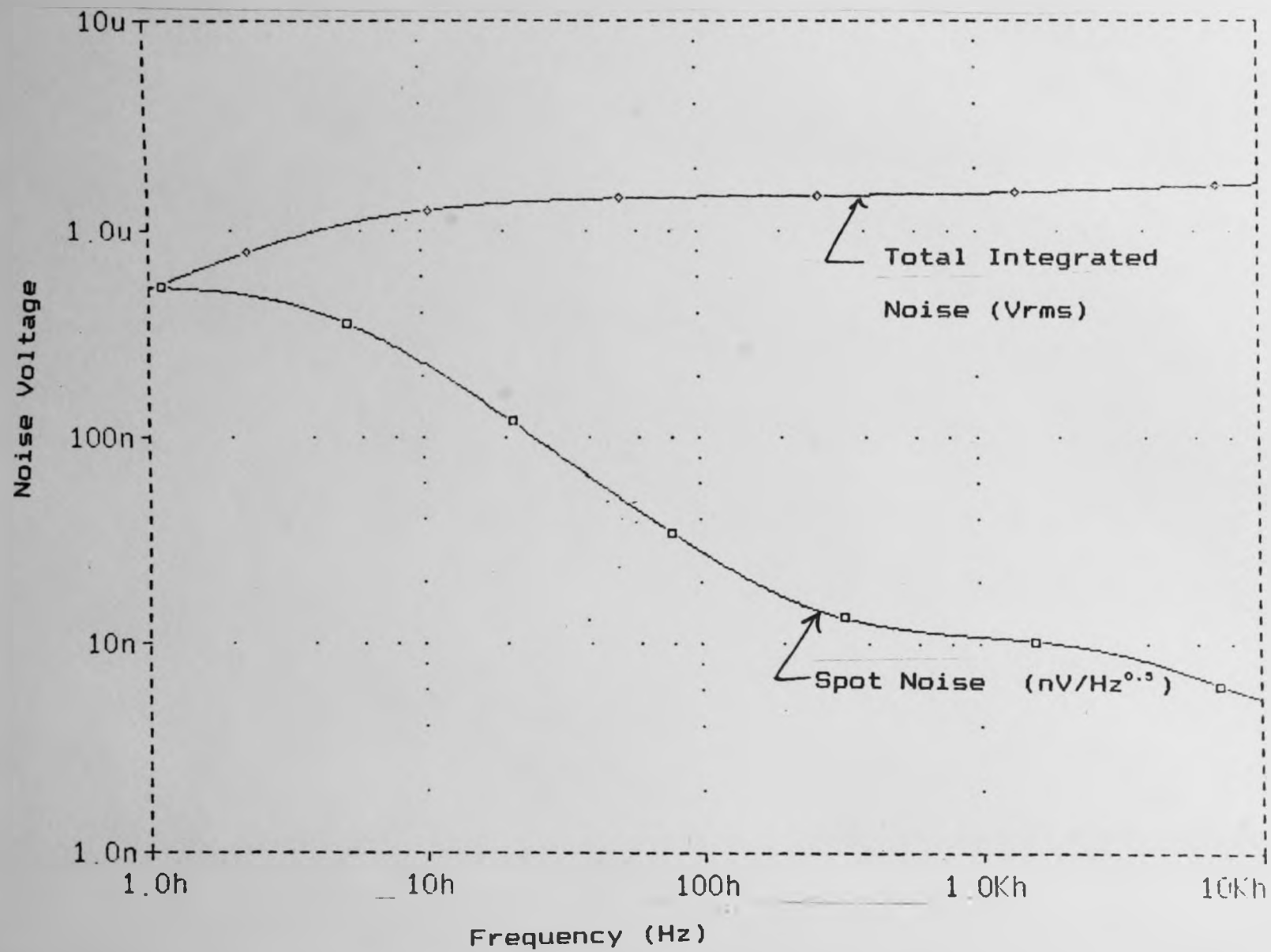


Figure 19 Total Output Noise for 10kg/cm<sup>2</sup> Applied Force

#### d) Evaluation of Force Sensing Resistor/Readout Circuitry

The Force Sensing Resistor/Readout Circuitry was evaluated by performing three separate tests to establish DC transfer characteristic, transient response and noise performance.

The DC transfer characteristic was evaluated by applying a calibrated uniform force over the entire sample FSR device with a custom aluminum test head of  $1.7 \times 1.7 \text{ cm}^2$  area, from  $47 \text{ g/cm}^2$  to  $9.397 \text{ kg/cm}^2$ , using an Instron Model 4206. A digital voltmeter was used to monitor the output voltage of the readout circuitry. First, the no load readout circuit voltage was observed to be  $0.1780 \text{ V}$ . Then the preload output voltage due to test head mass was observed to be  $0.1789 \text{ V}$ . The preload delta readout voltage of  $900 \text{ uV}$  is insignificant for the purposes of this test. A calibrated force was applied in a cyclic manner three times, to establish the transfer characteristic over the specified force per unit area range. The results (also see Appendix 3) are shown in Figure 20 on the following page.

It can be concluded that the FSR exhibits an approximate power law response. The response can be approximated by equation 1 below.

$$\text{Eq. 1 } R_{\text{fsr}}(F) = 10^{(-0.71454 * \log(F) + 3.79734)}$$

where  $R_{\text{fsr}}$  - is the FSR's terminal resistance (ohms)

$F$  - is applied force ( $\text{Kg/cm}^2$ )

This equation is different than the one used for the macromodel in simulations, since this is a different device. Full analysis of the test data is contained in Appendix 4. The observed maximum hysteresis and repeatability error were determined to be

$\pm 6.072\%$  and  $\pm 3.445\%$  of full scale range respectively. The repeatability error is approximately 50% higher than specified by the manufacture. The manufacturer did not specify hysteresis.

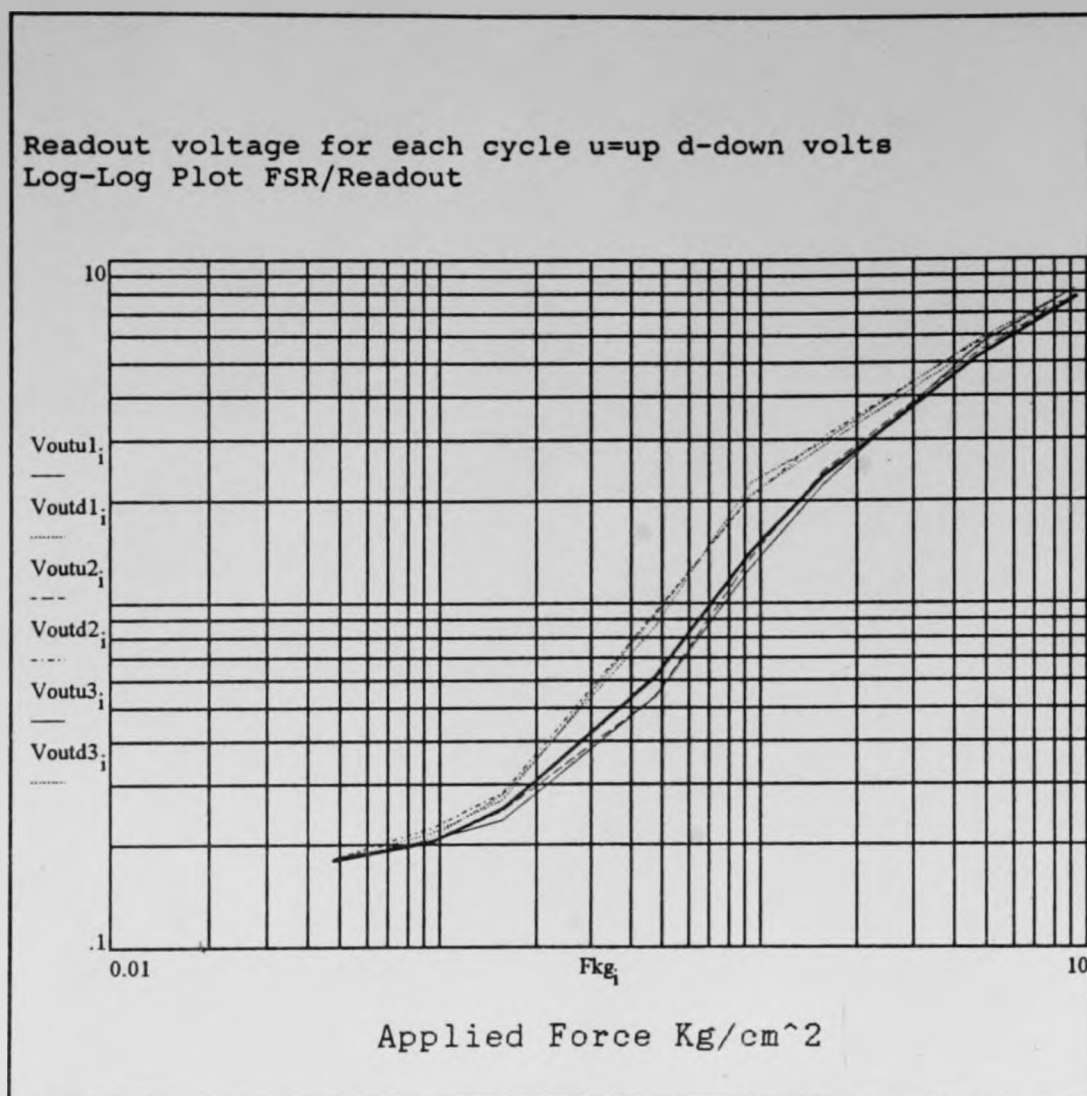


**Figure 20** DC Transfer Characteristic, 3 Cycles

The transient response was measured by hitting the custom aluminum test head, while it completely covers the FSR device, with a rubber mallet and monitoring the output voltage of the readout circuitry on a storage oscilloscope. The test results are shown in Figure 21 below. (Poor quality of photo has required retracing it.)

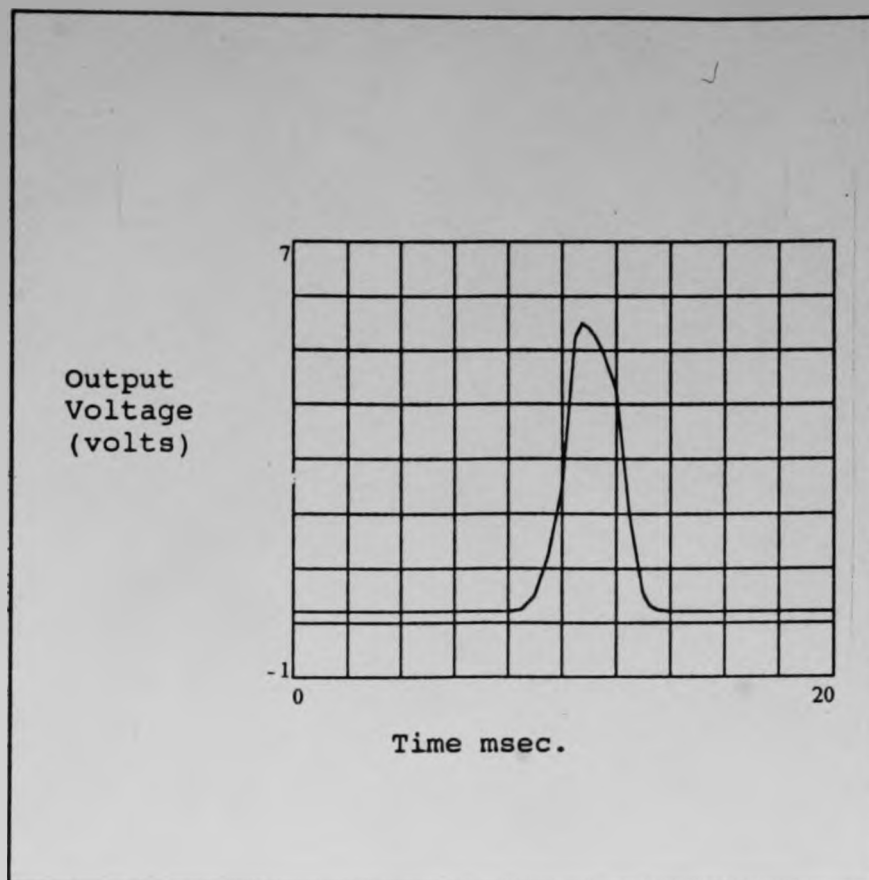


**Figure 21** FSR Transient Response

From these results it can be determined that the rise time is 1msec.

The no load output noise of the FSR/Readout circuitry was measured using an HP3562A dynamic signal analyzer. The results are shown in Figure 22 on the following page. Total output noise was measured to be 3.2  $\mu\text{V}_{\text{rms}}$  in a 1-10 kHz bandwidth. The measured value is approximately 6X higher than the no load simulation results. It was anticipated that the FSR would exhibit excess  $1/f$  noise, which it did when compared with the predicted noise performance assuming the FSR exhibited thermal noise only, as shown in Table 1. However it is not significant enough to effect measurement accuracy, since for a 3.5 V range 12 bits of resolution

is 835 uV and the peak to peak wideband output noise was measured to be less than 50 uV, as shown in Figure 23 on the following page. This is more than acceptable to achieve better than 0.1% resolution of a 10 kg/cm<sup>2</sup> full scale force.

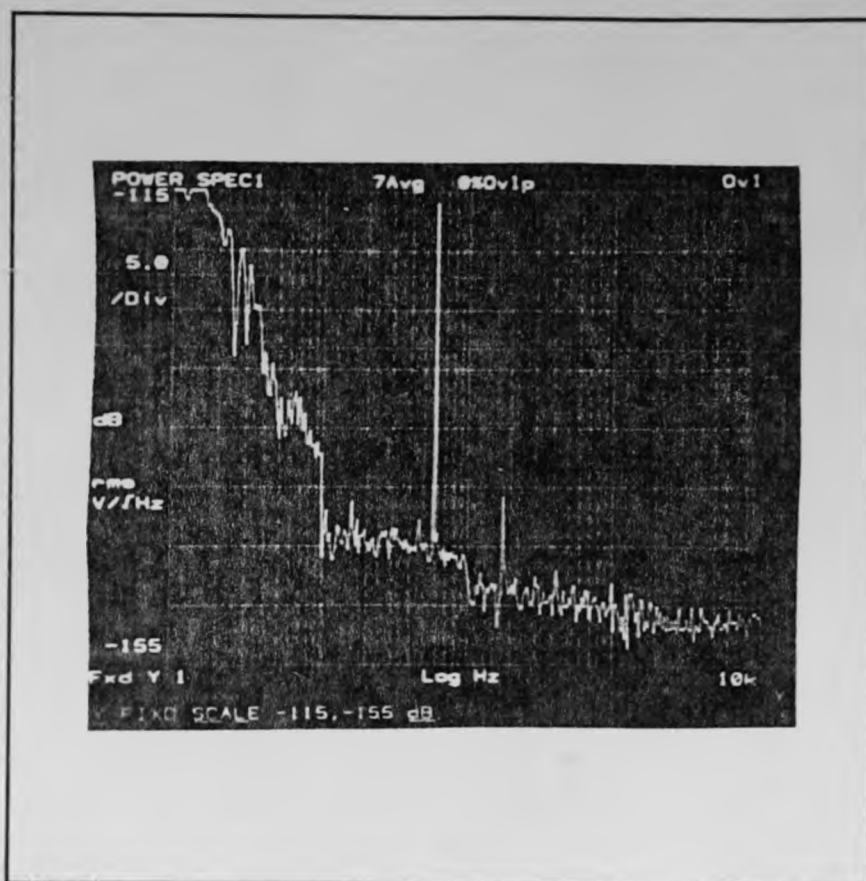


Figure 22 Output Noise

Table 1

Frequency(Hz)	Predicted	Measured
	Spot Noise	Spot Noise (nVrms/Hz <sup>0.5</sup> )
1	39	3162
10	16	51.2
100	7.8	44.7

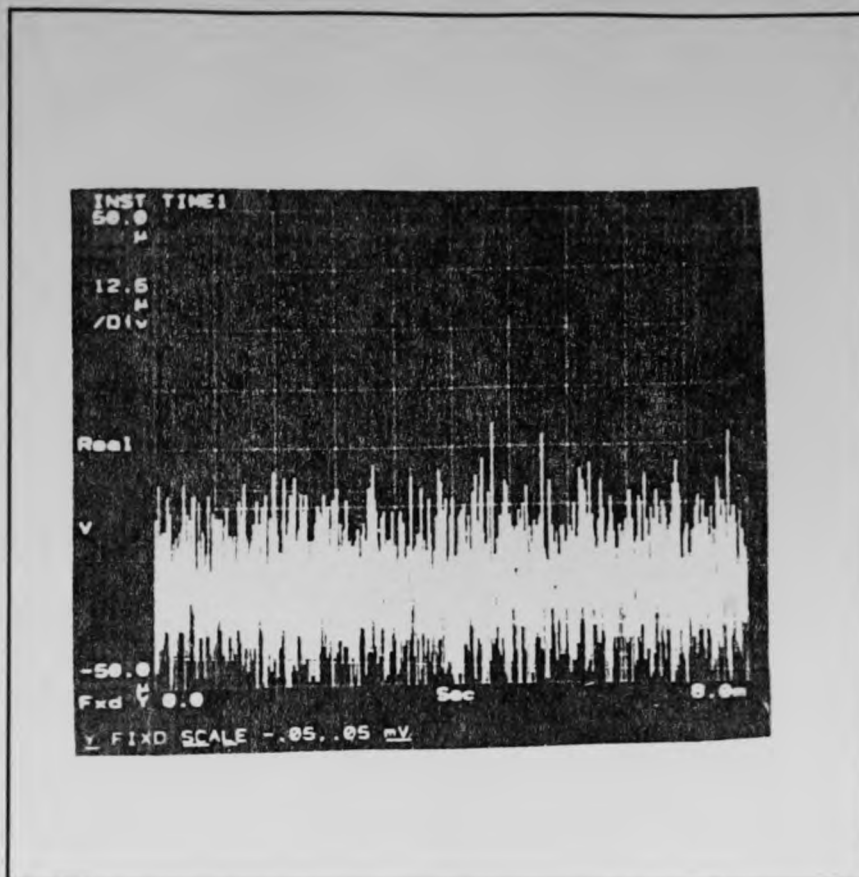


Figure 23 Wideband Output Noise

In conclusion the FSR sample device's performance nearly satisfies all the requirements for it to be acceptable for plantar force monitoring. The repeatability of this device at  $\pm 3.445\%$  exceeds the  $\pm 2\%$  requirement. However rise time at less than 1 msec. and noise performance which allows resolution exceeding 12 bits are more than adequate. The FSR's hysteresis at  $\pm 6.072\%$  needs improvement, however, since plantar force returns to zero at the end of each foot fall, rising force measurement accuracy of  $\pm 3.445\%$  could be achieved based upon the test data.

## CHAPTER IV

### A PROPOSED LOW POWER PORTABLE PLANTAR FORCE READOUT SYSTEM

In the following a proposal is presented , which describes a configuration for a "LOW POWER PORTABLE PLANTAR FORCE READOUT SYSTEM" based upon the FSR device manufactured by Interlink Electronics of Santa Barbara CA.

#### 4.0 Force Sensing Resistor Configuration

The FSR as manufactured by Interlink is a simple structure which can be manufactured in custom sizes, shapes, and profiles. It can be combined with others to form an array of FSR's on a common substrate. The size of each individual FSR can range from 0.2" to 24" diameter or square. Complete flexibility in the choice of material for the substrate and conductors, as well as overlap, allows for optimal terminal and environmental characteristics for a given application. In this case, a common bus array of FSR's can be custom designed and fabricated in mass quantities for different shoe sizes with the sensors located in critical areas, which are the heel, metatarsal heads and toes.[1] A clinical device for higher resolution would be possible but power dissipation and data storage requirements would be excessive for truly portable applications. In Figure 24 an engineering sketch of the Plantar Force Common Bus FSR Array is shown, for a size ten male foot.

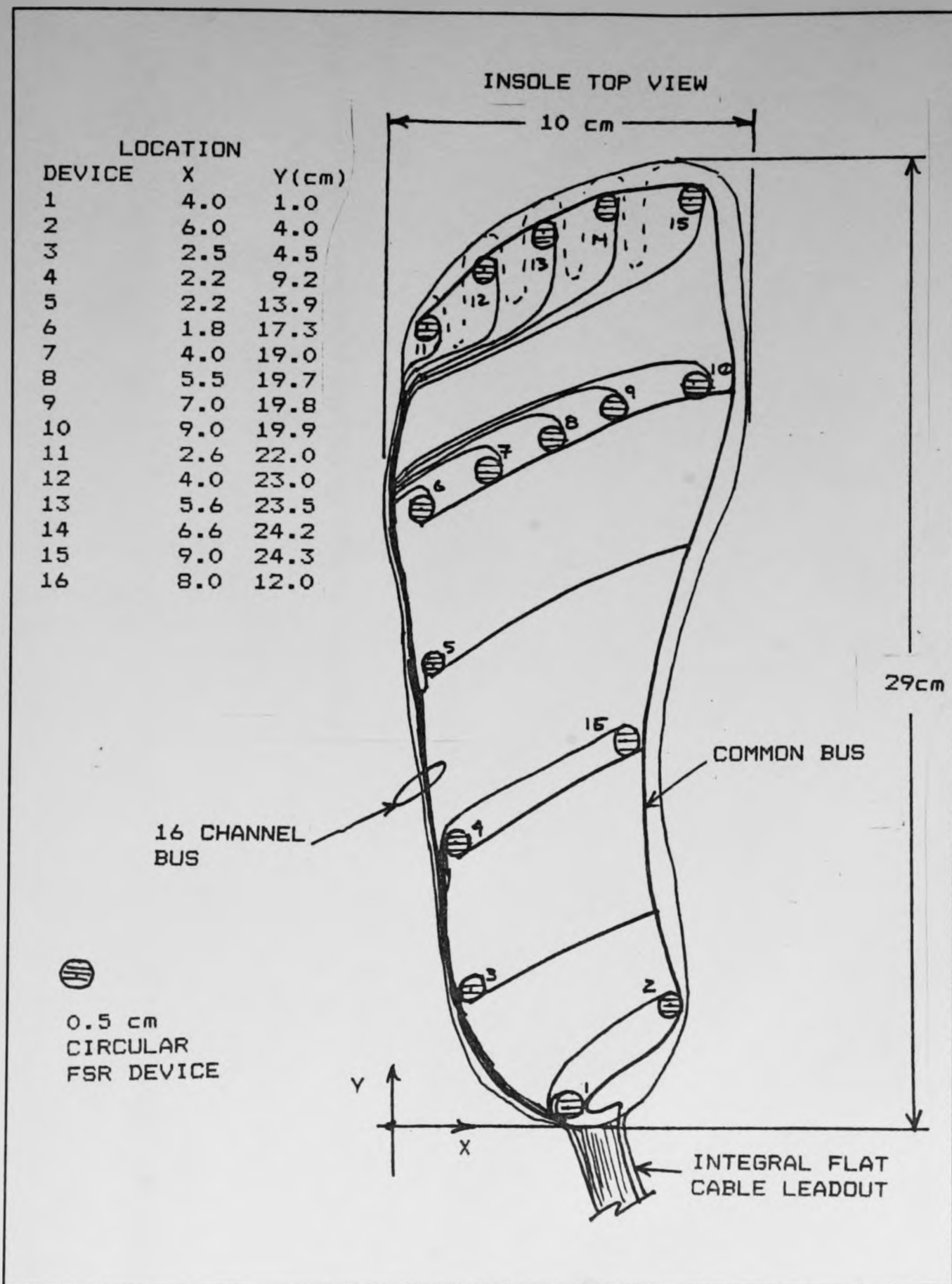


**Figure 24** Plantar Force Common Bus FSR Array Sensor.

#### 4.1 Readout Electronics Configuration

The proposed readout circuitry can best be described as a "Common Bus Array Transimpedance Amplifier/Sampling ADC Converter with Serial Output". A simplified schematic diagram of this architecture is shown in Figure 25, on the following page. This circuit has many advantages. 1) It requires only one amplifier to readout all the sensors in a serial multiplexed fashion. 2) The common reference only needs to bias a single FSR sensing element at one time.[1] 3) Only a small amount of glue logic is required to drive the multiplexer and completely integrated sampling analog to digital converter, which also contains the voltage reference. 4) Switch mode regulators provide efficient power conversion and allow for low battery end of life terminal voltage. The lifetime of this circuit with low power CMOS electronics should be more than adequate with a 9V cell.



## CHAPTER 5

### CONCLUSIONS

In this project the possible sensor types for monitoring plantar force were reviewed. The reasons for monitoring plantar force were stated and are many. It has been shown that the FSR could be a suitable device for monitoring plantar force with a 50% improvement in repeatability. This is likely possible since specified performance of the FSR device at  $\pm 2\%$  repeatability is more than adequate. A common bus FSR array which can be designed in the shape of an insole, with an array of these devices in critical areas has been proposed. Readout electronics for these devices are very simple.

## APPENDIX 1

### PSPICE CIRCUIT FILE LISTING for FSR READOUT CIRCUITRY

#### READOUT CIRCUIT FOR FORCE SENSING RESISTOR

\*\*\*\*U1 REF01AJ VOLTAGE REFERENCE

x3 11 0 13 14 REF01A

RTRIM1 14 13 5K

RTRIM2 13 0 5K

\*\*\*\*\*

\*\*\*\*INVERTING LOWPASS FILTER

R2 14 15 10K

R4 15 1B 5K

C3 15 1B 6.8UF

\*\*\*\*AR1 OP27AJ

X4 0 15 11 12 1B OP-27A

\*\*\*\*\*

\*\*\*\*SET RESISTOR

R6 1B 2B 56k

\*\*\*\*\*

\*\*\*\*LUMPED CABLE MODEL WITH LOSS

RCABLE1 1A 1B 0.072

RCABLE2 2A 2B 0.072

LCABLE1 1 1A 928NH

LCABLE2 2 2A 928NH

cCABLE 1B 2B 92.8pf

\*\*\*\*\*

\*\*\*\*TRANSIMPEDANCE AMPLIFIER

R9 2B 10 2k

C9 2B 10 20nf

\*\*\*\*AR2 OP27AJ

x2 0 2B 11 12 10 OP-27A

\*\*\*\*\*

\*\*\*\*DC POWER SUPPLIES

vsp 11 0 dc 15

vsn 12 0 dc -15

\*\*\*\*\*

\* REF01A SPICE MACROMODEL[9]

5/91, Rev. A

\* Copyright 1991 by Analog Devices, Inc.

\* NODE NUMBERS

\* VIN

\* | GND

\* | | TRIM

\* | | | VOUT

\* | | | |

.SUBCKT REF01A 2 4 5 6

\* 1.23V REFERENCE

I1 4 10 537.719E-9

R1 10 4 2.284E6 TC=8.5E-6

G1 4 10 2 4 54.0E-12

F1 4 10 VS 43.2E-9

\* INTERNAL OP AMP

G2 4 11 10 19 2E-3

R2	4	11	150E6
C1	4	11	2.1E-10
D1	11	12	DX
V1	2	12	2.0

\* SECONDARY POLE

G3	4	13	11	0	1E-6
R3	4	13	1E6		
C2	4	13	1.2E-13		

\* OUTPUT STAGE

ISY	2	4	0.78E-3		
FSY	2	4	V1	-1	
G4	4	14	13	0	25E-6
R4	4	14	40E3		
R7	17	19	14.2114E3		
R8	19	4	2E3		
R9	19	5	52.97E3		
R10	5	4	1E12		
Q1	16	14	17	QN	
VS	18	17	DC	0	
L1	18	6	1E-7		

\* OUTPUT CURRENT LIMIT

Q2	15	2	16	QN	
R6	2	16	21		
R5	2	15	18E3		
C3	2	15	1E-6		
G5	14	4	2	15	1

.MODEL QN NPN(IS=1E-15 BF=1000)

.MODEL DX D(IS=1E-15)

.ENDS REF01A

\* OP-27A SPICE Macro-model [9]

12/90, Rev. B

\* Node assignments

\* non-inverting input

\* | inverting input

\* | | positive supply

\* | | | negative supply

\* | | | | output

\* | | | | |

.SUBCKT OP-27A 1 2 99 50 39

\* INPUT STAGE & POLE AT 80 MHZ

R3 5 97 0.0619

R4 6 97 0.0619

CIN 1 2 4E-12

C2 5 6 16.07E-9

I1 4 51 1

IOS 1 2 17.5E-9

EOS 9 10 POLY(1) 30 33 25E-6 1

Q1 5 2 7 QX

Q2 6 9 8 QX

R5 7 4 0.0107

R6 8 4 0.0107

D1 2 1 DX

D2 1 2 DX

EN 10 1 12 0 1

GN1 0 2 15 0 1

GN2 0 1 18 0 1

\*

EREF 98 0 33 0 1

EPLUS 97 0 99 0 1

ENEG 51 0 50 0 1

\* VOLTAGE NOISE SOURCE WITH FLICKER NOISE

DN1 11 12 DEN

DN2 12 13 DEN

VN1 11 0 DC 2

VN2 0 13 DC 2

\* CURRENT NOISE SOURCE WITH FLICKER NOISE

DN3 14 15 DIN

DN4 15 16 DIN

VN3 14 0 DC 2

VN4 0 16 DC 2

\* SECOND CURRENT NOISE SOURCE

DN5 17 18 DIN

DN6 18 19 DIN

VN5 17 0 DC 2

VN6 0 19 DC 2

\* FIRST GAIN STAGE

RG1 40 98 1

GG1 98 40 5 6 79.86

DG3 40 41 DX

DG4	42	40	DX
EG1	97	41	POLY(1) 97 33 -2.1 1
EG2	42	51	POLY(1) 97 33 -2.1 1
* GAIN STAGE & DOMINANT POLE AT 7.2 HZ			
R7	20	98	37.58E3
C3	20	98	588E-9
G1	98	20	40 33 0.333
V1	97	21	1.9
V2	22	51	1.9
D5	20	21	DX
D6	22	20	DX
* POLE - ZERO AT 2.9MHZ / 6MHZ			
R8	23	98	1
R9	23	24	0.935
C4	24	98	28.4E-9
G2	98	23	20 33 1
* ZERO - POLE AT 6.8MHZ / 40MHZ			
R10	25	26	1
R11	26	98	4.88
L1	26	98	19.4E-9
G3	98	25	23 33 1
* POLE AT 60 MHZ			
R12	27	98	1
C5	27	98	2.65E-9
G4	98	27	25 33 1
* ZERO AT 28 MHZ			

```

R13  28 29      1
C6   28 29     -5.68E-9
R14  29 98     1E-6
E1   28 98     27 33  1E6

* COMMON-MODE GAIN NETWORK WITH ZERO AT 11.9 KHZ
R15  30 31      1
L2   31 98     13.3E-6
G5   98 30     POLY(2) 1  33  2  33  0  997.6E-9  997.6E-9
D7   30 97     DX
D8   51 30     DX

* POLE AT 80 MHZ
R16  32 98      1
C7   32 98     1.99E-9
G6   98 32     29 33  1

* OUTPUT STAGE
R17  33 97      1
R18  33 51      1
GSY  99 50     POLY(1) 99 50 3.47E-3 40E-6
F1   34  0     V3  1
F2   0  34     V4  1
R19  34 99     180
R20  34 50     180
L3   34 39     1E-7
G7   37 50     32 34  5.56E-3
G8   38 50     34 32  5.56E-3
G9   34 99     99 32  5.56E-3

```

G10 50 34 32 50 5.56E-3

V3 35 34 2.5

V4 34 36 3.1

D9 32 35 DX

D10 36 32 DX

D11 99 37 DX

D12 99 38 DX

D13 50 37 DY

D14 50 38 DY

\* MODELS USED

.MODEL QX NPN(BF=12.5E6)

.MODEL DX D(IS=1E-15)

.MODEL DY D(IS=1E-15 BV=50)

.MODEL DEN D(IS=1E-12, RS=1.74K, KF=4.01E-16, AF=1)

.MODEL DIN D(IS=1E-12, RS=43.5E-6, KF=11.1E-15, AF=1)

.ENDS OP-27A

\*\*\*\*FORCE INPUT

VIN 5A 0 pwl(0 0.02 0.02 0.02 10 10)

\*\*\*\*\*

\*\*\*VARIABLE RESISTOR MACROMODEL MODEL

RVIN 5A 5 1K

CMECH 5 0 455NF

ELOG 4 0 VALUE = {PWR(10,-0.49465\*LOG10(V(5))+3.9260)}

RELOG 4 0 1E3

EINREC 3 0 VALUE = {(1V/(V(4)))}

REINREC 3 0 1E3

RIRES 1 2 1E10

X1 1 2 3 VARISTR

.SUBCKT VARISTR 1 2 3

G 1 2 POLY(2) 1 2 3 0 0 0 0 0 1

.ENDS

\*\*\*\*\*

\*\*\*\*ANALYSIS CONTROL STATEMENTS

.PROBE v(5) v(10)

.TRAN 0.01 10 0.02 0.01

.END

## APPENDIX 2

### Technical Overview Force and Position Sensing Resistors.[2]

#### ABSTRACT

BY  
DR. STUART I. YANIGER  
VICE PRESIDENT  
AND CHIEF SCIENTIST

Force Sensing Resistor™ devices (FSR™) superficially resemble a membrane switch, but unlike the conventional switch, change resistance inversely with applied force. For example, with a typical FSR sensor, a human finger applying from 10g to 1kg will cause the sensor to change resistance continuously from 400K $\Omega$  to 40k $\Omega$ . These sensors are ideal for touch control, and may be applied where a semi-quantitative sensor is called for that is relatively inexpensive, thin (>0.15mm), durable (10,000,000 actuations), and environmentally resistant. These sensors can be made into arrays or single elements up to 60cm x 80cm, and cover forces in the tens of grams to tens of kilograms range.

Force and Position Sensing Resistor™ devices (FPSR™) can sense the position and normal force of a single actuator, such as a finger or a stylus, along either a straight line (a Linear Potentiometer) or on a planar surface (an XYZ Pad). Depending on the mechanical arrangement, positional resolution of 0.05 mm is possible.

#### INTRODUCTION

Force and position sensing are integral to a wide range of dynamical measurements. These range from podiatric gait analysis to electronic music to computer input devices. New sensor options for the designer are the Force Sensing Resistor (FSR) and the Force and Position Sensing Resistor (FPSR).

We will first deal with the simpler FSR. The construction of a typical FSR is shown in figure 1, and is based on two polymer films or sheets. A conducting pattern is deposited on one polymer in the form of a set of interdigitating electrodes. The electrode pattern is typically on the order of 0.4 mm finger width and spacing.

Next, a proprietary semiconductive polymer is deposited on the other sheet. The sheets are faced together so that the conducting fingers are shunted by the conducting polymer. When no force is applied to the sandwich, the resistance between the interdigitating electrodes is quite high, usually 1M $\Omega$  or more. With increasing force, the resistance drops, following an approximate power law.

A typical plot of resistance versus force is shown in Figure 2.

Note that, unlike a conventional load cell or strain gauge, the FSR resistance changes by nearly 3 decades.

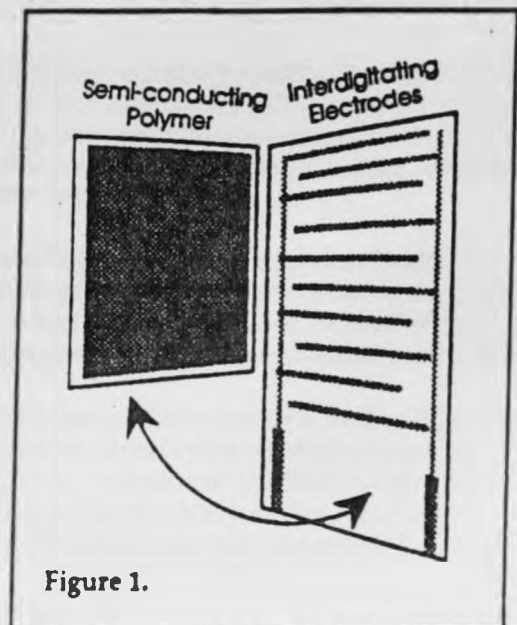
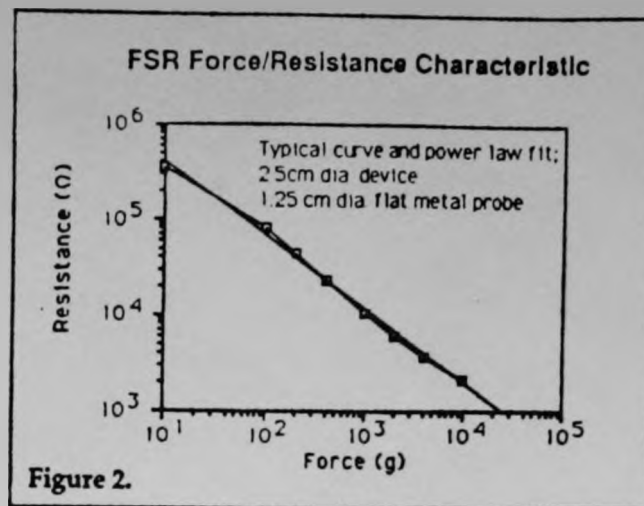


Figure 1.

UNLIKE  
PIEZOELECTRIC  
TRANSDUCERS,  
THE **FSR** IS  
INSENSITIVE TO  
VIBRATION AND  
ACOUSTIC NOISE PICKUP  
AND IS A SLOW DEVICE



With proper mechanical arrangement, repeatability of this curve cycle-to-cycle is better than  $\pm 2\%$  over a specified force range. For the device from which the data in figure 2 was obtained (a 2.5 cm diameter circular **FSR**), the specified force range was 200 g-10 kg. Device-to-device variation is typically  $\pm 15\%$  over that range.

The curve of Figure 2 does not show forces above a 10 kg load. At higher forces, the force/resistance characteristic starts to deviate from the power law response, eventually reaching a saturation force, beyond which the resistance does not vary strongly with force. The saturation force is a function of the ratio of the area of the applied force to the spacing between the **FSR** conductive inter

digitating electrodes. As we will discuss, the finer the lines and spaces, for a given area of applied force, the higher the saturation force. With real world areas and sensors, this saturation force can be designed to be from 3-50 kg.

**FSRs** can be fabricated in various sizes, from 0.5 to 4800 cm<sup>2</sup>, as single sensors or as arrays. The resistance range can also be tailored to specific applications. Varying the force range is also possible, but is best accomplished in the mechanical de-

sign. Zero travel is also a feature of the **FSR**. Where tactile feedback is desired, elastomeric overlays or molded domes can be laid over the parts to give travel or a tactile "snap."

The thickness of an **FSR** depends on several design variables. These include desired sensitivity, presence of overlays, and specified flexibility. Nearly all **FSR** designs to date have been in the thickness range of 0.1-1 mm.

Unlike piezoelectric transducers, the **FSR** is a slow device (typical mechanical rise time of 1-2 ms), and is relatively insensitive to vibration and acoustic noise pickup.

## EFFECT OF MECHANICAL DESIGN ON **FSR** RESPONSE

### a. Area Effects

The force/resistance response of an **FSR** is an extremely sensitive function of the manner in which it is mechanically addressed. A true force sensor will give a constant reading at a constant force, independent of the area over which the force is applied, or its distribution. A true pressure sensor will give, with the same constant force, a reading which is inversely proportional to the area of the applied force.

In actuality, the **FSR** lies somewhere between a force and a pressure transducer. A typical **FSR** will show a resistance that varies roughly as the reciprocal of the square root of the area of the applied force. This holds true under the condition where the force footprint is smaller than the **FSR** active area, and large compared to the spacing between the conducting fingers.

The sensitivity of the **FSR** resistance to the area and distribution of the force means that either the **FSR** must be used as a qualitative sensor, or that by proper mechanical arrangement, the force footprint can be held constant in area, position, and distribution. Other tradeoffs must be considered in the actual sensor design; for example, tailoring the sensor for minimum creep under load conflicts with some application requirements that the **FSR** have a very large no-load resistance.

The **FSR** can be used as a pressure sensor when the applied force is large compared to the **FSR** active area. Semi-quantitative biomedical gauging has been accomplished by orthopedists attaching small **FSRs** to various body parts in configurations such that the force is constant across the sensor active area.

THE **FSR** LIES  
SOMEWHERE  
BETWEEN A FORCE  
AND A PRESSURE  
TRANSDUCER

THE COMPLIANCE  
OF THE FORCE  
ACTUATOR  
IS A KEY ISSUE

## b. Actuator Characteristics

The compliance of the force actuator (i.e., the actual component or finger that physically contacts and transfers force to the FSR) is also a key issue. Frequently, a rubber or other elastomeric overlay is placed over the part to help spread the force out, extending the dynamic range.

Figure 3 shows how a typical force/resistance characteristic is changed by the use of overlays of varying thickness and hardness (or durometer, Shore A). Note that the greatest effect is seen at low to intermediate forces.

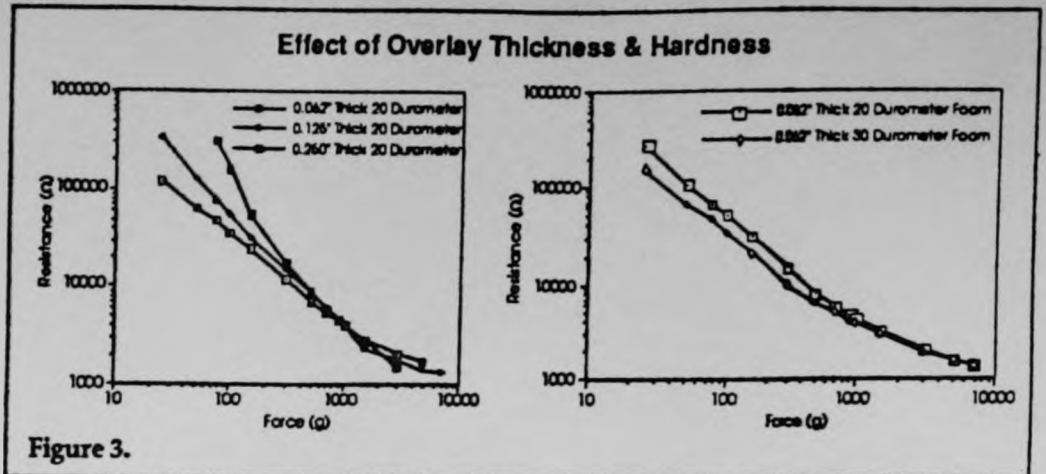


Figure 3.

A KEY ELEMENT  
IN PROPER FSR  
SENSOR DESIGN IS  
THE FINENESS OF  
PITCH OF THE  
CONDUCTIVE  
FINGERS

## c. Conductor Design

A key element in proper FSR sensor design is the fineness of pitch of the conductive fingers. For a given area, the finer the pitch (or "space and trace"), the greater the number of fingers actuated. The effect of the greater number of shunted fingers can be seen to increase the dynamic range of the device. With a fine space and trace, the force-resistance characteristic maintains its power-law characteristic over a greater force range (i.e., linearity on a log-log plot). Additionally, there is often an increase in the slope of this characteristic (i.e., a larger exponent in the power law). For example, a standard FSR formulation was tested with 0.020", 0.015" and 0.010" (0.50, 0.38 and 0.25mm) conductor pitch. The results are plotted in Figure 4, and clearly show the performance advantages of the fine pitch.

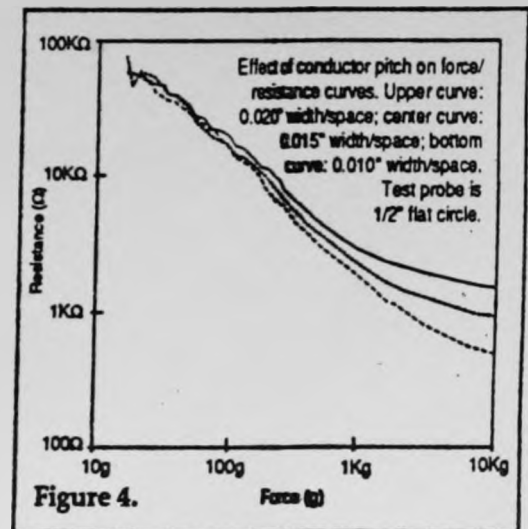


Figure 4.

The trade-off here is cost. With a finer space and trace, quality assurance inspection takes longer and the rejection rate is higher. This needs to be balanced against the real-world requirements of a given design.

## DEVICE DURABILITY

THE FSR IS  
A RUGGED,  
DURABLE  
DEVICE

The FSR is a rugged, durable device. The temperature range of our standard devices extends to 170°C, continuous. Higher temperature range devices are also available, with use temperatures as high as 400°C (750°F). Typical temperature coefficients are in the range of 1000 ppm/kg/°C near room temperature. The FSR is relatively insensitive to humidity.

Figure 5 shows the results of repeated use. For these data, a 2.5 cm diameter circular FSR was placed in a cycling force tester. A

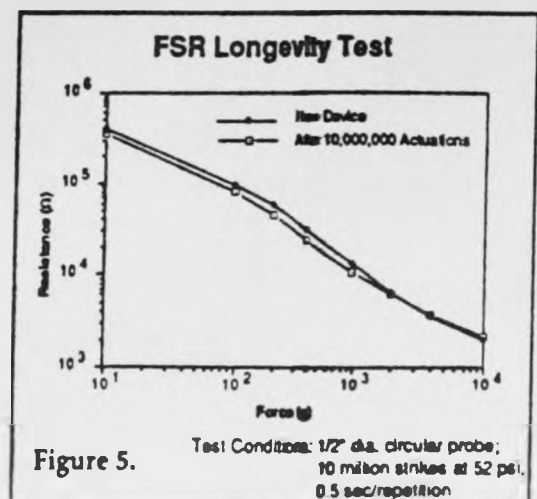


Figure 5.

12 lb. force was applied over ca. 1.5 cm<sup>2</sup>, through a 3 mm thick 45 Shore A rubber foot. The force was applied and released at a 2.5 Hz rate, with a 50% duty cycle. A small change toward lower resistance is observed after 10,000,000 cycles; however, this represents less than a 5% deviation (logarithmic) from the new part characteristic.

## ELECTRICAL INTERFACING

As we have seen, the FSR changes resistance dramatically with applied pressure. Additionally, its impedance is nearly purely resistive. These properties make FSR electrical interfaces extremely simple. Unlike strain-gauge sensors with their low  $\Delta R/R$ , no bridge is needed in FSR circuits, and the signals are usually in the 0-5 volt range.

Two general rules must be kept in mind, however: first, the FSR force-resistance response characteristic is a power law, so it may make sense to measure the logarithm of resistance changes; second, the maximum permissible device current is about 1 milliamp per cm<sup>2</sup> of applied force. Typical FSR current excitation is in the tens of microamps. You can use the FSR to control larger loads by using suitable buffer circuits.

The most unpredictable part of the FSR force/resistance characteristic is the pressure range under about 100 grams/cm<sup>2</sup>. If it is necessary to measure small forces in that range, you can pre-load the FSR with 100-200 grams/cm<sup>2</sup>, and measure the change in resistance when the small load is applied. At a somewhat higher part cost, high sensitivity can be designed in (e.g., by using a thinner substrate), but it is generally more economical to achieve this in the mechanical interface.

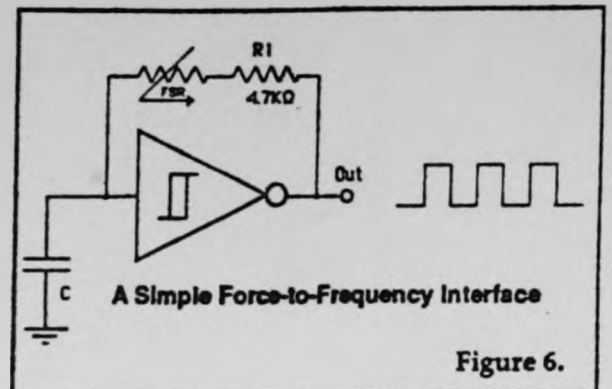


Figure 6.

The high dynamic range of the FSR simplifies electrical interfacing. For instance, a simple force to frequency converter is shown in Figure 6. In this circuit, the FSR is used as a feedback element around an inverter, with the time constant set by the FSR resistance and the capacitor. At zero force, the FSR resistance is very high, and the oscillator does not run. With increasing force, the output repetition rate is a linear function of the FSR resistance. R1 is included to limit current through the sensor. A great deal of control of the force/frequency curve is possible by including other elements in the feedback system. For example, bypassing R1 with a capacitor causes the curve to be steeper at higher forces; connecting a large value resistor in parallel with the capacitor C quenches any tendency to oscillate at low applied forces.

Analog interfaces are also quite simple. The FSR is placed in series with a current source (current kept within the maximum FSR rating). The voltage measured across the FSR is then related to the applied force. Alternately, the FSR can be used as one element in a voltage divider, with a fixed resistor as the other element. A voltage is applied to the divider, and the output voltage, taken from the resistor/FSR junction, is measured (Figure 7).

This type of interface is quite adequate for qualitative force sensing (for example, a touch panel). Precision measurements, however, are difficult, due to the shape of the power law curve. For higher precision measurements, it is usually most economic to go to the digital domain as soon as possible so that the log/log characteristic of the device can be translated to something more linear. If a design calls for a measurement of an impact (for example, a data entry keypad adhered behind a rigid plate) the FSR can be placed in a voltage divider, as above, and the junction of the voltage divider capacitively coupled to the succeeding stages. This eliminates any offset problems due to a preload. In the application just cited, denting the keypad protective plate with a hammer did not affect the operation of the pad; the offset created by the constant resistance of the FSR under the dent was blocked by the coupling capacitor.

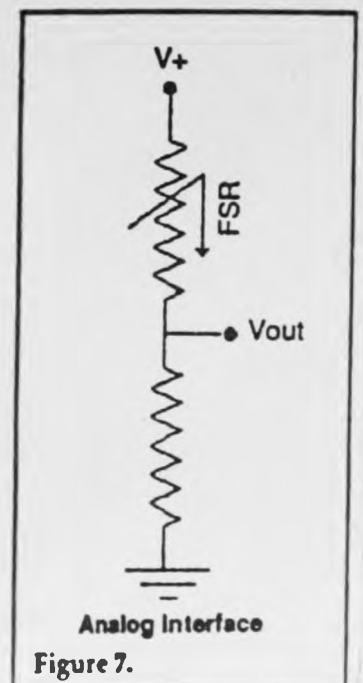


Figure 7.

THE HIGH DYNAMIC RANGE  
OF THE FSR  
SIMPLIFIES ELECTRICAL  
INTERFACING

RUGGEDIZED  
KEYPADS EVEN  
WITHSTAND  
HAMMERS

## FORCE AND POSITION SENSING RESISTORS

TWO BASIC TYPES  
OF **FPSRs** ARE AVAILABLE,  
THE LINEAR POTENTIOMETER AND  
THE XYZ PAD

Two basic types of *FPSRs* are available, the Linear Potentiometer (*FSR-LP*) and the XYZ Pad. The *FSR-LP*, besides being force sensitive, measures the position of an applied force along its sensing strip. The XYZ Pad is similar, but is used to measure position of an applied force in a plane.

The construction of an *FSR-LP* is shown in Figure 8. Generally, a voltage is applied between the Hot and Ground ends of the fixed resistor strip. When force is applied to the Force Sensing layer, the wiper contacts are shunted through that layer to one of the conducting fingers of the resistor strip. The voltage read from the wiper is thus proportional to the distance along the strip that the force is applied. An equivalent circuit for this arrangement is shown in Figure 9. The wiper series resistance varies with force.

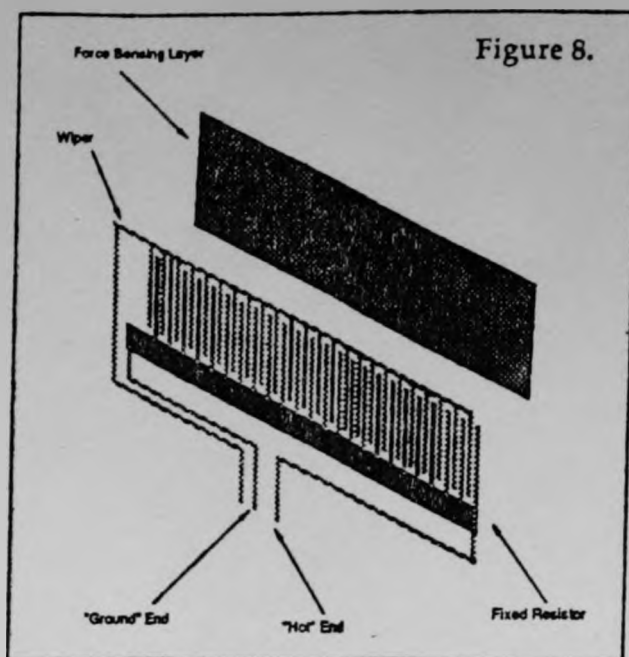


Figure 8.

To sense force, a resistance measurement is made between the wiper terminal and either the Hot or Ground end (or both, connected together) of the fixed resistor strip. The two alternate connections (force and position) are also shown in Figure 9.

DEPENDENT ON  
CONNECTION, **FPSRs** CAN  
MEASURE BOTH  
POSITION AND FORCE.

It is obvious that force and position measurements are not totally independent. However, the position measurement can be made unambiguously if the measuring device draws negligible current ( $< 1 \mu A$ ) so that there is no voltage drop across the wiper resistance. For example, an LF411 or similar low  $V_{ce}$  and  $i_{ce}$  device is suitable for this application. Also, the contact between the wiper and the resistor is momentary – some sort of sample and hold must be used in the interface. Connection of a small capacitor between wiper and ground is usually sufficient.

Force measurements are not quite so unambiguous, but good approximate measurements can be obtained by shorting the two fixed resistor ends (Hot and Ground) together, and measuring the resistance between the combined leads and the wiper. Some error can result from the fixed resistor being in series with the Force Sensing Resistor unless it is compensated for in the product design.

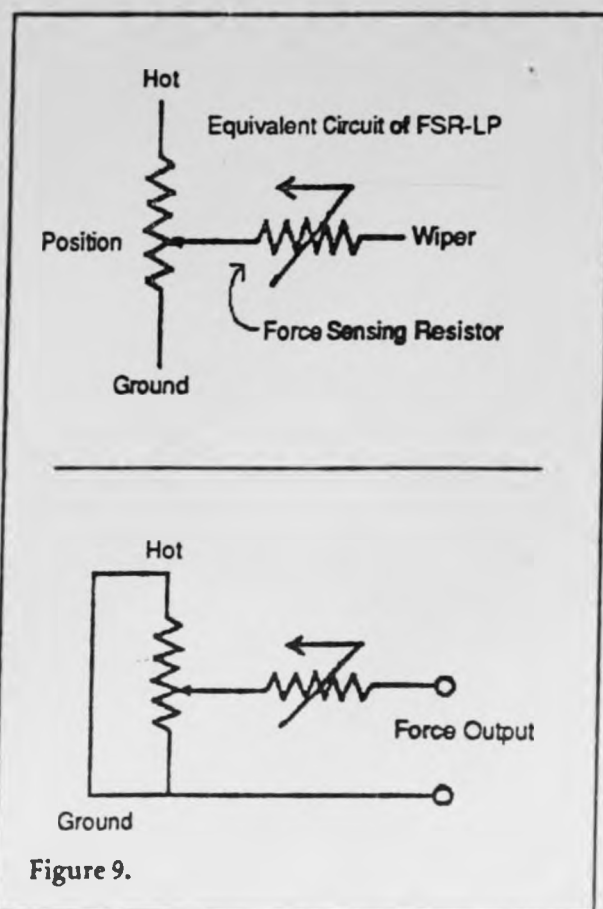


Figure 9.

For example, if the force is applied at the middle of the *FSR-LP*, the *FSR* part will have an additional series resistance of  $1/2$  of the total fixed resistance, because the resulting middle contact effectively parallels the two halves of the fixed resistor. If, on the other hand, force

THE USER CAN  
FINELY CONTROL  
THE **FSR-LP** OUTPUT  
BY A GENTLE ROCK  
OF THE FINGER

is applied to either end of the device active area, the fixed resistance is essentially shorted out. This problem can be mostly overcome by making the *FSR* resistance high compared to the potentiometer resistance, making low-current position measurement a must.

The force measurement error can also be subtracted out with a simple analog circuit or, given a position measurement, compensated for in software.

With the above topologies, force measurement is of one point only. It can be shown that the measured force position corresponds to the barycentric position, that is, a positional average weighted over the force distribution<sup>2</sup>. For the common case of a finger actuation, the point sensed by the *FSR-LP* is the center of the area covered by the fingertip; the user can finely control the *FSR-LP* output by a gentle rock of the finger.

### Positional Resolution and Accuracy

Resolution of a measurement device must be distinguished from accuracy. Resolution refers to the smallest change in position that can be detected. The positional resolution of a *FPSR* depends on the width of the applied force distribution and the fineness of the conductive fingers on the *FSR-LP*. It is typically in the 10-100 micron range.

Resolution can be approximated by  $\Delta x = 2w_f^2/w_i$ , where  $w_f$  is the width of the conductive fingers and  $w_i$  is the width of the applied force. This approximation assumes a relatively constant force across the force footprint. Typical numbers for a finger and an inexpensive *FPSR* are  $\Delta x = (2)(.5 \text{ mm})^2/(15 \text{ mm}) = 0.033 \text{ mm}$  (or 0.0013"). In practice, it is easy to achieve 300 counts per inch with a finger as the actuator. The resolution could be increased by decreasing the width of the conductive fingers and spaces; the trade-off is a more expensive part.

Positional accuracy refers to the absolute knowledge of a point's position, as opposed to resolution, which refers to the relative knowledge of position. The absolute positional accuracy of an *FPSR* is 1% or better.

## THE XYZ PAD

As we have seen, the *FSR-LP* gives a measurement of normal force and position along a line. It is often desirable to measure the position of an applied force in a plane (e.g., a graphics input pad for a computer).

If linear position of a point is measured in two orthogonal directions, then the position of the point on a plane is completely specified. Conceptually, by placing two *FSR-LPs* back-to-back and perpendicular to each other, one can measure the position of a force on a plane, as well as the magnitude of the force. The XYZ pad is so called since it can measure plane coordinates (X and Y) and normal force (Z).

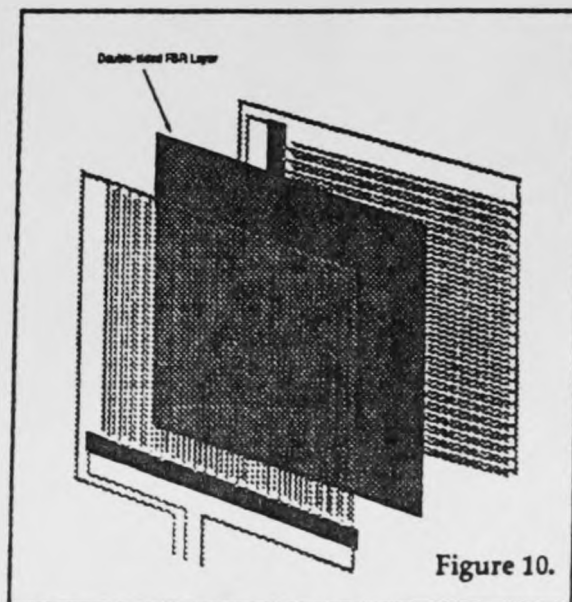


Figure 10.

Figure 10 shows the construction of an XYZ pad. Note that an unambiguous position can only be measured for a single applied force; multiple contacts will have degeneracies (that is, a non-unique set of solutions) in force-position measurements. This is not a problem for, e.g., graphics pads, but it does mean that the XYZ Pad cannot be used for complex pattern recognition.

# APPENDIX 3

## Test Data Sheet FSR/Readout Electronics DC Transfer Characteristic

Test Date: NOV 5 / 92 Time: 9:38 AM

Cycle Applied Force(lbs) Readout (volts)

<u>0</u>	<u>NO LOAD</u>	<u>0.1780</u>	↑ FORCE INCREASING
<u>0</u>	<u>TEST HEAD</u>	<u>0.1789</u>	↓ FORCE DECREASING
<u>1↑</u>	<u>0.3</u>	<u>0.1789</u>	
<u>1↑</u>	<u>0.6</u>	<u>0.2003</u>	
<u>1↑</u>	<u>1.0</u>	<u>0.2528</u>	
<u>1↑</u>	<u>3.0</u>	<u>0.6180</u>	
<u>1↑</u>	<u>6.0</u>	<u>1.415</u>	
<u>1↑</u>	<u>10.0</u>	<u>2.338</u>	
<u>1↑</u>	<u>30.0</u>	<u>5.222</u>	
<u>1↑</u>	<u>60.0</u>	<u>7.685</u>	
<u>1↓</u>	<u>30.0</u>	<u>5.515</u>	
<u>1↓</u>	<u>10.0</u>	<u>2.864</u>	
<u>1↓</u>	<u>6.0</u>	<u>2.060</u>	
<u>1↓</u>	<u>3.0</u>	<u>0.9317</u>	
<u>1↓</u>	<u>1.0</u>	<u>0.2689</u>	
<u>1↓</u>	<u>0.6</u>	<u>0.2143</u>	
<u>1↓</u>	<u>0.3</u>	<u>0.1792</u>	
<u>2↑</u>	<u>0.6</u>	<u>0.1993</u>	
<u>2↑</u>	<u>1.0</u>	<u>0.2486</u>	
<u>2↑</u>	<u>3.0</u>	<u>0.5342</u>	
<u>2↑</u>	<u>6.0</u>	<u>1.358</u>	

<u>2↑</u>	<u>10.0</u>	<u>1.358</u>
<u>2↑</u>	<u>30.0</u>	<u>5.349</u>
<u>2↑</u>	<u>60.0</u>	<u>7.800</u>
<u>2↓</u>	<u>30.0</u>	<u>5.705</u>
<u>2↓</u>	<u>10.0</u>	<u>3.015</u>
<u>2↓</u>	<u>6.0</u>	<u>2.051</u>
<u>2↓</u>	<u>3.0</u>	<u>0.9436</u>
<u>2↓</u>	<u>1.0</u>	<u>0.2816</u>
<u>2↓</u>	<u>0.6</u>	<u>0.2182</u>
<u>2↓</u>	<u>0.3</u>	<u>0.1802</u>
<u>3↑</u>	<u>0.6</u>	<u>0.2029</u>
<u>3↑</u>	<u>1.0</u>	<u>0.2326</u>
<u>3↑</u>	<u>3.0</u>	<u>0.5375</u>
<u>3↑</u>	<u>6.0</u>	<u>1.276</u>
<u>3↑</u>	<u>10.0</u>	<u>2.213</u>
<u>3↑</u>	<u>30.0</u>	<u>5.614</u>
<u>3↑</u>	<u>60.0</u>	<u>8.230</u>
<u>3↓</u>	<u>30.0</u>	<u>5.805</u>
<u>3↓</u>	<u>10.0</u>	<u>2.916</u>
<u>3↓</u>	<u>6.0</u>	<u>2.236</u>
<u>3↓</u>	<u>3.0</u>	<u>0.8550</u>
<u>3↓</u>	<u>1.0</u>	<u>0.2753</u>
<u>3↓</u>	<u>0.6</u>	<u>0.2077</u>
<u>2↓</u>	<u>0.3</u>	<u>0.1789</u>
<u>    </u>	<u>END TEST</u>	<u>11.32 AM</u>

## APPENDIX 4

### Test Data Analysis DC Transfer Characteristic.

#### FSR/READOUT CIRCUITRY DC TRANSFER CHARACTERISTIC CYCLIC TEST

$F :=$	$V_{out1} :=$	$V_{outd1} :=$
0.3	.1789	.1792
0.6	.2003	.2143
1.0	.2528	.2689
3.0	.6180	.9317
6.0	1.415	2.060
10.0	2.338	2.864
30.0	5.222	5.515
60.0	7.685	7.685

Applied lbs force.

Readout Voltage

$i := 0..7$	$V_{out2} :=$	$V_{outd2} :=$
$F_{kg_i} := \frac{F_i}{6.38486}$	.1792	.1802
	.1993	.2182
	.2486	.2816
	.5342	.9436
	1.358	2.051
	2.404	3.015
	5.349	5.705
	7.800	7.800

Convert to kg/cm<sup>2</sup>

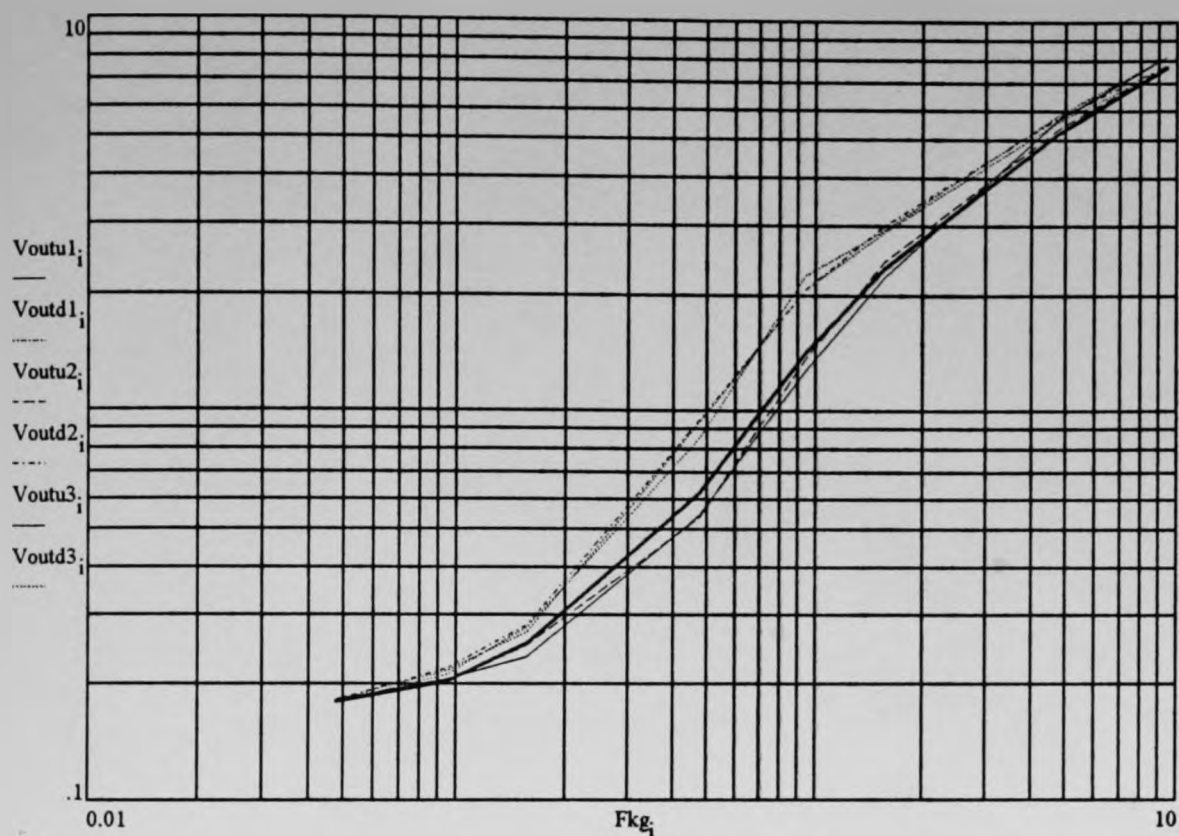
$F_{kg_i}$	$V_{out3} :=$	$V_{outd3} :=$
0.047	.1802	.1789
0.094	.2029	.2077
0.157	.2326	.2753
0.47	.5375	.8550
0.94	1.276	2.236
1.566	2.213	2.916
4.699	5.614	5.805
9.397	8.230	8.230

Applied force per  
unit area kg/cm<sup>2</sup>

$$V_{out_i} := \frac{10000}{10^{-0.71454 \cdot \log(F_{kg_i}) + 3.79734}}$$

End point power law approximation

Readout voltage for each cycle u=up d-down volts Log-Log Plot  
FSR/Readout



Applied Force kg/cm<sup>2</sup>

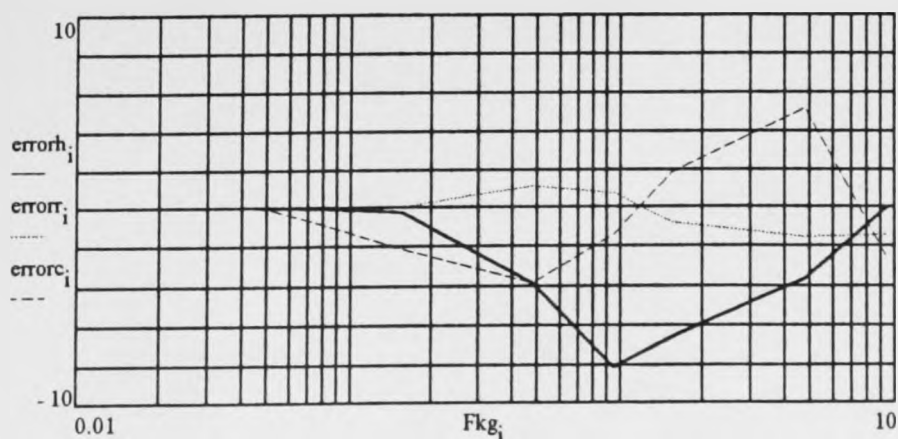
Calculate hysteresis error-errorh, repeatability-errorr & against  
power law errorc

$$\text{errorh}_i = \frac{V_{out1_i} - V_{outd1_i}}{0.07905}$$

$$\text{errorr}_i = \frac{V_{out1_i} - V_{outu2_i}}{0.07905}$$

$$\text{errorc}_i = \frac{V_{out1_i} - V_{out_i}}{0.07905}$$

Error % of full scale



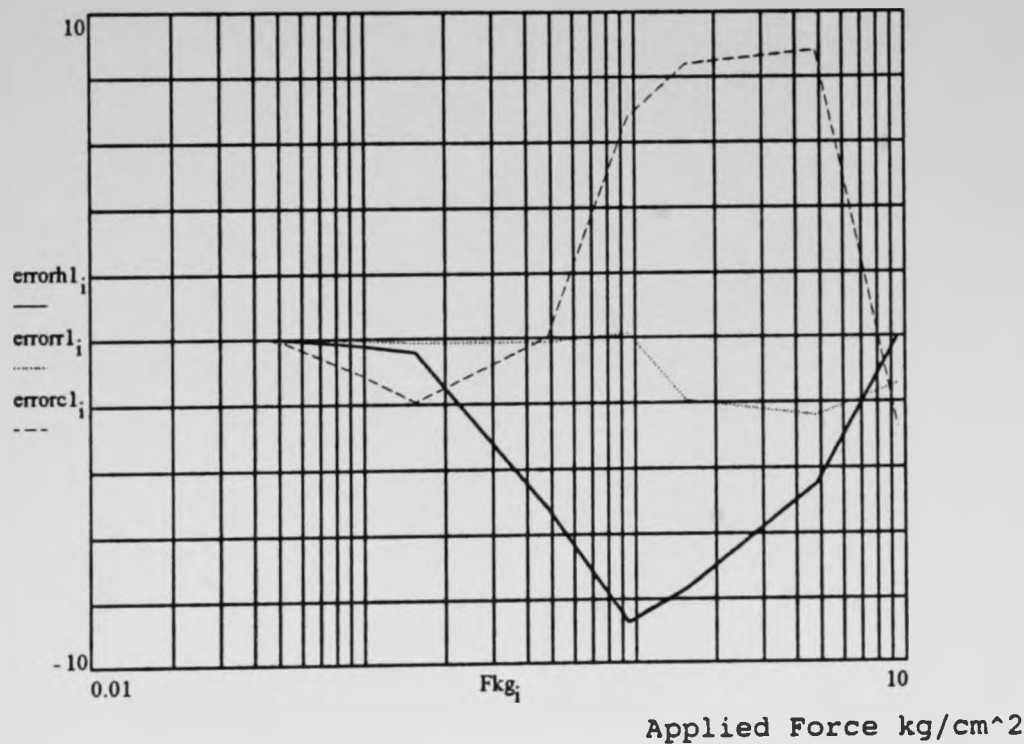
Applied Force kg/cm<sup>2</sup>

further error calaculations for other cycles

$$\text{errorh1}_i = \frac{\text{Voutu2}_i - \text{Voutd2}_i}{0.07905} \qquad \text{errorr1}_i = \frac{\text{Voutd1}_i - \text{Voutd2}_i}{.07905}$$

$$\text{errorcl}_i = \frac{\text{Voutd1}_i - \text{Vout}_i}{0.07905}$$

Error % of full scale



$$\text{erru1}_i = \frac{\text{Voutu1}_i - \text{Voutu2}_i}{0.07905} \qquad \text{erru2}_i = \frac{\text{Voutu1}_i - \text{Voutu3}_i}{0.07905}$$

erru1 <sub>i</sub>	erru2 <sub>i</sub>
-0.004	-0.016
0.013	-0.033
0.053	0.256
1.06	1.018
0.721	1.758
-0.835	1.581
-1.607	-4.959
-1.455	-6.894

Increasing force repeatability error

$$\text{errd1}_i := \frac{\text{Voutd1}_i - \text{Voutd2}_i}{0.07905}$$

$$\text{errd2}_i := \frac{\text{Voutd1}_i - \text{Voutd3}_i}{0.07905}$$

errd1<sub>i</sub>

-0.013
-0.049
-0.161
-0.151
0.114
-1.91
-2.404
-1.455

errd2<sub>i</sub>

0.004
0.083
-0.081
0.97
-2.226
-0.658
-3.669
-6.894

Decreasing force repeatability error % of full scale

$$\text{errh1}_i := \frac{\text{Voutu1}_i - \text{Voutd1}_i}{0.07905}$$

$$\text{errh2}_i := \frac{\text{Voutu2}_i - \text{Voutd2}_i}{0.07905}$$

$$\text{errh3}_i := \frac{\text{Voutu3}_i - \text{Voutd3}_i}{0.07905}$$

errh1<sub>i</sub>

-0.004
-0.177
-0.204
-3.968
-8.159
-6.654
-3.707
0

errh2<sub>i</sub>

-0.013
-0.239
-0.417
-5.179
-8.767
-7.729
-4.503
0

errh3<sub>i</sub>

0.016
-0.061
-0.54
-4.016
-12.144
-8.893
-2.416
0

Hysteresis error by cycle % of full scale

Calculate vave minimum error piecewise curve fit

$$vave_i := \frac{Voutu1_i + Voutu2_i + Voutu3_i + Voutd1_i + Voutd2_i + Voutd3_i}{6}$$

vave =	0.179
	0.207
	0.26
	0.737
	1.733
	2.625
	5.535
	7.905

Calculate error against curve fit

$$erau1_i := \frac{vave_i - Voutu1_i}{0.07905}$$

$$erau2_i := \frac{vave_i - Voutu1_i}{0.07905}$$

$$erau3_i := \frac{vave_i - Voutu3_i}{0.07905}$$

$$erad1_i := \frac{vave_i - Voutd1_i}{0.07905}$$

$$erad2_i := \frac{vave_i - Voutd2_i}{0.07905}$$

$$erad3_i := \frac{vave_i - Voutd3_i}{0.07905}$$

**% error by cycle against curve fit**

erau1 <sub>i</sub>	erau2 <sub>i</sub>	erau3 <sub>i</sub>	erad1 <sub>i</sub>	erad2 <sub>i</sub>	erad3 <sub>i</sub>
0.007	0.007	-0.01	0.003	-0.01	0.007
0.086	0.086	0.053	-0.091	-0.14	-0.007
0.091	0.091	0.346	-0.113	-0.274	-0.194
1.501	1.501	2.52	-2.467	-2.618	-1.497
4.019	4.019	5.777	-4.141	-4.027	-6.367
3.631	3.631	5.212	-3.023	-4.934	-3.681
3.96	3.96	-0.999	0.253	-2.151	-3.416
2.783	2.783	-4.111	2.783	1.328	-4.111

# Active Component Data Sheets for FSR Evaluation Readout Circuitry.[6]

## OP-27

### LOW-NOISE PRECISION OPERATIONAL AMPLIFIER

#### FEATURES

- Low Noise .....  $80\text{nV}_{\text{p-p}}$  (0.1Hz to 10Hz)  
.....  $3\text{nV}/\sqrt{\text{Hz}}$
- Low Drift .....  $0.2\mu\text{V}/^\circ\text{C}$
- High Speed .....  $2.8\text{V}/\mu\text{s}$  Slew Rate  
..... 8MHz Gain Bandwidth
- Low  $V_{\text{OS}}$  .....  $10\mu\text{V}$
- Excellent CMRR ..... 126dB at  $V_{\text{CM}}$  of  $\pm 11\text{V}$
- High Open-Loop Gain ..... 1.8 Million
- Fits 725, OP-07, OP-05, AD510, AD517, 5534A sockets
- Available in Die Form

#### ORDERING INFORMATION<sup>1</sup>

$T_A = +25^\circ\text{C}$ $V_{\text{OS}}$ MAX (mV)	PACKAGE				OPERATING TEMPERATURE RANGE
	TO-99	CERDIP 8-PIN	PLASTIC 8-PIN	LCC 20-CONTACT	
25	OP27AJ*	OP27AZ*	-	-	MIL
25	OP27EJ	OP27EZ	OP27EP	-	IND/COM
80	OP27BJ*	OP27BZ*	-	OP27BR/883	MIL
80	OP27FJ	OP27FZ	OP27FP	-	IND/COM
100	OP27CJ	OP27CZ	-	-	MIL
100	OP27GJ	OP27GZ	OP27GP	-	XIND
100	-	-	OP27GS <sup>††</sup>	-	XIND

\* For devices processed in total compliance to MIL-STD-883, add /883 after part number. Consult factory for 883 data sheet.

† Burn-in is available on commercial and industrial temperature range parts in CerDIP, plastic DIP, and TO-can packages. For ordering information, see 1990/91 Data Book, Section 2.

†† For availability and burn-in information on SO and PLCC packages, contact your local sales office.

#### GENERAL DESCRIPTION

The OP-27 precision operational amplifier combines the low offset and drift of the OP-07 with both high-speed and low-noise. Offsets down to  $25\mu\text{V}$  and drift of  $0.6\mu\text{V}/^\circ\text{C}$  maximum make the OP-27 ideal for precision instrumentation applications. Exceptionally low noise,  $e_n = 3.5\text{nV}/\sqrt{\text{Hz}}$ , at 10Hz, a low 1/f noise corner frequency of 2.7Hz, and high gain (1.8 million), allow accurate high-gain amplification of low-level

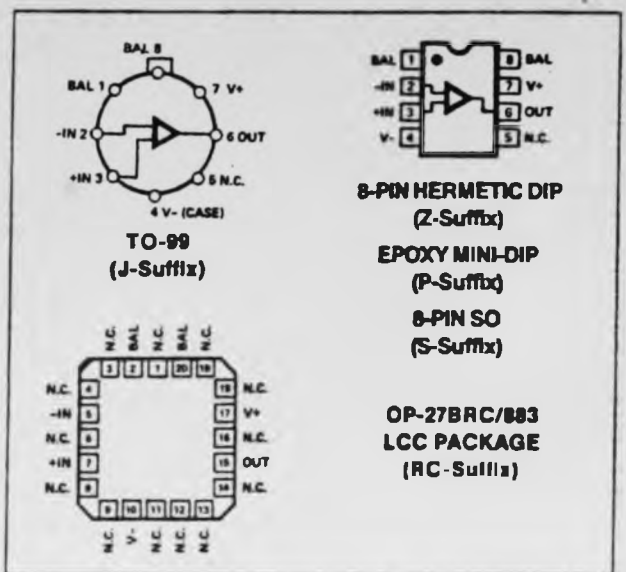
signals. A gain-bandwidth product of 8MHz and a  $2.8\text{V}/\mu\text{sec}$  slew rate provides excellent dynamic accuracy in high-speed data-acquisition systems.

A low input bias current of  $\pm 10\text{nA}$  is achieved by use of a bias-current-cancellation circuit. Over the military temperature range, this circuit typically holds  $I_B$  and  $I_{\text{OS}}$  to  $\pm 20\text{nA}$  and  $15\text{nA}$  respectively.

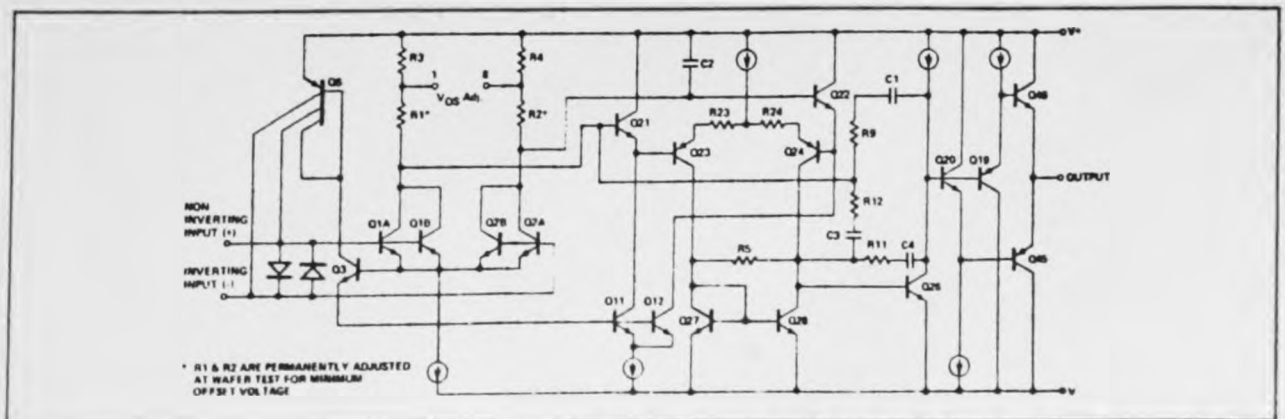
The output stage has good load driving capability. A guaranteed swing of  $\pm 10\text{V}$  into  $600\Omega$  and low output distortion make the OP-27 an excellent choice for professional audio applications.

PSRR and CMRR exceed 120dB. These characteristics, coupled with long-term drift of  $0.2\mu\text{V}/\text{month}$ , allow the circuit designer to achieve performance levels previously attained only by discrete designs.

#### PIN CONNECTIONS



#### SIMPLIFIED SCHEMATIC





Low cost, high-volume production of OP-27 is achieved by using an on-chip zener-zap trimming network. This reliable and stable offset trimming scheme has proved its effectiveness over many years of production history.

The OP-27 provides excellent performance in low-noise high-accuracy amplification of low-level signals. Applications include stable integrators, precision summing amplifiers, precision voltage-threshold detectors, comparators, and professional audio circuits such as tape-head and microphone preamplifiers.

The OP-27 is a direct replacement for 725, OP-06, OP-07 and OP-05 amplifiers; 741 types may be directly replaced by removing the 741's nulling potentiometer.

#### ABSOLUTE MAXIMUM RATINGS (Note 4)

Supply Voltage .....	$\pm 22\text{V}$
Input Voltage (Note 1) .....	$\pm 22\text{V}$
Output Short-Circuit Duration .....	Indefinite
Differential Input Voltage (Note 2) .....	$\pm 0.7\text{V}$
Differential Input Current (Note 2) .....	$\pm 25\text{mA}$
Storage Temperature Range .....	$-65^\circ\text{C}$ to $+150^\circ\text{C}$

#### Operating Temperature Range

OP-27A, OP-27B, OP-27C (J, Z, RC) .....	$-55^\circ\text{C}$ to $+125^\circ\text{C}$
OP-27E, OP-27F (J, Z) .....	$-25^\circ\text{C}$ to $+85^\circ\text{C}$
OP-27E, OP-27F (P) .....	$0^\circ\text{C}$ to $+70^\circ\text{C}$
OP-27G (P, S, J, Z) .....	$-40^\circ\text{C}$ to $+85^\circ\text{C}$
Lead Temperature Range (Soldering, 60 sec) .....	$300^\circ\text{C}$
Junction Temperature .....	$-65^\circ\text{C}$ to $+150^\circ\text{C}$

PACKAGE TYPE	$\theta_{JA}$ (Note 3)	$\theta_{JC}$	UNITS
TO-99 (J)	150	18	$^\circ\text{C/W}$
8-Pin Hermetic DIP (Z)	148	18	$^\circ\text{C/W}$
8-Pin Plastic DIP (P)	103	43	$^\circ\text{C/W}$
20-Contact LCC (RC)	98	38	$^\circ\text{C/W}$
8-Pin SO (S)	158	43	$^\circ\text{C/W}$

#### NOTES:

- For supply voltages less than  $\pm 22\text{V}$ , the absolute maximum input voltage is equal to the supply voltage.
- The OP-27's inputs are protected by back-to-back diodes. Current limiting resistors are not used in order to achieve low noise. If differential input voltage exceeds  $\pm 0.7\text{V}$ , the input current should be limited to  $25\text{mA}$ .
- $\theta_{JA}$  is specified for worst case mounting conditions, i.e.,  $\theta_{JA}$  is specified for device in socket for TO, CerDIP, P-DIP, and LCC packages;  $\theta_{JA}$  is specified for device soldered to printed circuit board for SO package.
- Absolute maximum ratings apply to both DICE and packaged parts, unless otherwise noted.

#### ELECTRICAL CHARACTERISTICS at $V_S = \pm 15\text{V}$ , $T_A = 25^\circ\text{C}$ , unless otherwise noted.

PARAMETER	SYMBOL	CONDITIONS	OP-27A/E			OP-27B/F			OP-27C/G			UNITS
			MIN	TYP	MAX	MIN	TYP	MAX	MIN	TYP	MAX	
Input Offset Voltage	$V_{OS}$	(Note 1)	—	10	25	—	20	60	—	30	100	$\mu\text{V}$
Long-Term $V_{OS}$ Stability	$V_{OS}/\text{Time}$	(Notes 2, 3)	—	0.2	1.0	—	0.3	1.5	—	0.4	2.0	$\mu\text{V}/\text{Mo}$
Input Offset Current	$I_{OS}$		—	7	35	—	9	50	—	12	75	nA
Input Bias Current	$I_B$		—	$\pm 10$	$\pm 40$	—	$\pm 12$	$\pm 55$	—	$\pm 15$	$\pm 80$	nA
Input Noise Voltage	$e_{np-p}$	0.1Hz to 10Hz (Notes 3, 5)	—	0.08	0.18	—	0.08	0.18	—	0.08	0.25	$\mu\text{Vp-p}$
Input Noise Voltage Density	$e_n$	$f_O = 10\text{Hz}$ (Note 3)	—	3.5	5.5	—	3.5	5.5	—	3.8	8.0	$\text{nV}/\sqrt{\text{Hz}}$
		$f_O = 30\text{Hz}$ (Note 3)	—	3.1	4.5	—	3.1	4.5	—	3.3	5.6	
		$f_O = 1000\text{Hz}$ (Note 3)	—	3.0	3.8	—	3.0	3.8	—	3.2	4.5	
Input Noise Current Density	$i_n$	$f_O = 10\text{Hz}$ (Notes 3, 6)	—	1.7	4.0	—	1.7	4.0	—	1.7	—	$\text{pA}/\sqrt{\text{Hz}}$
		$f_O = 30\text{Hz}$ (Notes 3, 6)	—	1.0	2.3	—	1.0	2.3	—	1.0	—	
		$f_O = 1000\text{Hz}$ (Notes 3, 6)	—	0.4	0.6	—	0.4	0.6	—	0.4	0.6	
Input Resistance — Differential-Mode	$R_{in}$	(Note 7)	1.3	6	—	0.94	5	—	0.7	4	—	M $\Omega$
Input Resistance — Common-Mode	$R_{inCM}$		—	3	—	—	2.5	—	—	2	—	G $\Omega$
Input Voltage Range	IVR		$\pm 11.0$	$\pm 12.3$	—	$\pm 11.0$	$\pm 12.3$	—	$\pm 11.0$	$\pm 12.3$	—	V
Common-Mode Rejection Ratio	CMRR	$V_{CM} = \pm 11\text{V}$	114	128	—	106	123	—	100	120	—	dB
Power Supply Rejection Ratio	PSRR	$V_S = \pm 4\text{V}$ to $\pm 18\text{V}$	—	1	10	—	1	10	—	2	20	$\mu\text{V/V}$
Large-Signal Voltage Gain	$A_{VO}$	$R_L \geq 2\text{k}\Omega$ , $V_O = \pm 10\text{V}$	1000	1800	—	1000	1800	—	700	1500	—	V/mV
		$R_L \geq 600\Omega$ , $V_O = \pm 10\text{V}$	800	1500	—	800	1500	—	600	1500	—	
Output Voltage Swing	$V_O$	$R_L \geq 2\text{k}\Omega$	$\pm 12.0$	$\pm 13.8$	—	$\pm 12.0$	$\pm 13.8$	—	$\pm 11.5$	$\pm 13.5$	—	V
		$R_L \geq 600\Omega$	$\pm 10.0$	$\pm 11.5$	—	$\pm 10.0$	$\pm 11.5$	—	$\pm 10.0$	$\pm 11.5$	—	
Slew Rate	SR	$R_L \geq 2\text{k}\Omega$ (Note 4)	1.7	2.8	—	1.7	2.8	—	1.7	2.8	—	V/ $\mu\text{s}$



# REF-01

+10V PRECISION  
VOLTAGE REFERENCE

Precision Monolithics Inc.

## FEATURES

- 10 Volt Output .....  $\pm 0.3\%$  Max
- Adjustment Range .....  $\pm 3\%$  Min
- Excellent Temperature Stability .....  $8.5\text{ppm}/^\circ\text{C}$  Max
- Low Noise .....  $30\mu\text{V}_{\text{p-p}}$  Max
- Low Supply Current .....  $1.4\text{mA}$  Max
- Wide Input Voltage Range .....  $12\text{V}$  to  $40\text{V}$
- High Load-Driving Capability .....  $20\text{mA}$
- No External Components
- Short-Circuit Proof
- MIL-STD-883 Screening Available
- Available in Die Form

## ORDERING INFORMATION<sup>1</sup>

$T_A = 25^\circ\text{C}$ $\Delta V_{00} \text{ MAX}$ (mV)	PACKAGE				OPERATING TEMPERATURE RANGE
	TO-99	CERDIP 8-PIN	PLASTIC 8-PIN	LCC 20-CONTACT	
$\pm 30$	REF01AJ*	REF01AZ*	—	—	MIL
$\pm 30$	REF01EJ	REF01EZ*	—	—	COM
$\pm 50$	REF01J*	REF01Z*	—	REF01RC/883	MIL
$\pm 50$	REF01HJ	REF01HZ	REF01HP	—	COM
$\pm 100$	REF01CJ	REF01CZ	—	—	COM
$\pm 100$	—	—	REF01CP	—	XIND
$\pm 100$	—	—	REF01CS††	—	XIND

\* For devices processed in total compliance to MIL-STD-883, add /883 after part number. Consult factory for 883 data sheet.

† Burn-in is available on commercial and industrial temperature range parts in CerDIP, plastic DIP, and TO-can packages. For ordering information, see 1990/91 Data Book, Section 2.

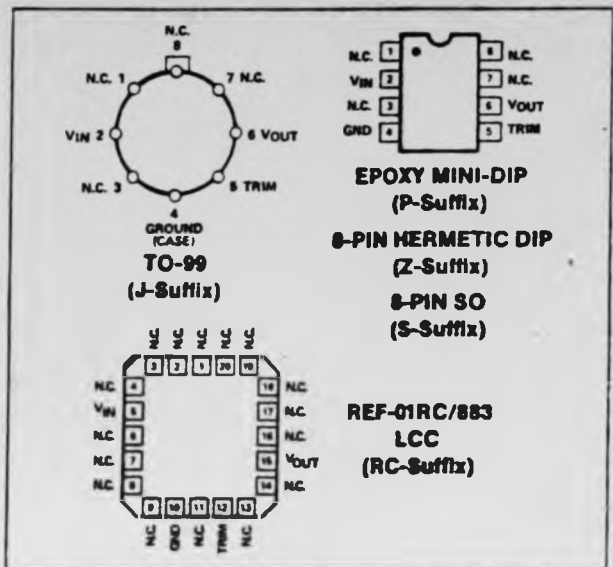
†† For availability and burn-in information on SO and PLCC packages, contact your local sales office.

## GENERAL DESCRIPTION

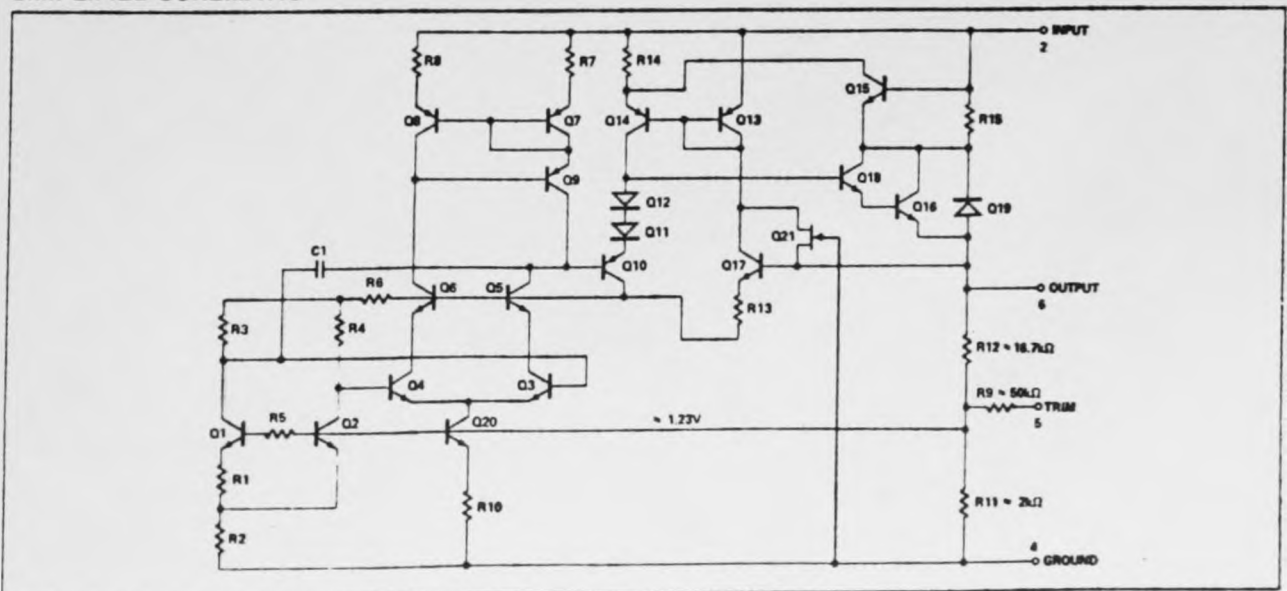
The REF-01 precision voltage reference provides a stable

+10V output which can be adjusted over a  $\pm 3\%$  range with minimal effect on temperature stability. Single-supply operation over an input voltage range of  $12\text{V}$  to  $40\text{V}$ , low current drain of  $1\text{mA}$ , and excellent temperature stability are achieved with an improved bandgap design. Low cost, low noise, and low power make the REF-01 an excellent choice whenever a stable voltage reference is required. Applications include D/A and A/D converters, portable instrumentation, and digital voltmeters. Full military temperature range devices with screening to MIL-STD-883 are available. For guaranteed long-term drift see the REF-10 data sheet.

## PIN CONNECTIONS

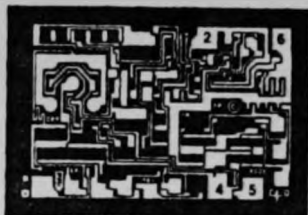


## SIMPLIFIED SCHEMATIC





## DICE CHARACTERISTICS (125°C TESTED DICE AVAILABLE)



DIE SIZE 0.074 × 0.048 inch, 3552 sq. mils  
(1.88 × 1.22 mm, 2.29 sq. mm)

2. INPUT VOLTAGE ( $V_{IN}$ )  
4. GROUND  
5. TRIM  
6. OUTPUT VOLTAGE ( $V_{OUT}$ )

For additional DICE ordering information,  
refer to 1990/91 Data Book, Section 2.

**WAFER TEST LIMITS** at  $V_{IN} = +15V$ ,  $T_A = 25^\circ C$  for REF-01N and REF-01G devices;  $T_A = 125^\circ C$  for REF-01NT and REF-01GT devices, unless otherwise noted. (Note 1)

PARAMETER	SYMBOL	CONDITIONS	REF-01NT LIMIT	REF-01N LIMIT	REF-01GT LIMIT	REF-01G LIMIT	UNITS
Output Voltage	$V_O$	$I_L = 0$	10.05 9.95	10.03 9.97	10.10 9.90	10.05 9.95	V MAX V MIN
Output Adjustment Range	$V_{trim}$	$R_P = 10k\Omega$	—	$\pm 3.0$	—	$\pm 3.0$	% MIN
Line Regulation		$V_{IN} = 13V$ to $33V$	0.015	0.01	0.015	0.01	%/V MAX

**NOTE:**

Electrical tests are performed at wafer probe to the limits shown. Due to variations in assembly methods and normal yield loss, yield after packaging is not guaranteed for standard product dice. Consult factory to negotiate specifications based on dice lot qualification through sample lot assembly and testing.

**TYPICAL ELECTRICAL CHARACTERISTICS** at  $V_{IN} = +15V$ ,  $T_A = 25^\circ C$ , unless otherwise noted.

PARAMETER	SYMBOL	CONDITIONS	REF-01NT TYPICAL	REF-01N TYPICAL	REF-01GT TYPICAL	REF-01G TYPICAL	UNITS
Load Regulation		$I_L = 0$ to $10mA$ $I_L = 0$ to $8mA$ , NT, GT @ $+125^\circ C$	0.007	0.005	0.009	0.006	%/mA
Output Voltage Noise	$e_{np-p}$	0.1Hz to 10Hz	20	20	20	20	$\mu V_{p-p}$
Turn-On Settling Time	$t_{ON}$	To $\pm 0.1\%$ of Final Value NT, GT @ $+125^\circ C$	7.5	5.0	7.5	5.0	$\mu s$
Quiescent Current	$I_{qv}$	No Load, NT, GT @ $+125^\circ C$	1.4	1.0	1.4	1.0	mA
Load Current	$I_L$		21	21	21	21	mA
Sink Current	$I_S$		-0.5	-0.5	-0.5	-0.5	mA
Short-Circuit Current	$I_{SC}$	$V_O = 0$	30	30	30	30	mA
Output Voltage Temperature Coefficient	$TCV_O$		10	10	10	10	ppm/ $^\circ C$

**NOTE:**

1. For  $+25^\circ C$  specifications of REF-01NT and REF-01GT, see REF-01N and REF-01G respectively.

Active Component Data Sheets for Proposed Readout Circuitry.[6,7]

19-4729, Rev. Q, 12/91



16-Channel/Dual 8-Channel High Performance CMOS Analog Multiplexers

General Description

The DG406/DG407 are monolithic CMOS analog multiplexers (muxes). The DG406 is a single-ended 1-of-16 device, and the DG407 is a differential 2-of-8 device. Both are pin and functionally compatible with the industry-standard DG506A/DG507A.

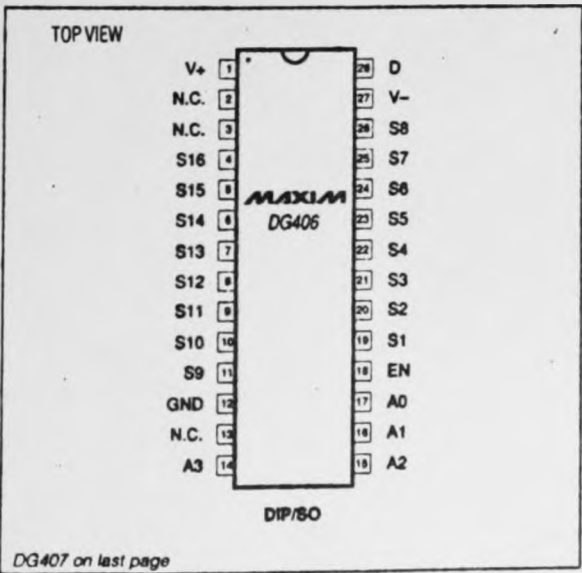
The DG406/DG407 are fabricated with Maxim's new improved silicon gate process. Both parts offer low on resistance (100Ω max), improved leakage over temperature, low power consumption ( $I_{SUPPLY} = 75\mu A$  max) and fast switching speeds ( $t_{TRANS} = 250ns$  max). The 44V maximum breakdown voltage allows switch-off blocking capability rail-to-rail.

These muxes can be used with a single positive supply (+12V to +30V) or split supplies ( $\pm 4.5V$  to  $\pm 20V$ ) while retaining CMOS logic input compatibility. CMOS inputs provide reduced input loading.

Applications

- Sample-and-Hold Circuits
- Test Equipment
- Winchester Disk Drives
- Heads-Up Displays
- Guidance and Control Systems
- Military Radios
- Communications Systems
- Battery-Operated Systems
- PBX, PABX

Pin Configurations



DG407 on last page

Features

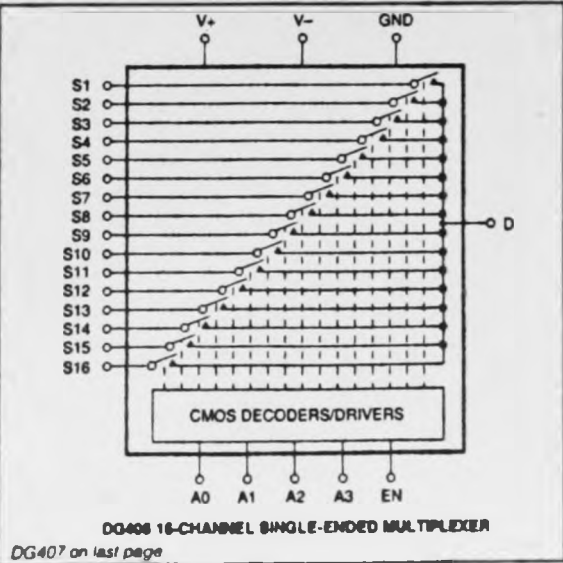
- $r_{DS(ON)}$ : 100Ω Max,  $\Delta r_{DS(ON)}$ : 15Ω Max
- $t_{TRANS}$ : 250ns Max
- Leakage -  $T_A = T_{MIN}$  to  $T_{MAX}$ 
  - $I_{S(OFF)}$ : 50nA Max
  - $I_{D(OFF)}$ : 100nA Max (DG407), 200nA Max (DG406)
  - $I_{-ION}$ : 100nA Max (DG407), 200nA Max (DG406)
- Q: 20pC Typ
- $I_{SUPPLY}$ : 75μA Max
- Single- or Bipolar-Supply Operation
- TTL/CMOS Logic Compatible

Ordering Information

PART	TEMP. RANGE	PIN-PACKAGE
DG406C/D	0°C to +70°C	Dice*
DG406DJ	-40°C to +85°C	28 Plastic DIP
DG406DN	-40°C to +85°C	28 PLCC
DG406DK	-40°C to +85°C	28 CERDIP
DG406AK	-55°C to +125°C	28 CERDIP**
DG407C/D	0°C to +70°C	Dice*
DG407DJ	-40°C to +85°C	28 Plastic DIP
DG407DN	-40°C to +85°C	28 PLCC
DG407DK	-40°C to +85°C	28 CERDIP
DG407AK	-55°C to +125°C	28 CERDIP**

\* Contact factory for dice specifications.  
\*\* Contact factory for availability and processing to MIL-STD-883.

Functional Diagrams



DG407 on last page

DG406/DG407

1

# 16-Channel/Dual 8-Channel High Performance CMOS Analog Multiplexers

## ABSOLUTE MAXIMUM RATINGS

Voltage Referenced to V-

V+	44V
GND	25V
Digital Inputs $V_S, V_D$ (Note 1)	V- -2V to V+ +2V or 30mA (whichever occurs first)
Current (any terminal, except S or D)	30mA
Continuous Current, S or D	20mA
Peak Current, S or D (pulsed at 1ms, 10% duty cycle max)	40mA

Continuous Power Dissipation ( $T_A = +70^\circ\text{C}$ ) (Note 2)

28-Pin Plastic DIP (derate 9.09mW/°C above +70°C)	727mW
28-Pin PLCC (derate 10.53mW/°C above +70°C)	842mW
28-Pin Cerdip (derate 16.67mW/°C above +70°C)	1333mW

Operating Temperature Ranges:

DG406/407C/D	0°C to +70°C
DG406/407D	-40°C to +85°C
DG406/407AK	-55°C to +125°C
Storage Temperature Range	-65°C to +150°C
Lead Temperature (soldering, 10 sec)	+300°C

**Note 1:** Signals on Sx, Dx, or INx exceeding V+ or V- are clamped by internal diodes. Limit forward current to maximum current ratings.

**Note 2:** All leads are soldered or welded to PC board.

Stresses beyond those listed under "Absolute Maximum Ratings" may cause permanent damage to the device. These are stress ratings only, and functional operation of the device at these or any other conditions beyond those indicated in the operational sections of the specifications is not implied. Exposure to absolute maximum rating conditions for extended periods may affect device reliability.

## ELECTRICAL CHARACTERISTICS (Dual Supplies)

(V+ = 15V, V- = -15V, GND = 0V,  $V_{AH} = +2.4\text{V}$ ,  $V_{AL} = +0.8\text{V}$ ,  $T_A = T_{MIN}$  to  $T_{MAX}$ , unless otherwise noted.)

PARAMETER	SYMBOL	CONDITIONS			MIN	TYP (Note 3)	MAX	UNIT
SWITCH								
Analog Signal Range	V <sub>ANALOG</sub>	(Note 4)			-15		15	V
Drain-Source On Resistance	r <sub>DS(ON)</sub>	I <sub>S</sub> = -10mA, V <sub>D</sub> = ±10V		T <sub>A</sub> = +25°C		50	100	Ω
				T <sub>A</sub> = T <sub>MIN</sub> to T <sub>MAX</sub>			125	
r <sub>DS(ON)</sub> Matching Between Channels	Δr <sub>DS(ON)</sub>	V <sub>D</sub> = ±10V (Note 5)		T <sub>A</sub> = +25°C			15	Ω
Source-Off Leakage Current	I <sub>S(OFF)</sub>	V <sub>D</sub> = ±10V, V <sub>S</sub> = ±10V, V <sub>EN</sub> = 0V		T <sub>A</sub> = +25°C	-0.5		0.5	nA
				T <sub>A</sub> = T <sub>MIN</sub> to T <sub>MAX</sub>	-50		50	
Drain-Off Leakage Current	I <sub>D(OFF)</sub>	V <sub>S</sub> = ±10V, V <sub>D</sub> = ±10V, V <sub>EN</sub> = 0V	DG406	T <sub>A</sub> = +25°C	-2		2	nA
				T <sub>A</sub> = T <sub>MIN</sub> to T <sub>MAX</sub>	-200		200	
			DG407	T <sub>A</sub> = +25°C	-2		2	nA
				T <sub>A</sub> = T <sub>MIN</sub> to T <sub>MAX</sub>	-100		100	
Drain-On Leakage Current	I <sub>D(ON)</sub> + I <sub>S(ON)</sub>	V <sub>D</sub> = ±10V, V <sub>S</sub> = ±10V, sequence each switch on	DG406	T <sub>A</sub> = +25°C	-2		2	nA
				T <sub>A</sub> = T <sub>MIN</sub> to T <sub>MAX</sub>	-200		200	
			DG407	T <sub>A</sub> = +25°C	-2		2	nA
				T <sub>A</sub> = T <sub>MIN</sub> to T <sub>MAX</sub>	-100		100	

# MAXIM

## High-Speed, Micropower Op Amps

### General Description

The MAX402/MAX403 high-speed, micropower op amps are fabricated with Maxim's high-frequency complementary bipolar process. These devices feature a combination of high-speed performance and low-power operation that offers significant improvement over other available op amps.

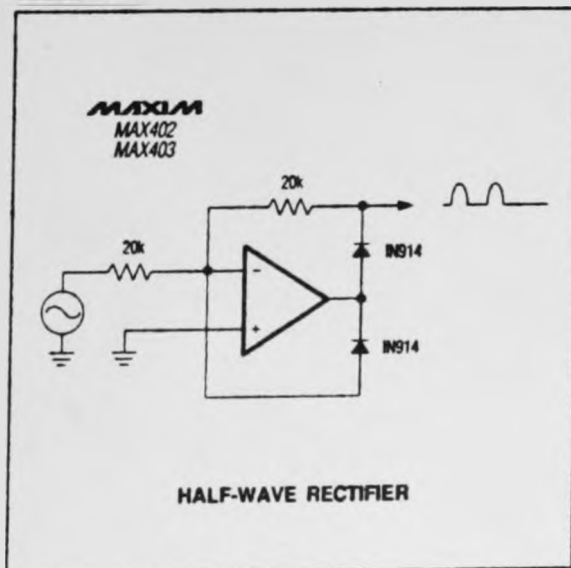
The MAX402 guarantees a 5V/ $\mu$ s slew rate and 1.4MHz bandwidth while drawing only 75 $\mu$ A of supply current. For applications requiring increased speed, the MAX403 guarantees a 25V/ $\mu$ s slew rate and 7MHz bandwidth while drawing a maximum supply current of 375 $\mu$ A. These micropower op amps have excellent load-driving capability:  $\pm 3.6$ V into a 10k $\Omega$  load for both amplifiers, and  $\pm 3.3$ V into a 2k $\Omega$  load for the MAX403. Both op amps are unity-gain stable and operate from  $\pm 3$ V to  $\pm 5$ V supplies, or a single supply from +6V to +10V.

The combination of high speed and low power makes the MAX402/MAX403 ideal for high-speed, battery-powered applications.

### Applications

- Low-Power Signal Processing
- Portable Instruments
- Remote Sensors

### Typical Application Circuit



### Features

#### MAX402

- ◆ 1.4MHz Min Unity Gain Bandwidth
- ◆ 5V/ $\mu$ s Min Slew Rate
- ◆ 75 $\mu$ A Max Supply Current

#### MAX403

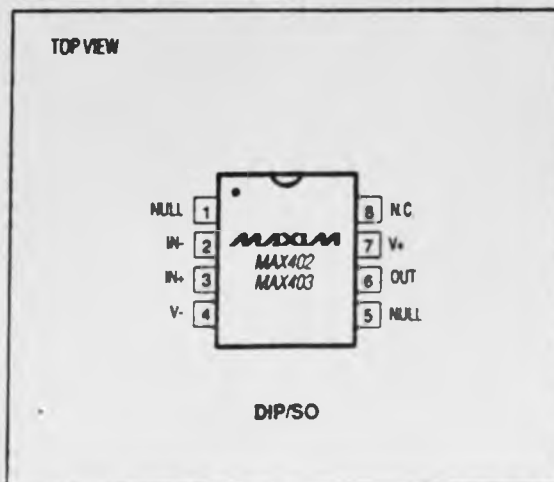
- ◆ 7MHz Min Unity Gain Bandwidth
- ◆ 25V/ $\mu$ s Min Slew Rate
- ◆ 375 $\mu$ A Max Supply Current

### Ordering Information

PART	TEMP. RANGE	PIN-PACKAGE
MAX402CPA	0°C to +70°C	8 Plastic DIP
MAX402CSA	0°C to +70°C	8 SO
MAX402C/D	0°C to +70°C	Dice*
MAX402EPA	-40°C to +85°C	8 Plastic DIP
MAX402ESA	-40°C to +85°C	8 SO
MAX403CPA	0°C to +70°C	8 Plastic DIP
MAX403CSA	0°C to +70°C	8 SO
MAX403C/D	0°C to +70°C	Dice*
MAX403EPA	-40°C to +85°C	8 Plastic DIP
MAX403ESA	-40°C to +85°C	8 SO
MAX403MJA	-55°C to +125°C	8 CERDIP

\* Contact factory for dice specifications and military temperature range availability.

### Pin Configuration



MAX402/MAX403

3

## High-Speed, Micropower Op Amps

### ABSOLUTE MAXIMUM RATINGS (Note 1)

Supply Voltage ( $V^+$ to $V^-$ )	12V
Input Voltage Range	( $V^+ + 0.3V$ ) to ( $V^- - 0.3V$ )
Differential Input Voltage	$V^+$ to $V^-$
Short-Circuit Current Duration	Indefinite
Maximum Current into Any Pin	50mA
Continuous Power Dissipation ( $T_A = +25^\circ\text{C}$ )	
8-Pin Plastic DIP	375mW
8-Pin CERDIP	500mW
8-Pin SO	471mW

### Operating Temperature Ranges

MAX402C	$0^\circ\text{C}$ to $+70^\circ\text{C}$
MAX402E	$-40^\circ\text{C}$ to $+85^\circ\text{C}$
MAX403MJA	$-55^\circ\text{C}$ to $+125^\circ\text{C}$
Storage Temperature Range	$-65^\circ\text{C}$ to $+150^\circ\text{C}$
Lead Temperature (soldering, 10 sec)	$+300^\circ\text{C}$

**Note 1:** Absolute maximum ratings apply to packaged parts only, unless otherwise noted.

Stresses beyond those listed under "Absolute Maximum Ratings" may cause permanent damage to the device. These are stress ratings only, and functional operation of the device at these or any other conditions beyond those indicated in the operational sections of the specifications is not implied. Exposure to absolute maximum rating conditions for extended periods may affect device reliability.

### ELECTRICAL CHARACTERISTICS

( $V^+ = 5V$ ,  $V^- = -5V$ ,  $T_A = +25^\circ\text{C}$ , unless otherwise noted.)

PARAMETER	SYMBOL	CONDITIONS	MAX402			MAX403			UNITS
			MIN	TYP	MAX	MIN	TYP	MAX	
Input Offset Voltage	$V_{OS}$			0.5	2		0.5	2	mV
Offset Voltage Tempco $\Delta V_{OS}/\Delta T$	$TCV_{OS}$	$T_A = T_{MIN}$ to $T_{MAX}$		25			25		$\mu\text{V}/^\circ\text{C}$
Input Bias Current	$I_B$			$\pm 2$	$\pm 5$		$\pm 10$	$\pm 25$	nA
Input Voltage Range	IVR		$\pm 3.5$	$\pm 3.8$		$\pm 3.5$	$\pm 3.8$		V
Differential Input Resistance	$R_{IN}$ (DIFF)			90			18		M $\Omega$
Common-Mode Input Resistance	$R_{IN}$ (CM)			1			1		G $\Omega$
Input Noise Voltage Density	$e_n$	$f_O = 10\text{Hz}$		43			33		$\text{nV}/\sqrt{\text{Hz}}$
		$f_O = 1000\text{Hz}$		26			14		
Input Noise Current Density	$i_n$	$f_O = 10\text{Hz}$		0.06			0.25		$\text{pA}/\sqrt{\text{Hz}}$
		$f_O = 1000\text{Hz}$		0.03			0.07		
Common-Mode Rejection Ratio	CMRR	$V_{CM} = \pm 3.5V$	75	95		66	80		dB
Power-Supply Rejection Ratio	PSRR	$V_S = \pm 4.5V$ to $\pm 5.5V$	56	65		60	70		dB
Large-Signal Gain	$A_{VOL}$	$R_L = 10k\Omega$	68	75			80		dB
		$R_L = 2k\Omega$				68	75		
Output Voltage Swing	$V_{OUT}$	$R_L = 10k\Omega$	$\pm 3.6$	$\pm 3.9$		$\pm 3.6$	$\pm 3.9$		V
		$R_L = 2k\Omega$				$\pm 3.3$	$\pm 3.6$		
Short-Circuit Output Current	$I_{SC}$			3			5		mA
Slew Rate	SR	$10k\Omega$    $20\text{pF}$ load	5	7		25	40		$\text{V}/\mu\text{s}$
Gain Bandwidth	GBW	$10k\Omega$    $20\text{pF}$ load	1.4	2		7	10		MHz
Quiescent Current	$I_Q$		40	50	75	200	250	375	$\mu\text{A}$

# MAXIM

## Dual, Low-Noise Low-Voltage Precision Op Amp

MAX412

### General Description

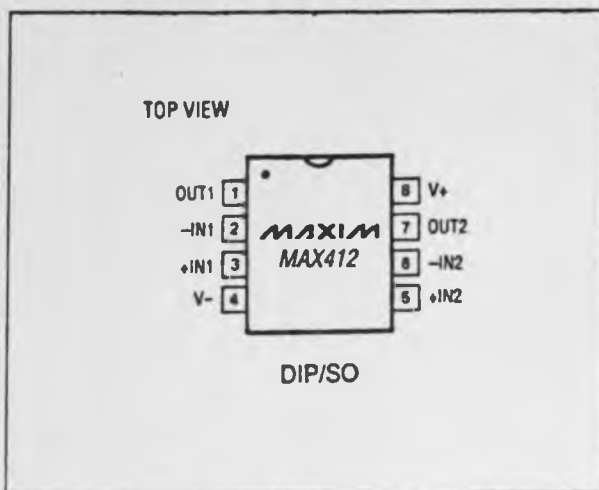
The MAX412 dual operational amplifier sets a new standard for noise performance in low-voltage systems. Input voltage noise density is 100% tested and is guaranteed to be less than  $2.4\text{nV}/\sqrt{\text{Hz}}$  at 1kHz. A unique design not only combines low noise with  $\pm 5\text{V}$  operation, but also consumes less than 2.5mA supply current per amplifier. Low voltage operation is assured with a guaranteed output voltage swing of  $\pm 3.6\text{V}$  into  $2\text{k}\Omega$ . The MAX412 also operates from supply voltages between  $\pm 2.4\text{V}$  and  $\pm 5\text{V}$  for greater supply flexibility.

Unity-gain stability, 28MHz bandwidth, and  $4.5\text{V}/\mu\text{s}$  slew rate ensure low noise performance in a variety of wideband and measurement applications. The MAX412 is available in 8-pin DIP and SO packages in the industry-standard dual op amp pin configuration.

### Applications

- Low Noise-Frequency Synthesizers
- Infrared Detectors
- High-Quality Audio Amplifiers
- Accelerometer and Gyro Amplifiers
- Magnetic Search Coil Amplifiers
- Ultra-Low Noise Instrumentation Amplifiers
- Bridge Signal Conditioning

### Pin Configuration



### Features

- ◆ 100% Tested Voltage Noise:  $2.4\text{nV}/\sqrt{\text{Hz}}$  Max at 1kHz
- ◆ 2.5mA Supply Current Per Amplifier
- ◆ Low Supply Voltage Operation:  $\pm 2.4\text{V}$  to  $\pm 5\text{V}$
- ◆ 28MHz Unity-Gain Bandwidth
- ◆  $4.5\text{V}/\mu\text{s}$  Slew Rate
- ◆  $250\mu\text{V}$  Max Offset Voltage
- ◆ 115dB Min Voltage Gain
- ◆ 2 Amplifiers in One 8-Pin DIP/SO

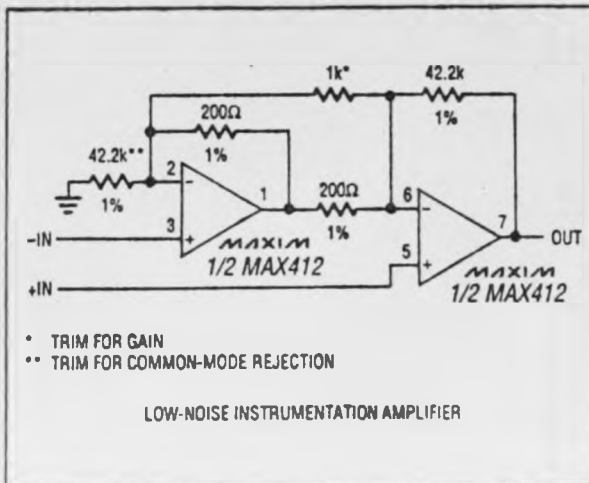
### Ordering Information

PART	TEMP. RANGE	PIN-PACKAGE
MAX412CPA	$0^\circ\text{C}$ to $+70^\circ\text{C}$	8 Plastic DIP
MAX412CSA	$0^\circ\text{C}$ to $+70^\circ\text{C}$	8 SO
MAX412C/D	$0^\circ\text{C}$ to $+70^\circ\text{C}$	Dice*
MAX412EPA	$-40^\circ\text{C}$ to $+85^\circ\text{C}$	8 Plastic DIP
MAX412ESA	$-40^\circ\text{C}$ to $+85^\circ\text{C}$	8 SO
MAX412MJA	$-55^\circ\text{C}$ to $+125^\circ\text{C}$	8 CERDIP

\* Dice are specified at  $T_A = +25^\circ\text{C}$ , DC parameters only.

3

### Typical Operating Circuit



## Dual, Low-Noise, Low-Voltage Precision Op Amp

### ABSOLUTE MAXIMUM RATINGS

Supply Voltage ( $V^+$  to  $V^-$ ) ..... 12V  
 Differential Input Current (Note 1) .....  $\pm 20\text{mA}$   
 Differential Input Voltage .....  $V^+$  to  $V^-$   
 Common-Mode Input Voltage ..... ( $V^+ + 0.3\text{V}$ ) to ( $V^- - 0.3\text{V}$ )  
 Short-Circuit Current Duration ..... Indefinite  
 Continuous Power Dissipation ( $T_A = +70^\circ\text{C}$ )  
   8-pin Plastic DIP (derate  $6.9\text{mW}/^\circ\text{C}$  above  $+70^\circ\text{C}$ ) .. 552mW  
   8-pin SO (derate  $5.88\text{mW}/^\circ\text{C}$  above  $+70^\circ\text{C}$ ) ..... 471mW  
   8-pin CERDIP (derate  $8.0\text{mW}/^\circ\text{C}$  above  $+70^\circ\text{C}$ ) ... 640mW

#### Operating Temperature Ranges:

MAX412C\_A .....  $0^\circ\text{C}$  to  $+70^\circ\text{C}$   
 MAX412E\_A .....  $-40^\circ\text{C}$  to  $+85^\circ\text{C}$   
 MAX412MJA .....  $-55^\circ\text{C}$  to  $+125^\circ\text{C}$   
 Storage Temperature .....  $-65^\circ\text{C}$  to  $+150^\circ\text{C}$   
 Lead Temperature (soldering, 10 sec) .....  $+300^\circ\text{C}$

**Note 1:** The amplifier inputs are connected by internal back-to-back clamp diodes. In order to minimize noise in the input stage, current-limiting resistors are not used. If differential input voltages exceeding  $\pm 1.0\text{V}$  are applied, input current should be limited to  $20\text{mA}$ .

Stresses beyond those under "Absolute Maximum Ratings" may cause permanent damage to the device. These are stress ratings only, and functional operation of the device at these or any other conditions beyond those indicated in the operational sections of the specification is not implied. Exposure to absolute maximum rating conditions for extended periods may affect the device reliability.

### ELECTRICAL CHARACTERISTICS

( $V^+ = 5\text{V}$ ,  $V^- = -5\text{V}$ ,  $T_A = +25^\circ\text{C}$ , unless otherwise noted.)

PARAMETER	SYMBOL	CONDITIONS	MIN	TYP	MAX	UNITS
Input Offset Voltage	$V_{OS}$			$\pm 120$	$\pm 250$	$\mu\text{V}$
Input Bias Current	$I_B$			$\pm 80$	$\pm 150$	nA
Input Offset Current	$I_{OS}$			$\pm 40$	$\pm 80$	nA
Differential Input Resistance	$R_{IN}(\text{Diff})$			20		k $\Omega$
Common-Mode Input Resistance	$R_{IN}(\text{CM})$			40		M $\Omega$
Input Capacitance	$C_{IN}$			4		pF
Input Noise-Voltage Density	$e_n$	$f_o = 10\text{Hz}$		7		nV/ $\sqrt{\text{Hz}}$
		$f_o = 1000\text{Hz}$ (100% tested)		1.8	2.4	
Input Noise-Current Density	$i_n$	$f_o = 10\text{Hz}$		2.6		pA/ $\sqrt{\text{Hz}}$
		$f_o = 1000\text{Hz}$		1.2		
Common-Mode Input Voltage	$V_{CM}$		+3.5 -3.5	+3.7 -3.8		V
Common-Mode Rejection Ratio	CMRR	$V_{CM} = \pm 3.5\text{V}$	115	130		dB
Power-Supply Rejection Ratio	PSRR	$V_S = \pm 2.4\text{V}$ to $\pm 5.25\text{V}$	96	103		dB
Large-Signal Gain	$A_{VOL}$	$R_L = 2\text{k}\Omega$ , $V_O = 3.6\text{V}$ to $-3.7\text{V}$	115	122		dB
		$R_L = 600\Omega$ , $V_O = \pm 3.5\text{V}$	110	120		
Output Voltage Swing	$V_{OUT}$	$R_L = 2\text{k}\Omega$	+3.6 -3.7	+3.7 -3.8		V
Short-Circuit Output Current	$I_{SC}$			35		mA
Slew Rate	SR	10k $\Omega$ /20pF load		4.5		V/ $\mu\text{s}$
Unity-Gain Bandwidth	GBW	10k $\Omega$ /20pF load		28		MHz
Settling Time	$t_S$	To 0.1%		1.3		$\mu\text{s}$
Channel Separation	CS	$f_o = 1\text{kHz}$		135		dB
Operating-Supply Voltage Range	$V_S$		$\pm 2.4$		$\pm 5.25$	V
Supply Current	$I_S$	Both amplifiers		5	5.25	mA

EVALUATION KIT  
AVAILABLE

MAXIM

# Low-Power Single-Supply 12-Bit Sampling ADC

## General Description

The MAX190 is a complete monolithic CMOS 12-bit analog-to-digital converter (ADC) that features a differential input, track-and-hold (T/H), adjustable voltage reference, internal or external clock, and both parallel and serial  $\mu$ P interfaces. It has a conversion time of 7.5 $\mu$ s and tested sampling rate of 76kHz while requiring only 5mA from a single 5V supply. A 50 $\mu$ A power-down mode saves power in slow sampling rate applications.

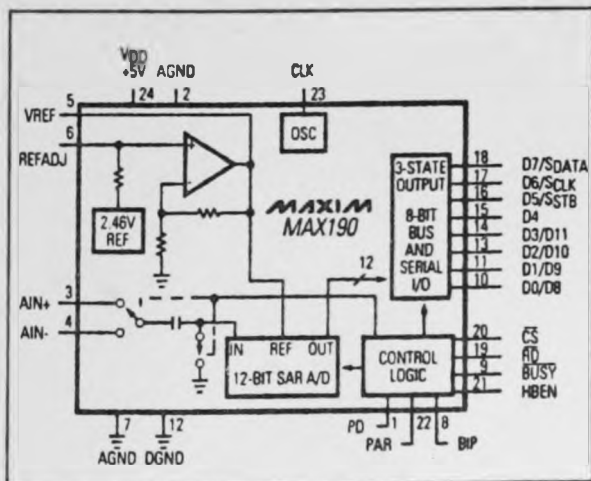
No external components are needed other than decoupling capacitors for the power supply and reference. This ADC operates with an internal or external reference. The internal reference features an adjustment input for trimming system gain errors.

The MAX190 provides three interface modes. Two 8-bit parallel modes, and a serial interface mode that is compatible with common serial interface standards.

## Applications

- Battery-Powered Data Logging
- High-Accuracy Process Control
- Electro-Mechanical Systems
- Data-Acquisition Boards for PCs
- Automatic Testing Systems
- Telecommunications
- Digital-Signal Processing (DSP)

## Functional Diagram



## Features

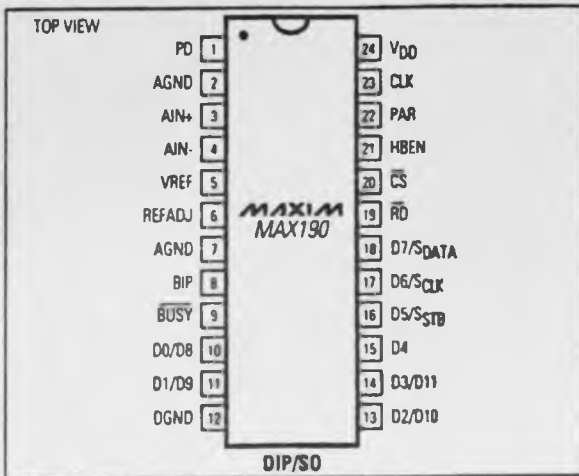
- ◆ 12-Bit Resolution, 1/2LSB Linearity
- ◆ Single +5V Operation 5mA Max Current
- ◆ Power-Down Mode-50 $\mu$ A Max
- ◆ Built-In Track-and-Hold
- ◆ 7.5 $\mu$ s Conversion Time (12.5 $\mu$ s including T/H Acquisition)
- ◆ Internal Reference with Adjustment Capability
- ◆ Serial and 8-Bit Parallel  $\mu$ P Interface
- ◆ 24-Pin Narrow DIP and Wide SO Packages

## Ordering Information

PART	TEMP. RANGE	PIN-PACKAGE	ERROR (LSBs)
MAX190ACNG	0°C to +70°C	24 Narrow Plastic DIP	$\pm 1/2$
MAX190BCNG	0°C to +70°C	24 Narrow Plastic DIP	$\pm 1$
MAX190ACWG	0°C to +70°C	24 Wide SO	$\pm 1/2$
MAX190BCWG	0°C to +70°C	24 Wide SO	$\pm 1$
MAX190BC/D	0°C to +70°C	Dice*	$\pm 1$
MAX190AENG	-40°C to +85°C	24 Narrow Plastic DIP	$\pm 1/2$
MAX190BENG	-40°C to +85°C	24 Narrow Plastic DIP	$\pm 1$
MAX190AEWG	-40°C to +85°C	24 Wide SO	$\pm 1/2$
MAX190BEWG	-40°C to +85°C	24 Wide SO	$\pm 1$
MAX190AMRG	-55°C to +125°C	24 Narrow CERDIP	$\pm 1/2$
MAX190BMRG	-55°C to +125°C	24 Narrow CERDIP	$\pm 1$

\*Contact factory for dice specifications.

## Pin Configuration



# Low-Power Single-Supply 12-Bit Sampling ADC

## ABSOLUTE MAXIMUM RATINGS

$V_{DD}$ to DGND	-0.3V, +7V
AGND, VREF, REFADJ to DGND	-0.3V, $V_{DD} + 0.3V$
AIN+, AIN-, PD to $V_{SS}$	-0.3V, $V_{DD} + 0.3V$
$\overline{CS}$ , $\overline{RD}$ , CLK, BIP, HBEN,	
PAR to DGND	-0.3V, $V_{DD} + 0.3V$
$\overline{BUSY}$ , D0-D7 to DGND	-0.3V, $V_{DD} + 0.3V$

Continuous Power Dissipation (any package)	
to +75 °C	941mW
derate above +75°C	12mW/°C
Operating Temperature Ranges:	
MAX190_C	0°C to +70°C
MAX190_E	-40°C to +85°C
MAX190_M	-55°C to +125°C
Storage Temperature Range	-65°C to +160°C
Lead Temperature (soldering, 10 sec)	+300°C

Stresses beyond those listed under "Absolute Maximum Ratings" may cause permanent damage to the device. These are stress ratings only, and functional operation of the device at these or any other conditions beyond those indicated in the operational sections of the specifications is not implied. Exposure to absolute maximum rating conditions for extended periods may affect device reliability.

## ELECTRICAL CHARACTERISTICS

$V_{DD} = +5V \pm 5\%$ ,  $f_{CLK} = 1.8MHz$ , 50% duty cycle, AIN- = AGND, BIP = GND, Slow-Memory Mode, Internal Reference Mode, External Compensation Mode, Synchronous Operation, Figure 6,  $T_A = T_{MIN}$  to  $T_{MAX}$ , unless otherwise noted). (Note 1)

PARAMETER	SYMBOL	CONDITIONS		MIN	TYP	MAX	UNITS
DC ACCURACY (Note 2)							
Resolution				12			Bits
Integral Nonlinearity	INL		MAX190A	±1/2			LSB
			MAX190B	±1			
Differential Nonlinearity	DNL	Monotonic over temperature		±1			LSB
Offset Error			MAX190A	±1			LSB
			MAX190B	±2			
Full-Scale Error (Note 3)		T <sub>A</sub> = +25°C, includes reference error	MAX190A	±2			LSB
			MAX190B	±3			
Full-Scale Tempco (Note 4)		Excludes internal reference drift		±0.2			ppm/°C
Conversion Time (Note 5)	t <sub>CONV</sub>	Synchronous CLK (12 to 12.5 CLKs)		7.50		7.81	μs
		Internal CLK, C <sub>L</sub> = 120pf		6	12	18	
DYNAMIC ACCURACY (sample rate = 76kHz)							
Signal-to-Noise plus Distortion Ratio	SINAD	1kHz input signal, T <sub>A</sub> = +25°C		70			dB
Total Harmonic Distortion (up to the 5th harmonic)	THD	1kHz input signal, T <sub>A</sub> = +25°C				-80	dB
Spurious-Free Dynamic Range	SFDR	1kHz input signal, T <sub>A</sub> = +25°C		80			dB

EVALUATION KIT  
AVAILABLE

# MAXIM

## High-Efficiency, +5V Adjustable Step-Down Switching Regulator

### General Description

The MAX639 high-efficiency step-down switching regulator converts battery voltages between +5.5V and +11.5V to +5V, and supplies 100mA of output current over the entire input voltage range. 10 $\mu$ A quiescent current, greater than 90% efficiency, and 0.5V dropout (0.12V dropout at 25mA output current) extend battery life in portable applications. Additional features include a logic-level shutdown control and low-battery detection circuitry.

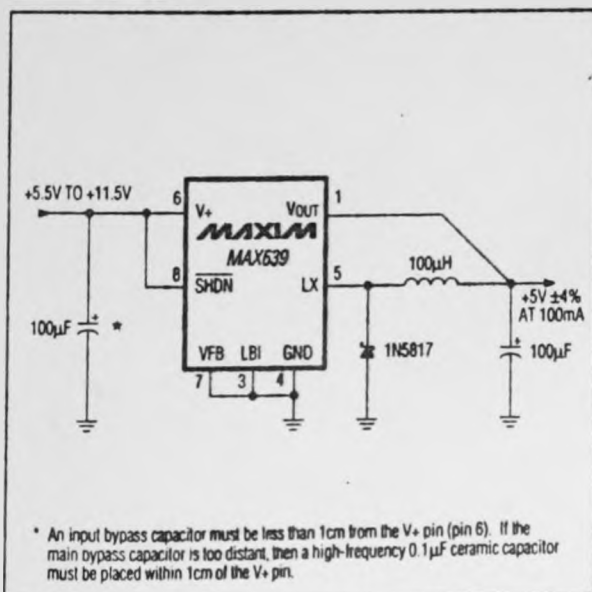
The MAX639 requires only four external components: a small low-cost inductor, a diode, an input bypass capacitor, and an output filter capacitor. No compensation components are needed. Voltages other than +5V can be generated by adding two resistors.

The MAX639 is pin compatible with the MAX638, except for the addition of the SHUTDOWN input, and is available in 8-pin DIP and SO packages.

### Applications

High-Efficiency DC-DC Step Down Regulation  
Linear Voltage Regulator Replacement  
+9V to +5V Conversion  
Battery-Life Extension  
Portable Instruments

### Typical Operating Circuit



### Features

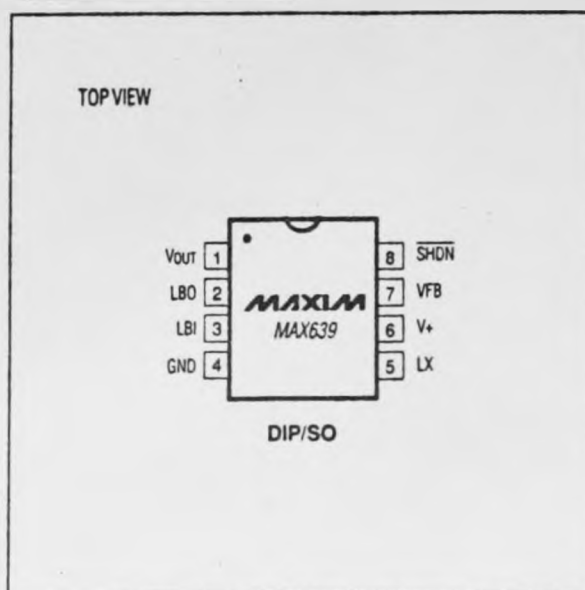
- ◆ High Efficiency
  - 84% at I<sub>OUT</sub> = 25mA
  - 91% at I<sub>OUT</sub> = 100mA
- ◆ Ultra Low 20 $\mu$ A (Max) Quiescent Current
- ◆ Output Currents Up to 225mA
- ◆ Preset +5V or Adjustable Output Voltage
- ◆ Only 4 External Components
- ◆ TTL/CMOS Compatible Shutdown Control
- ◆ Low-Battery Detector
- ◆ 500mV (Typ) Dropout Voltage (100mA Load)
- ◆ 8-Pin SO and Plastic DIP Packages

### Ordering Information

PART	TEMP. RANGE	PIN-PACKAGE
MAX639CPA	0°C to +70°C	8 Plastic DIP
MAX639CSA	0°C to +70°C	8 SO
MAX639C/D	0°C to +70°C	Dice*
MAX639EPA	-40°C to +85°C	8 Plastic DIP
MAX639ESA	-40°C to +85°C	8 SO
MAX639MJA	-55°C to +125°C	8 CERDIP

\*Contact factory for dice specifications.

### Pin Configuration



# High-Efficiency, +5V Adjustable Step-Down Switching Regulator

## ABSOLUTE MAXIMUM RATINGS

V+	12V
LX	(V+ - 12V) to (V+ + 0.3V)
LBI, LBO, VFB, SHDN, Vout	-0.3V to (V+ + 0.3V)
LX Output Current	1A
LBO Output Current	10mA
Continuous Power Dissipation	
Plastic DIP (derate 9.09mW/°C above +70°C)	727mW
SO (derate 5.88mW/°C above +70°C)	471mW
CERDIP (derate 8.00mW/°C above +70°C)	640mW

### Operating Temperature Ranges:

MAX639C	0°C to +70°C
MAX639E	-40°C to +85°C
MAX639MJA	-55°C to +125°C
Storage Temperature Range	-65°C to +160°C
Lead Temperature (soldering, 10 sec)	+300°C

Stresses beyond those listed under "Absolute Maximum Ratings" may cause permanent damage to the device. These are stress ratings only, and functional operation of the device at these or any other conditions beyond those indicated in the operational sections of the specifications is not implied. Exposure to absolute maximum rating conditions for extended periods may affect device reliability.

## ELECTRICAL CHARACTERISTICS

(V+ = 9V, I<sub>LOAD</sub> = 0mA, T<sub>A</sub> = T<sub>MIN</sub> to T<sub>MAX</sub>, unless otherwise noted.)

PARAMETER	CONDITIONS	MIN	TYP	MAX	UNITS
Supply Voltage		4.0		11.5	V
Supply Current	SHDN = V+, No load		10	20	μA
V <sub>OUT</sub> (Note 1)	V+ = 6.0V to 11.5V, 0mA < I <sub>OUT</sub> < 100mA	4.80	5.00	5.20	V
Dropout Voltage	I <sub>OUT</sub> = 100mA, L = 100μH		0.5		V
Efficiency	I <sub>OUT</sub> = 100mA, L = 100μH		91		%
	I <sub>OUT</sub> = 25mA, L = 470μH		94		
t <sub>ON</sub>	V+ = 9V, V <sub>OUT</sub> = 5V	11.0	12.5	14.0	μs
	V+ = 6V, V <sub>OUT</sub> = 3V	14.2	16.7	19.2	
t <sub>OFF</sub>	V+ = 9V, V <sub>OUT</sub> = 5V	8.5	10.0	11.5	μs
	V+ = 6V, V <sub>OUT</sub> = 3V	14.2	16.7	19.2	
LX Peak Current				600	mA
LX Switch r <sub>ON</sub>	V+ = 9V, T <sub>A</sub> = +25°C		0.8	1.5	Ω
	V+ = 6V			2.5	
LX Switch Leakage	V+ = 12V, V <sub>LX</sub> = 0V, T <sub>A</sub> = +25°C		0.003	1.0	μA
	V+ = 12V, V <sub>LX</sub> = 0V			30	
VFB I <sub>BIAS</sub>	VFB = 2V		4	15	nA
VFB Dual Mode Trip Point			50		mV
VFB Threshold	MAX639C	1.26	1.28	1.30	V
	MAX639E, M	1.24	1.28	1.32	
LBI I <sub>BIAS</sub>	V <sub>LBI</sub> = 2V		2	10	nA
LBI Threshold	MAX639C	1.26	1.28	1.30	V
	MAX639E, M	1.24	1.28	1.32	
LBO Sink Current	V <sub>LBO</sub> = 0.4V	0.80	2.50		mA
LBO Leakage Current	V <sub>LBO</sub> = 12V		0.001	0.1	μA
LBO Delay	50mV Overdrive		25		μs
SHDN Threshold		0.80	1.15	2.00	V
SHDN Pull-Up Current	V <sub>SHDN</sub> = 0V	0.10	0.20	0.40	μA

Note 1. Load regulation guaranteed by correlation to DC pulse measurements.

## Preset/Adjustable Output CMOS Inverting Switching Regulators

### ABSOLUTE MAXIMUM RATINGS

Supply Voltage, +Vs (Note 1)	+18V
Input Voltage, LBO, LBI, VFB	-0.3V to (+Vs + 0.3V)
LX Output Current	525mA Peak
LBO Output Current	50mA
Power Dissipation	
Plastic DIP (derate 8.33mW/°C above +50°C)	625mW
Small Outline (derate 6mW/°C above +50°C)	450mW
CERDIP (derate 8mW/°C above +50°C)	800mW

### Operating Temperature Range

MAX63_C	0°C to +70°C
MAX63_E	-40°C to +85°C
MAX63_M	-55°C to +125°C
Storage Temperature	-65°C to +160°C
Lead Temperature (Soldering, 10 sec.)	+300°C

Stresses beyond those listed under "Absolute Maximum Ratings" may cause permanent damage to the device. These are stress ratings only and functional operation of the device at these or any other conditions beyond those indicated in the operational sections of the specifications is not implied. Exposure to absolute maximum rating conditions for extended periods may affect device reliability.

### ELECTRICAL CHARACTERISTICS

(TA = +25°C, unless otherwise noted.)

PARAMETER	SYMBOL	CONDITIONS	MIN	TYP	MAX	UNITS
Supply Voltage (Note 1)	+Vs	TA = +25°C Over Temperature	2.3 2.6		16.5 16.5	V
Supply Current	IS	No Load, LX Off, Over Temperature +Vs = +5V +Vs = +15V		80 260	150 500	μA
Reference Voltage	VREF	TA = +25°C Over Temperature	1.24 1.20	1.31	1.38 1.42	V
VOUT Voltage (Note 2)		No Load, VFB = VREF, +Vs = +5V Over Temperature MAX635A } MAX636A } 5% Output Accuracy MAX637A } MAX635B } MAX636B } 10% Output Accuracy MAX637B }	-4.75 -11.4 -14.25 -4.5 -10.8 -13.5	-5.0 -12.0 -15.0 -5.0 -12.0 -15.0	-5.25 -12.6 -15.75 -5.5 -13.2 -16.5	V
Efficiency				85		%
Line Regulation (Note 2)		+5V < +Vs < +15V		0.5		%VOUT
Load Regulation (Note 2)		POUT = 0mW to 150mW		0.2		%VOUT
Oscillator Frequency	fO	+Vs = +5V    MAX63_A MAX63_B	45 40	50 50	56 65	kHz
Oscillator Duty Cycle		+Vs = +5V	40	50	60	%
LX On Resistance	RON	Ix = 100mA, +Vs = +5V = +15V		9 4	16 8	Ω
LX Leakage Current	IXL	+Vs = +16.5V TA = +25°C Over Temperature		0.01	1.0 30	μA
VFB Input Bias Current	IFB			0.01	10	nA
Low Battery Threshold	VLBI			1.31		V
Low Battery Input Bias Current	ILBI			0.01	10	nA
Low Battery Output Current	ILBO	V2 = +0.4V, V3 = +1.1V TA = 25°C Over Temperature	0.5	1.0		mA
Low Battery Output Leakage Current	ILBOL	V2 = +16.5V, V3 = +1.4V		0.01	3.0	μA

Note 1: In addition to the Absolute Maximum Rating of +18V, the input voltage also must not exceed 24V - | -VOUT |.

Note 2: Guaranteed by correlation with DC pulse measurements.



## Preset/Adjustable Output CMOS Inverting Switching Regulators

### General Description

The MAX635/MAX636/MAX637 inverting switching regulators are designed for minimum component DC-DC conversion in the 5mW to 500mW range.

Low power applications require only a diode, output filter capacitor, and a low-cost inductor. An additional MOSFET and driver are needed for higher power applications. Low battery detection circuitry is included on chip.

The MAX635/636/637 are preset for -5V, -12V, and -15V outputs, respectively. However, the regulators can be set to other levels by adding 2 resistors.

Maxim manufactures a broad line of step-up, step-down, and inverting DC-DC converters, with features such as logic-level shutdown, adjustable oscillator frequency, and external MOSFET drive.

### Applications

- Minimum Component, High-Efficiency DC-DC Converters
- Portable Instruments
- Battery Power Conversion
- Board Level DC-DC Conversion

### Features

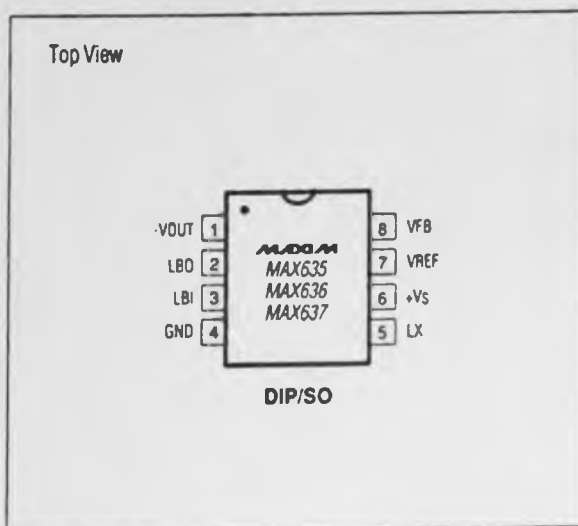
- ◆ Preset -5V, -12V, -15V Output Voltages
- ◆ Adjustable Output with 2 Resistors
- ◆ 85% Typ Efficiency
- ◆ Only 3 External Components
- ◆ 80μA Typ Operating Current
- ◆ Low Battery Detector

### Ordering Information

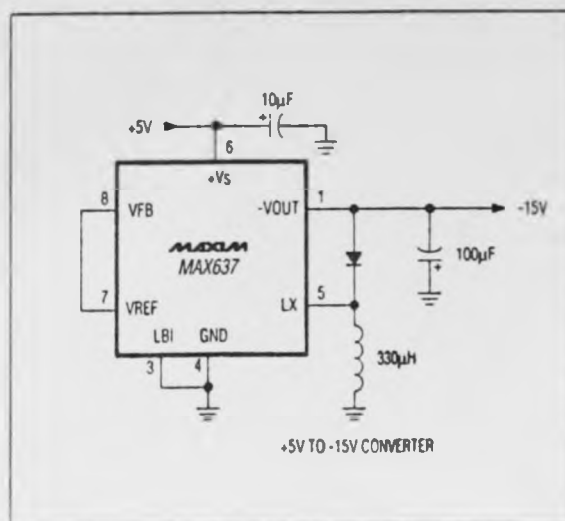
PART*	TEMP. RANGE	PIN-PACKAGE
MAX635XCPA	0°C to +70°C	8 Plastic DIP
MAX635XCSA	0°C to +70°C	8 Narrow SO
MAX635XC/D	0°C to +70°C	Dice
MAX635XEPA	-40°C to +85°C	8 Plastic DIP
MAX635XESA	-40°C to +85°C	8 Narrow SO
MAX635XEJA	-40°C to +85°C	8 CERDIP
MAX635XMJA	-55°C to +125°C	8 CERDIP
MAX636XCPA	0°C to +70°C	8 Plastic DIP
MAX636XCSA	0°C to +70°C	8 Narrow SO
MAX636XC/D	0°C to +70°C	Dice
MAX636XEPA	-40°C to +85°C	8 Plastic DIP
MAX636XESA	-40°C to +85°C	8 Narrow SO
MAX636XEJA	-40°C to +85°C	8 CERDIP
MAX636XMJA	-55°C to +125°C	8 CERDIP

\*X = A for 5% Output Accuracy, X = B for 10% Output Accuracy.  
Ordering information continued on last page.

### Pin Configuration



### Typical Operating Circuit



## Preset/Adjustable Output CMOS Inverting Switching Regulators

### ABSOLUTE MAXIMUM RATINGS

Supply Voltage, +Vs (Note 1)	+18V
Input Voltage, LBO, LBI, VFB	-0.3V to (+Vs + 0.3V)
LX Output Current	525mA Peak
LBO Output Current	50mA
Power Dissipation	
Plastic DIP (derate 8.33mW/°C above +50°C)	625mW
Small Outline (derate 6mW/°C above +50°C)	450mW
CERDIP (derate 8mW/°C above +50°C)	800mW

### Operating Temperature Range

MAX63_C	0°C to +70°C
MAX63_E	-40°C to +85°C
MAX63_M	-55°C to +125°C
Storage Temperature	-65°C to +160°C
Lead Temperature (Soldering, 10 sec.)	+300°C

Stresses beyond those listed under "Absolute Maximum Ratings" may cause permanent damage to the device. These are stress ratings only and functional operation of the device at these or any other conditions beyond those indicated in the operational sections of the specifications is not implied. Exposure to absolute maximum rating conditions for extended periods may affect device reliability.

### ELECTRICAL CHARACTERISTICS

(TA = +25°C, unless otherwise noted.)

PARAMETER	SYMBOL	CONDITIONS	MIN	TYP	MAX	UNITS
Supply Voltage (Note 1)	+Vs	TA = +25°C Over Temperature	2.3 2.6		16.5 16.5	V
Supply Current	IS	No Load, LX Off, Over Temperature +Vs = +5V +Vs = +15V		80 260	150 500	μA
Reference Voltage	VREF	TA = +25°C Over Temperature	1.24 1.20	1.31	1.38 1.42	V
VOUT Voltage (Note 2)		No Load, VFB = VREF, +Vs = +5V Over Temperature				V
		MAX635A } 5% Output Accuracy MAX636A } MAX637A } MAX635B } 10% Output Accuracy MAX636B } MAX637B }	-4.75 -11.4 -14.25	-5.0 -12.0 -15.0	-5.25 -12.6 -15.75	
Efficiency				85		%
Line Regulation (Note 2)		+5V < +Vs < +15V		0.5		%VOUT
Load Regulation (Note 2)		POUT = 0mW to 150mW		0.2		%VOUT
Oscillator Frequency	fO	+Vs = +5V MAX63_A MAX63_B	45 40	50 50	56 65	kHz
Oscillator Duty Cycle		+Vs = +5V	40	50	60	%
LX On Resistance	RON	Ix = 100mA, +Vs = +5V = +15V		9 4	16 8	Ω
LX Leakage Current	IXL	+Vs = +16.5V TA = +25°C Over Temperature		0.01	1.0 30	μA
VFB Input Bias Current	IFB			0.01	10	nA
Low Battery Threshold	VLBI			1.31		V
Low Battery Input Bias Current	ILBI			0.01	10	nA
Low Battery Output Current	ILBO	V2 = +0.4V, V3 = +1.1V TA = 25°C Over Temperature	0.5	1.0		mA
Low Battery Output Leakage Current	ILBOL	V2 = +16.5V, V3 = +1.4V		0.01	3.0	μA

Note 1: In addition to the Absolute Maximum Rating of +18V, the input voltage also must not exceed 24V - |VOUT|.

Note 2: Guaranteed by correlation with DC pulse measurements.

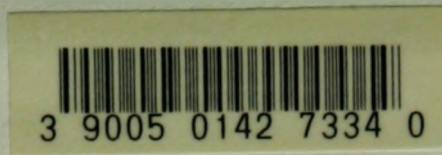
## REFERENCES

- 1)Suggested Interfaces, Tech Notes. Interlink Electronics, Sept.,1990
- 2)Technical Overview, Force and Position Sensing Resistors. interlink Electronics, 1990
- 3)FSR Technical Specification. Interlink Electronics
- 4)Force Sensing Resistors, Unlock the Power of Touch. Interlink Electronics
- 5)The Design Center Analysis-Reference Manual Version 5.1, Irvine, CA Microsim Corporation ,Jan 1992
- 6)Volume 10 Data Book Analog Integrated Circuits, Santa Clara, CA, Precision Monolithics Inc.
- 7)Maxim 1993 New Release Data Book Volume II, Sunnyvale, CA, Maxim Integrated Products Inc. 1993
- 8)Maxim 1992 New Release Data Book, Sunnyvale, CA Maxim Integrated Products Inc. 1992
- 9)SPICE Model Library, Analog Devices Release F, 4/92
- 10)Pressure Sensor Handbook, Sunnyvale, CA SenSyn Inc. 1987
- 11)Blake C.D., Brewerton D.A., Goodbody A., Soames R.W., Staff J.R.R. "Measurement of pressure under foot during function." Med. & Biol. Eng. & Comput.,1982,20,489-495.
- 12)Gerber H. "A system for measuring dynamic pressure distribution under the human foot." J. Biomechanics Vol. 15. No.3 pp 225-227,1982

- 13)Ishida A., Miyazaki S. "Capacitive transducer for continuous measurement of vertical foot force." Med. & Biol. Eng. & Comput.,1984, 22, 309-316.
- 14)Albert H.T., Cavanagh P.R., Hennig E.M., Macmillan N.H. "A piezoelectric method for measuring the vertical contact stress beneath the human foot." J. Biomed. Eng. 1982, Vol. 4, july pp 213-222.
- 15)Tompkins Willis J., Webster John G., Wertsch Jacqueline J., "A portable insole plantar pressure measurement system." Journal of Rehabilitation Research and development Vol. 29 No. 1, 1992 pp 13-18.
- 16)Maliniak David "Piezoelectric-Film sensors Leave Niches Behind", Electronic Design 1991, Dec. 5 p. 37.
- 17)"Pressure Sensors & Transducers" EDN 1986, May 1, pp 100-113.
- 18)Shiengold Daniel H., Transducer Interface Handbook. Norwood, MA Analog Devices Inc., 1980.
- 19)Webster John G., Medical Instrumentation Application and Design. Boston, MA. Houghton Mifflin Company, 1978.
- 20)Wobschall Darold, Sensors: Interfaces and Applications, McGraw Hill Seminar Center, 1985
- 21)Hymowitz Charles E., Meares Lawrence G. Simulating with SPICE, SanPedro CA Intusoft, 1988.

NOTE: Certain Figures (as noted by [\*] in the figures caption) contained in this report were taken from these references.





Thode

R

857

.T7 H54

1992

c.2

ADU 1199